

Supplementary Materials

Supplementary Material 1.1 Annotation List

Supplementary Table 1.2 Glossary

Supplementary Fig. 1.3 – Molecular Interaction Map (MIM) referred to HT29

Supplementary Table 1.4 - Pathways present in our MIMs

Supplementary Table 2.1 - Reaction list

Supplementary Table 2.2 - Species Initial Concentration

Supplementary Material 3.1 Cell cultures and reagents

Supplementary Material 3.2 Western Blots: Methods and raw results

Supplementary Fig. 4.1 Illustration of the transcription factors and transcription factor binding sites considered in the Promoter/TF/RNAP and TFBS/TF/RNAP systems.

Supplementary Material 4.2 Literature background describing the involvement of key transcription factors and transcription factor binding sites in regulation of MYC and CCND1 transcription

Supplementary Material 4.3 Derivation of the transcription rate function for MYC and CCND1

Supplementary Material 4.4 Derivation of the regulation factor $F_{\text{Promoter/TF/RNAP}}$ in terms of the regulation factors of independent TFBS/TF/RNAP subsystems

Supplementary Material 4.5 Example: Detailed derivation of the regulation factor $F_{E2F-DP1}$ for the TFBS/TF/RNAP subsystem associated with the E2F-DP1 transcription factor binding site

Supplementary Material 4.6 Final expression for the transcription rate of MYC and CCND1

Supplementary Table 4.7 Computation of regulation factor $F_{E2F-DP1}$

Supplementary Table 4.8 Computation of regulation factor F_{TCF7L2}

Supplementary Table 4.9 Computation of regulation factor F_{SMAD4}

Supplementary Table 4.10 Computation of regulation factor F_{AP1}

Supplementary Table 4.11 Computation of regulation factor F_{TP53}

Supplementary Table 4.12 Summary of regulation factor expressions

Supplementary Material 5.1 Examples of behaviors of the model

Supplementary Material 5.2 Starting from physiologic model: no mutations, KRAS mutation. Inhibitors: no inhibitors, panErb inhibitor, MEK inhibitor, both inhibitors

Supplementary Material 6 Simulated and Experimental Data

Supplementary Table 6.1 ERKPP and AKTP levels in HCT116 cell line

Supplementary Table 6.2 ERKPP and AKTP levels in HT29 cell line

Supplementary Table 6.3 MYC and CCND1 mRNA levels HCT116 cell line

Supplementary Table 6.4 MYC and CCND1 mRNA levels HT29 cell line

Supplementary Material 1.1 - Annotation List referred to the MIM of Fig.1 and Supplementary Fig. 1.3

Supplementary Material 1.1 shows an Annotation List of the reference sources of the interactions reconstructed in our MIMs. In order to keep the reference list as short and relevant as possible, recent articles or review articles were often cited that contained references to the original works. Whenever possible these sources of biochemical interactions where also utilized for preliminary extrapolations of kinetic parameters to reconstruct a reasonable global dynamic behavior. Additional information contained in publications were utilized. Corresponding numbers appear in Fig. 1- main text, Supplementary Fig. 1.3 and in the Annotation List.

(# followed by an Arabic number indicates an interaction or a contingency depicted in the MIM)

#1-3, coord. 1-2, G: EGF (EGF family proteins) binds the extracellular domain of ErbB family receptors (#1); the EGF:ErbB family receptors complex then forms a dimer (homo or hetero-dimer) (#2) which induces reciprocal multiple tyrosine autophosphorylations (#3) in the intracellular portion of the receptors, and provides specific docking sites for cytoplasmatic proteins [1-3]. In this MIM, we represented only one site of autophosphorylation.

#4-9, coord.2-3, G-H: Following activation of the ErbB family kinases and autophosphorylation, the adaptor protein Grb2 can bind either directly (#4) [4] or through tyrosyl-phosphorylated Shc (#5,#6, #7), to specific docking sites on the receptor [5]. The complex of the ErbB family receptors with the adaptor protein Grb2 and /or ShcP:Grb2 complex (#9), can bind SOS and is then recruited to the plasma membrane [6]. The Grb2:SOS complex can bind the ErbB family receptors activated (#8), directly.

#10, coord. 2-3, H-I: SOS can act on membrane-bound KRAS and is then able to increase KRAS-GTP levels by catalyzing nucleotide exchange on KRAS, resulting in KRAS activation (KRAS-GTP) (#10) [6, 7].

#11-12, coord. 1-3, G-H: Association of GAP with receptors tyrosine kinase phosphorylated (#11) induces GAP protein binding to KRAS-GTP and accelerates the conversion of KRAS-GTP to KRAS-GDP (#12), which terminates signaling [7, 8].

#13-14, coord. 2-3, G: Phosphorylation of Shc (#13) decreases the affinity of the protein for the EGFR activated receptor: Shc dissociated from the receptor does not contribute to RAS activation [9]. Shc:P can be dephosphorylated by cellular protein tyrosine phosphatase (PTPases): In this MIM, it was assumed that Shc:P can be dephosphorylated by PTPε phosphatase (#14) [10].

#15-17, coord. 2-4, H-I: KRAS:GTP binds to BRAF (#15) and recruits BRAF from the cytosol to the cell membrane, where BRAF activation takes place. BRAF activation (#16) is regulated by an interplay of complex and still incompletely understood mechanisms [11-14]. In this MIM, it was assumed that BRAF-P1 can be dephosphorylated by an unknown phosphatase, P-ase 1 (#17).

#18-23, coord. 4-6, G-I: Activated BRAF can phosphorylate and activate MEK (#18, #19), which in turn phosphorylates (#20, #21) and activates extracellular-signal-regulated kinase (ERK). In this MIM, it was assumed that an unknown phosphatase P-ase 7 dephosphorylates MEK-P and MEK-PP (#22); MKP3 phosphatase dephosphorylates ERK-P and ERK-PP (#23). It was reported that inactivation of ERK-PP could be carried out by multiple phosphatases [11-13].

#24-28, coord. 6-9, D-L: ERK-PP translocates to the nucleus and can phosphorylate Elk1 transcription factor (not shown in this MIM) [15], leading to elevated AP-1 activity via c-fos induction. AP1 complexes, depending on their composition, have been shown to activate or repress CCND1, and their activity can be modulated by phosphorylation [16, 17]. In the model, we assume a net-positive effect of AP1 on CCND1 transcription, which has a consensus AP1 (TFBS_{AP1}) site in its promoter (#27), [17-20] and on c-MYC transcription (#28) [21-23]. In this MIM, it was assumed that ERK-PP can bind (#24) and phosphorylate a pre-existing AP-1 transcription factor (#25) and not newly synthesized AP-1 components or AP-1 complexes. In this MIM, it was assumed that an unknown phosphatase (P-ase 11) dephosphorylates AP-1-P (#26).

#29-31, coord. 2-6, H-L: Feedback inhibition from ERK-PP to SOS provides an additional mechanism for the inhibition of KRAS signaling: SOS phosphorylation by ERK-PP (#29) causes the dissociation of SOS from its complexes with Grb2 (#30). SOS-P can't bind KRAS [11, 24, 25]. In this MIM, it was assumed that an unknown phosphatase (P-ase 5) dephosphorylates SOS-P (#31).

#32-35, coord. 2-6, F-I: Activated ERK kinase can bind (#32) and phosphorylate CDC25C on several residues (#33), leading to activation of its phosphatase activity [26]. Activated CDC25C can dephosphorylate EGFR receptor (#34). An activating KRAS mutation or a BRAF (V600F) constitutive activation in mutant colon cancer tumors [27] causes a feedback dephosphorylation of EGFR-P. In this MIM, it was assumed that an unknown phosphatase (P-ase 11) dephosphorylates CDC25C-P (#35).

#36-44, coord. 1-4, G-P: Binding of PLC γ to activated ErbB family receptors (#36) results in the phosphorylation of PLC γ (#37), [1]. In this MIM, it was assumed that PLC γ :P can be dephosphorylated by an unknown phosphatase P-ase 2 (#38). Active PLC γ binds and cleaves (#39, #40) the PtdIns(4,5)-P₂ to yield the second messengers 1,2-diacylglycerol (DAG) that stays in the plasma membrane and the soluble inositol 1,3,5-trisphosphate (IP₃) that induces a Ca²⁺ release from the endoplasmic reticulum (not shown in this MIM). DAG (#41) and IP₃ (#42) are degraded. The increased concentration of diacylglycerol (DAG) can activate, alone and in combination with calcium, various PKC isoforms (#43) [28, 29]. An activated PKC can phosphorylate and activate BRAF (#44) [30].

#45-54, coord. 1-3, G-L: Upon growth factor stimulation, receptors tyrosine kinase phosphorylated can activate PI3K via two major mechanisms: direct binding (#45,#46) [31, 32] or indirect via GAB1 [25]. The association of GAB1 with ErbB family receptors is thought to occur via Grb2 (#47) or ShP:Grb2 (#48), resulting in tyrosine phosphorylation of GAB1 (#49,#50); GAB1-P binds (#51) and activates PI3K and recruits them to the plasma membrane (#52) [33]. In this MIM, we assumed that a PK inactivator protein (#53) inactivates PI3K and unknown phosphatase P-ase 3 dephosphorylates GAB1-P (#54).

#55-56, coord.2-3, I-L: RasGTP can bind (#55) and activate (#56) PI3K [34].

#57-58, coord. 1-3, H-M: GAB1 and GAB1-P can bind PIP3 and lead to a further recruitment of GAB1 (#57) to the membrane [33], and activate PI3K pathway. In addition, the tyrosyl-phosphorylated GAB1 can bind GAP (#58) [33]. This association induces GAP protein binding to KRAS-GTP and accelerates the conversion of KRAS-GTP to KRAS-GDP (#12), and negatively regulates KRAS [7, 8, 33]. Negative feedback regulation of GAB can be achieved by serine phosphorylation by ERKPP (#152) [35, 36].

#59-6 , coord. 2-3, I-N: Activated PI3K binds PIP2 (#59) and catalyzes the formation of PIP3 from PIP2, on the plasma membrane (#60). PTEN directly antagonizes PI3K signaling by dephosphorylating the 3-position of the inositol ring of PIP3 (#61) and thus inactivating downstream signaling [31-33].

#62-66, coord. 2-4, I-N: PIP3 directly binds to Akt (#62) and recruits Akt to the plasma membrane; PDK1 kinase phosphorylates and activates the Akt-PIP3 complex (#63). The phosphorylation of Akt at Thr 308 by PDK1 (#64) results in activation of this protein kinase; additional phosphorylation of Akt at Ser 473 is required for its full activation [37] (not shown in this MIM). PHLPP dephosphorylates Akt-P on Ser473, resulting in inhibition of its kinase activity (#65) [38]. The active phospho-Akt inhibits the activation of BRAF, by hyperphosphorylation on Ser-259 (BRAF-P2)(#66), [39].

#67-76, coord. 2-9, E-N: Activated Akt binds and phosphorylates several cellular proteins, including GSK3 β (#67) [37], MDM2 (#68,#69) [40]. In this MIM, we assumed that an unknown P-ase 13 dephosphorylates MDM2 (#70). MDM2-P binds (#71) and promotes ubiquitination, nuclear export and proteasomal degradation (#72) [41] of TP53 and blocks its ability to regulate target genes. TP53 can bind transcription binding sites (TFBS_{TP53})(#73) and can inhibit the expression of MYC transcription through a mechanism that involves histone deacetylation (#74) [42]. TP53 also represses CCND1 transcription indirectly, by downregulating a transcriptional coactivator [43]. The ARF protein can bind to the MDM2 (#75) protein and modulates down its ubiquitin ligase activity by inhibition of TP53 binding (#76), increasing the levels of the TP53 protein [41].

#77- 86, coord. 2-4, E-M: Activated Akt binds and phosphorylates GSK3 β : GSK3 β phosphorylated in Ser9 seems to result in inhibition of activity (#77), [37, 44, 45]. (*Some experimental reports [46, 47] have suggested a weak or controversial connection between the PI3K - AKT pathway and GSK3 β*). We assumed that unknown phosphatases P-ase 4 dephosphorylates GSK3 β (#78).

β -Catenin phosphorylation involves the sequential actions of casein kinase 1 (Ck1, not shown in this MIM) and GSK3 β , and takes place in a protein complex, the “destruction complex” assembled by Axin and APC. In the absence of Wnt signalling, GSK3 β binds (#79) and phosphorylates the scaffold protein Axin (#80). GSK3 β : Axin-P complex binds (#81) and phosphorylates (#82) APC, APC-P binds to GSK3 β : Axin-P complex; the “destruction complex” (GSK3 β : Axin-P : APC-P complex) promotes the binding (#83) and phosphorylation of cytosolic β -catenin (#84) [48-52]. Phosphorylation in residues 45, 41, 37 and 33 of cytosolic β -catenin (non E-Cadherin bound) by the destruction complex, leads to its degradation

[48-54] by the ubiquitin–proteasome pathway (#85). We assumed that an unknown phosphatase P-ase 6 can dephosphorylate Axin, APC and β -catenin in the “destruction complex” (P-ase 6 is also indicated as PP2A in [49, 54, 55]). P-ase 6 also dephosphorylates LRP5/6 (#86).

#87-99, coord. I-9, C-G: β -catenin normally, associates at the cellular membrane with the adhesion molecule E-cadherin, while any free cytoplasmic β -catenin is phosphorylated and targeted for ubiquination-dependent degradation. E-Cadherin binds PTP1B phosphatase (#87) promoting binding between β -catenin and the cytoplasmatic domain of E-Cadherin (#88) [56, 57]; this binding (#89) inhibits the binding with members of the TCF/LEF family of transcription factor. In the intestinal epithelium, TCF7L2 is the most prominently expressed TCF family member [58, 59]. E-cadherin and TCF7L2 forms mutually exclusive complexes with β -catenin (#94), [59]. An activated ErbB family receptor can phosphorylate β -catenin at Y654 (#90) and can inhibit E-Cadherin binding (#91) and adhesive function [56, 57]. PY654 of β -catenin is target of PTP1B phosphatase (#92) [57]. As a consequence of this phosphorylation β -catenin is not sequestered from E-Cadherin: it is in equilibrium with free β -catenin which can translocate to the nucleus where β -cateninY654 (#93) and β -catenin (#94) can bind the TCF7L2 transcription factor (#95) [60, 61] and can activate the expression of target genes (#96) (in this MIM: CCND1 and MYC genes), [62-66]. In the absence of nuclear β -catenin, TCF7L2 functions instead as transcriptional repressor by binding to co-repressors of the Groucho-TLE family (#97) and binds (#98) and inhibits transcription of target genes [67, 68]. In the absence of TGF β signaling, Smad4 binds the MYC promoter LEF/TCF-binding elements from the MYC promoter and activates MYC promoter activity (#99), [69]. In this MIM, it was assumed that SMAD4 also activates CCND1 gene transcription. The cadherin cytoplasmic domain binds to β -catenin, which in turn binds with weaker affinity to α -catenin [52]. This binding was omitted in this MIM (an example of simplification).

#100-105, coord. I-4, E-G: Upon ligand interaction, Wnt, Frizzled receptors and the Wnt co-receptor LRP6 form a ternary signaling complex which recruits Dishevelled proteins to the plasma membrane [70] by direct binding [71]. The scaffold protein Dishevelled promotes the formation of an LRP-associated Wnt ‘signalosome’ [72] and directly interacts with Axin [73] and recruits it, and also associates GSK3 β to the plasma membrane. Formation of signalosomes promotes sequential phosphorylation of LRP6 by GSK3 β and casein kinase 1, of cytoplasmic domain of LRP5 or LRP6 at five critical PPSP/TP repeats [74]. The association of the axin complex with the phosphorylated LRP6 leads to (via an as yet unknown mechanism) inhibition of β -catenin phosphorylation. The function of the degradation complex is inhibited by this canonical pathway: β -catenin accumulates, enter the nucleus, and engages in transcriptional activation (#94, #96).

To make it easy, in this MIM, it was assumed that activated Wnt binds Frizzled receptors (#100), then LRP5/6 co-receptors (#101) and the Wnt:Frizzled:LRP5/6 complex binds the Dishevelled protein (#102). It was assumed that activated Wnt:Frizzled:LRP5/6:Dishevelled complex recruits GSK3 β (#103) which phosphorylates LRP5 or LRP6 (#104): these sites allow docking of Axin (#105) and its recruitment to the plasma membrane. How Wnt signalling activates β -catenin through the blocking of GSK3 β remains one of the main open questions in this pathway: different model have been proposed [48, 49, 74, 75]. In this MIM, it was assumed that LRP5 (or LRP6) can be dephosphorylated by an unknown phosphatase, P-ase 6 (#86).

#106-107, coord. I-3, C-E: Kinase activity of TAK1 was stimulated in response to Wnt (#106, #107) [76].

#108-114, coord I-2, B-C: Dimeric TGF β (#108) binds with high affinity (#110) type II (TGF β R-II) receptors dimers (#109), on the cell surface. Dimeric TGF β type I (TGF β R-I) (#111) binds dimeric TGF β R-II:dimeric TGF β complex (#112). In the hetero-tetrameric receptor complex, type II receptors phosphorylate a serine/threonine-rich region (the GS region), located in the kinase domain of TGF β R-I (#113), which then propagates the signal [77-80]. PP1C can dephosphorylate active TGF β R-I (#114) [81].

#115-126, coord. I-5, C-D: An activated TGF β complex can bind (#115) and activate TAK1 (#116)[82]. In this MIM, it was assumed that P-ase 9 can dephosphorylate TAK1-P (#117). TAK1-P binds TAB2 scaffold protein (#118) [83] and phosphorylates NLK family of protein kinases and increases their kinase activity (#119-120). In this MIM, it was assumed that P-ase 10 can dephosphorylate NLK-P (#121). NLK-P can bind (#122) and directly phosphorylate TCF7L2 on two serine/threonine residues (#124) and can prevent the β -catenin:TCF7L2 complex from binding to DNA, thereby inhibiting the ability of β -catenin:TCF7L2 to activate transcription (#125). The TAK1-NLK pathway negatively regulates the canonical Wnt signaling pathway [83, 84]. In this MIM, it was assumed that P-ase 8 can dephosphorylate TCF7L2- P (#126).

#127-134, coord. 2-9, A-H: An activated TGF β complex can bind (#127) and phosphorylate Smad3 and propagate the signal (#128); an activated TGF β complex (via a region in the type I receptor) can bind Smad2 (#129) and phosphorylate Smad2 (#130) and propagate the signal. Smad4 can bind activated Smad2 and Smad3 (#132) [77-80] forming complexes that can translocate into the nucleus (#133). These SMAD complexes can then bind to a SMAD binding site ($TFBS_{SMAD}$) on MYC, repressing its transcription [85-87]. A similar inhibitory role of the TGF- β pathway on CCDN1 transcription has been

described [88, 89]. SMAD4 (most likely complexed with phosphorylated SMAD2 or SMAD3) binds to the promoter region of CCND1 upon TGF- β treatment, repressing transcription [90]. Dephosphorylation is accompanied with dissociation of the Smad2/3-Smad4 complex and export of its components to the cytoplasm (not shown in this MIM). PPM1A can dephosphorylate active Smad2 and Smad3, in the nucleus (#131) [91].

#135-147, coord. 6-7, M-P: Cdk4 binds exclusively to D-type cyclins (#135), Cdk2 binds to cyclins E (or A) (#136). Cyclin D:Cdk4 phosphorylates pRb at a subset of sites (#137, #138), Cyclin E:Cdk2 phosphorylates pRb at additional sites after the Cyclin D:Cdk4-specific sites have been phosphorylated. p16 competes with Cyclin D1 for binding to Cdk4 (#139) [92]. In this MIM, it was assumed that P-ase 14 can dephosphorylate pRb (#140, #141).

#142-147, coord. 7-8, F-P: Dimerization partner (DP) protein forms stable heterodimers with E2F (#142). Unphosphorylated (or hypophosphorylated) pRb (active form), can bind to DP:E2F complexes (#143) and block E2F-dependent transcription genes (#144, #145). Hyperphosphorylated pRb (inactive form), resulting from combined phosphorylation by Cyclin D:Cdk4 and Cyclin E:Cdk2 (#137, #138), abrogates the binding of pRb to DP:E2F complexes, leads to the release of E2F transcription factors and to the transcriptional activation of E2F-responsive genes (#146, #147). MYC and CCND1 are target genes of E2F [93, 94].

#148-151, coord. 8-9, B-P: In this MIM, MYC and CCND1 genes transcription has been described as importantly stimulated at least by the following: AP-1, AP1-P (#27), TCF7L2: β catenin, TCF7L2: β cateninY654 (#95), TCF7L2:SMAD4 (#99), E2F:DP1 (#146). They can bind DNA in different sites. Transcription has been described as inhibited by SMADIIP:SMAD4 (#133); SMADIIP:SMAD4 (#133); GROUCHO:TCF7L2 (#98); TP53 (#73, #74); E2F:DP1:RB (#144). Each transcription factor to activate gene expression, can recruit the transcriptional machinery such as RNA Polymerase II elongation complex (#148) to the promoter region. A completely operational RNA Polymerase II slides over the DNA CCND1 or MYC coding region (#149) and makes a copy of Cyclin D1 or c-myc mRNA (#150). The Cyclin D1 or c-Myc mRNA are degraded (#151), [95, 96].

References related to the MIM Annotation List

1. Jorissen RN, Walker F, Pouliot N, Garrett TP, Ward CW and Burgess AW. Epidermal growth factor receptor: mechanisms of activation and signalling. *Exp Cell Res.* 2003; 284(1):31-53.
2. Yarden Y and Sliwkowski MX. Untangling the ErbB signalling network. *Nat Rev Mol Cell Biol.* 2001; 2(2):127-137.
3. Citri A and Yarden Y. EGF-ERBB signalling: towards the systems level. *Nat Rev Mol Cell Biol.* 2006; 7(7):505-516.
4. Batzer AG, Rotin D, Urena JM, Skolnik EY and Schlessinger J. Hierarchy of binding sites for Grb2 and Shc on the epidermal growth factor receptor. *Mol Cell Biol.* 1994; 14(8):5192-5201.
5. Wills MK and Jones N. Teaching an old dogma new tricks: twenty years of Shc adaptor signalling. *Biochem J.* 2012; 447(1):1-16.
6. Markevich NI, Moehren G, Demin OV, Kiyatkina A, Hoek JB and Kholodenko BN. Signal processing at the Ras circuit: what shapes Ras activation patterns? *Systems biology.* 2004; 1(1):104-113.
7. Malumbres M and Barbacid M. RAS oncogenes: the first 30 years. *Nat Rev Cancer.* 2003; 3(6):459-465.
8. McCormick F. ras GTPase activating protein: signal transmitter and signal terminator. *Cell.* 1989; 56(1):5-8.
9. Suenaga A, Hatakeyama M, Kiyatkina AB, Radhakrishnan R, Taiji M and Kholodenko BN. Molecular Dynamics Simulations Reveal that Tyr-317 Phosphorylation Reduces Shc Binding Affinity for Phosphotyrosyl Residues of Epidermal Growth Factor Receptor. *Biophysical Journal.* 2009; 96(6):2278-2288.
10. Kraut-Cohen J, Muller WJ and Elson A. Protein-tirosine phosphatase epsilon regulates Shc signaling in a kinase-specific manner - Increasing coherence in tyrosine phosphatase signaling. *Journal of Biological Chemistry.* 2008; 283(8):4612-4621.
11. Brightman FA and Fell DA. Differential feedback regulation of the MAPK cascade underlies the quantitative differences in EGF and NGF signalling in PC12 cells. *Febs Letters.* 2000; 482(3):169-174.
12. Udell CM, Rajakulendran T, Sicheri F and Therrien M. Mechanistic principles of RAF kinase signaling. *Cellular and Molecular Life Sciences.* 2011; 68(4):553-565.
13. Roskoski R. RAF protein-serine/threonine kinases: Structure and regulation. *Biochemical and Biophysical Research Communications.* 2010; 399(3):313-317.

14. Matallanas D, Birtwistle M, Romano D, Zebisch A, Rauch J, von Kriegsheim A and Kolch W. Raf family kinases: old dogs have learned new tricks. *Genes Cancer*. 2011; 2(3):232-260.
15. Gille H, Kortenjann M, Thomae O, Moomaw C, Slaughter C, Cobb MH and Shaw PE. ERK phosphorylation potentiates Elk-1-mediated ternary complex formation and transactivation. *EMBO J*. 1995; 14(5):951-962.
16. Karin M, Liu Z and Zandi E. AP-1 function and regulation. *Curr Opin Cell Biol*. 1997; 9(2):240-246.
17. Shaulian E and Karin M. AP-1 in cell proliferation and survival. *Oncogene*. 2001; 20(19):2390-2400.
18. Albanese C, Johnson J, Watanabe G, Eklund N, Vu D, Arnold A and Pestell RG. Transforming p21ras mutants and c-Ets-2 activate the cyclin D1 promoter through distinguishable regions. *The Journal of biological chemistry*. 1995; 270(40):23589-23597.
19. Bakiri L, Lallemand D, Bossy-Wetzel E and Yaniv M. Cell cycle-dependent variations in c-Jun and JunB phosphorylation: a role in the control of cyclin D1 expression. *EMBO J*. 2000; 19(9):2056-2068.
20. Zhang HS, Yan B, Li XB, Fan L, Zhang YF, Wu GH, Li M and Fang J. PAX2 protein induces expression of cyclin D1 through activating AP-1 protein and promotes proliferation of colon cancer cells. *The Journal of biological chemistry*. 2012; 287(53):44164-44172.
21. Kerkhoff E, Houben R, Loffler S, Troppmair J, Lee JE and Rapp UR. Regulation of c-myc expression by Ras/Raf signalling. *Oncogene*. 1998; 16(2):211-216.
22. Iavarone C, Catania A, Marinissen MJ, Visconti R, Acunzo M, Tarantino C, Carlomagno MS, Bruni CB, Gutkind JS and Chiariello M. The platelet-derived growth factor controls c-myc expression through a JNK- and AP-1-dependent signaling pathway. *The Journal of biological chemistry*. 2003; 278(50):50024-50030.
23. Weston CR and Davis RJ. The JNK signal transduction pathway. *Curr Opin Genet Dev*. 2002; 12(1):14-21.
24. Holt KH, Waters SB, Okada S, Yamauchi K, Decker SJ, Saltiel AR, Motto DG, Koretzky GA and Pessin JE. Epidermal growth factor receptor targeting prevents uncoupling of the Grb2-SOS complex. *The Journal of biological chemistry*. 1996; 271(14):8300-8306.
25. Wolf J, Dronov S, Tobin F and Goryanin I. The impact of the regulatory design on the response of epidermal growth factor receptor-mediated signal transduction towards oncogenic mutations. *FEBS J*. 2007; 274(21):5505-5517.
26. Wang R, He G, Nelman-Gonzalez M, Ashorn CL, Gallick GE, Stukenberg PT, Kirschner MW and Kuang J. Regulation of Cdc25C by ERK-MAP kinases during the G2/M transition. *Cell*. 2007; 128(6):1119-1132.

27. Prahallas A, Sun C, Huang S, Di Nicolantonio F, Salazar R, Zecchin D, Beijersbergen RL, Bardelli A and Bernards R. Unresponsiveness of colon cancer to BRAF(V600E) inhibition through feedback activation of EGFR. *Nature*. 2012; 483(7387):100-103.
28. Fukami K, Inanobe S, Kanemaru K and Nakamura Y. Phospholipase C is a key enzyme regulating intracellular calcium and modulating the phosphoinositide balance. *Prog Lipid Res*. 2010; 49(4):429-437.
29. Todderud G, Wahl MI, Rhee SG and Carpenter G. Stimulation of phospholipase C-gamma 1 membrane association by epidermal growth factor. *Science*. 1990; 249(4966):296-298.
30. Kolch W, Heidecker G, Kochs G, Hummel R, Vahidi H, Mischak H, Finkenzeller G, Marme D and Rapp UR. Protein kinase C alpha activates RAF-1 by direct phosphorylation. *Nature*. 1993; 364(6434):249-252.
31. Bader AG, Kang S, Zhao L and Vogt PK. Oncogenic PI3K deregulates transcription and translation. *Nat Rev Cancer*. 2005; 5(12):921-929.
32. Chalhoub N and Baker SJ. PTEN and the PI3-kinase pathway in cancer. *Annu Rev Pathol*. 2009; 4:127-150.
33. Kiyatkin A, Aksamitiene E, Markevich NI, Borisov NM, Hoek JB and Kholodenko BN. Scaffolding protein Grb2-associated binder 1 sustains epidermal growth factor-induced mitogenic and survival signaling by multiple positive feedback loops. *The Journal of biological chemistry*. 2006; 281(29):19925-19938.
34. Rodriguez-Viciano P, Warne PH, Dhand R, Vanhaesebroeck B, Gout I, Fry MJ, Waterfield MD and Downward J. Phosphatidylinositol-3-OH kinase as a direct target of Ras. *Nature*. 1994; 370(6490):527-532.
35. Lehr S, Kotzka J, Avci H, Sickmann A, Meyer HE, Herkner A and Muller-Wieland D. Identification of major ERK-related phosphorylation sites in Gab1. *Biochemistry*. 2004; 43(38):12133-12140.
36. Verma S, Vaughan T and Bunting KD. Gab adapter proteins as therapeutic targets for hematologic disease. *Adv Hematol*. 2012; 2012:380635.
37. Hemmings BA and Restuccia DF. PI3K-PKB/Akt pathway. *Cold Spring Harb Perspect Biol*. 2012; 4(9):a011189.
38. Gao TY, Furnari F and Newton A. PHLPP: a novel phosphatase that directly dephosphorylates Akt, promotes apoptosis and suppresses tumor growth. *Faseb Journal*. 2005; 19(4):A258-A258.
39. Zimmermann S and Moelling K. Phosphorylation and regulation of Raf by Akt (protein kinase B). *Science*. 1999; 286(5445):1741-1744.
40. Ogawara Y, Kishishita S, Obata T, Isazawa Y, Suzuki T, Tanaka K, Masuyama N and Gotoh Y. Akt enhances Mdm2-mediated ubiquitination and degradation of p53. *Journal of Biological Chemistry*. 2002; 277(24):21843-21850.

41. Moll UM and Petrenko O. The MDM2-p53 interaction. *Molecular Cancer Research*. 2003; 1(14):1001-1008.
42. Ho JSI, Ma WL, Mao DYL and Benchimol S. p53-dependent transcriptional repression of c-myc is required for G(1) cell cycle arrest. *Molecular and Cellular Biology*. 2005; 25(17):7423-7431.
43. Rocha S, Martin AM, Meek DW and Perkins ND. p53 Represses cyclin D1 transcription through down regulation of Bcl-3 and inducing increased association of the p52 NF-kappa B subunit with histone deacetylase 1. *Molecular and Cellular Biology*. 2003; 23(13):4713-4727.
44. Cross DAE, Alessi DR, Cohen P, Andjelkovich M and Hemmings BA. Inhibition of Glycogen-Synthase Kinase-3 by Insulin-Mediated by Protein-Kinase-B. *Nature*. 1995; 378(6559):785-789.
45. Chappell WH, Steelman LS, Long JM, Kempf RC, Abrams SL, Franklin RA, Basecke J, Stivala F, Donia M, Fagone P, Malaponte G, Mazzarino MC, Nicoletti F, Libra M, Maksimovic-Ivanic D, Mijatovic S, et al. Ras/Raf/MEK/ERK and PI3K/PTEN/Akt/mTOR Inhibitors: Rationale and Importance to Inhibiting These Pathways in Human Health. *Oncotarget*. 2011; 2(3):135-164.
46. Ng SS, Mahmoudi T, Danenberg E, Bejaoui I, de Lau W, Korswagen HC, Schutte M and Clevers H. Phosphatidylinositol 3-kinase signaling does not activate the wnt cascade. *The Journal of biological chemistry*. 2009; 284(51):35308-35313.
47. Voskas D, Ling LS and Woodgett JR. Does GSK-3 provide a shortcut for PI3K activation of Wnt signalling? *F1000 Biol Rep*. 2010; 2:82.
48. Kikuchi A. Regulation of beta-catenin signaling in the Wnt pathway. *Biochem Biophys Res Commun*. 2000; 268(2):243-248.
49. Available at www.wnt.stanford.edu.
50. Wu D and Pan W. GSK3: a multifaceted kinase in Wnt signaling. *Trends Biochem Sci*. 2010; 35(3):161-168.
51. Kishida S, Yamamoto H, Ikeda S, Kishida M, Sakamoto I, Koyama S and Kikuchi A. Axin, a negative regulator of the wnt signaling pathway, directly interacts with adenomatous polyposis coli and regulates the stabilization of beta-catenin. *The Journal of biological chemistry*. 1998; 273(18):10823-10826.
52. Daugherty RL and Gottardi CJ. Phospho-regulation of Beta-catenin adhesion and signaling functions. *Physiology (Bethesda)*. 2007; 22:303-309.
53. Wu G and He X. Threonine 41 in beta-catenin serves as a key phosphorylation relay residue in beta-catenin degradation. *Biochemistry*. 2006; 45(16):5319-5323.

54. Su YY, Fu CJ, Ishikawa S, Stella A, Kojima M, Shitoh K, Schreiber EM, Day BW and Liu B. APC Is Essential for Targeting Phosphorylated beta-Catenin to the SCF(beta-TrCP) Ubiquitin Ligase. *Molecular Cell*. 2008; 32(5):652-661.
55. Zhang W, Yang J, Liu YJ, Chen X, Yu TX, Jia JH and Liu CM. PR55 alpha, a Regulatory Subunit of PP2A, Specifically Regulates PP2A-mediated beta-Catenin Dephosphorylation. *Journal of Biological Chemistry*. 2009; 284(34):22649-22656.
56. Lilien J and Balsamo J. The regulation of cadherin-mediated adhesion by tyrosine phosphorylation/dephosphorylation of beta-catenin. *Current Opinion in Cell Biology*. 2005; 17(5):459-465.
57. Wong NACS and Pignatelli M. beta-catenin - A linchpin in colorectal carcinogenesis? *American Journal of Pathology*. 2002; 160(2):389-401.
58. Korinek V, Barker N, Morin PJ, vanWichen D, deWeger R, Kinzler KW, Vogelstein B and Clevers H. Constitutive transcriptional activation by a beta-catenin-Tcf complex in APC(-/-) colon carcinoma. *Science*. 1997; 275(5307):1784-1787.
59. van de Wetering M, Sancho E, Verweij C, de Lau W, Oving I, Hurlstone A, van der Horn K, Batlle E, Coudreuse D, Haramis AP, Tion-Pon-Fong M, Moerer P, van den Born M, Soete G, Pals S, Eilers M, et al. The beta-catenin/TCF-4 complex imposes a crypt progenitor phenotype on colorectal cancer cells. *Cell*. 2002; 111(2):241-250.
60. Orsulic S, Huber O, Aberle H, Arnold S and Kemler R. E-cadherin binding prevents beta-catenin nuclear localization and beta-catenin/LEF-1-mediated transactivation. *Journal of Cell Science*. 1999; 112(8):1237-1245.
61. Bienz M and Clevers H. Linking colorectal cancer to Wnt signaling. *Cell*. 2000; 103(2):311-320.
62. He TC, Sparks AB, Rago C, Hermeking H, Zawel L, da Costa LT, Morin PJ, Vogelstein B and Kinzler KW. Identification of c-MYC as a target of the APC pathway. *Science*. 1998; 281(5382):1509-1512.
63. Tetsu O and McCormick F. beta-catenin regulates expression of cyclin D1 in colon carcinoma cells. *Nature*. 1999; 398(6726):422-426.
64. Shtutman M, Zhurinsky J, Simcha I, Albanese C, D'Amico M, Pestell R and Ben-Ze'ev A. The cyclin D1 gene is a target of the beta-catenin/LEF-1 pathway. *Proceedings of the National Academy of Sciences of the United States of America*. 1999; 96(10):5522-5527.
65. Piedra J, Martinez D, Castano J, Miravet S, Dunach M and de Herreros AG. Regulation of beta-catenin structure and activity by tyrosine phosphorylation. *Journal of Biological Chemistry*. 2001; 276(23):20436-20443.

66. van Veelen W, Le NH, Helvensteijn W, Blonden L, Theeuwes M, Bakker ERM, Franken PF, van Gurp L, Meijlink F, van der Valk MA, Kuipers EJ, Fodde R and Smits R. beta-catenin tyrosine 654 phosphorylation increases Wnt signalling and intestinal tumorigenesis. *Gut*. 2011; 60(9):1204-1212.
67. Daniels DL and Weis WI. beta-catenin directly displaces Groucho/TLE repressors from Tcf/Lef in Wnt-mediated transcription activation. *Nature Structural & Molecular Biology*. 2005; 12(4):364-371.
68. Arce L, Pate KT and Waterman ML. Groucho binds two conserved regions of LEF-1 for HDAC-dependent repression. *Bmc Cancer*. 2009; 9.
69. Lim SK and Hoffmann FM. Smad4 cooperates with lymphoid enhancer-binding factor 1/T cell-specific factor to increase c-myc expression in the absence of TGF-beta signaling. *Proceedings of the National Academy of Sciences of the United States of America*. 2006; 103(49):18580-18585.
70. Angers S and Moon RT. Proximal events in Wnt signal transduction. *Nature Reviews Molecular Cell Biology*. 2009; 10(7):468-477.
71. Wong HC, Bourdelas A, Krauss A, Lee HJ, Shao YM, Wu DQ, Mlodzik M, Shi DL and Zheng J. Direct binding of the PDZ domain of Dishevelled to a conserved internal sequence in the C-terminal region of frizzled. *Molecular Cell*. 2003; 12(5):1251-1260.
72. Bilic J, Huang YL, Davidson G, Zimmermann T, Cruciat CM, Bienz M and Niehrs C. Wnt induces LRP6 signalosomes and promotes dishevelled-dependent LRP6 phosphorylation. *Science*. 2007; 316(5831):1619-1622.
73. Fiedler M, Mendoza-Topaz C, Rutherford TJ, Miesczanek J and Bienz M. Dishevelled interacts with the DIX domain polymerization interface of Axin to interfere with its function in down-regulating beta-catenin. *Proceedings of the National Academy of Sciences of the United States of America*. 2011; 108(5):1937-1942.
74. Taelman VF, Dobrowolski R, Plouhinec JL, Fuentealba LC, Vorwald PP, Gumper I, Sabatini DD and De Robertis EM. Wnt Signaling Requires Sequestration of Glycogen Synthase Kinase 3 inside Multivesicular Endosomes. *Cell*. 2010; 143(7):1136-1148.
75. Zeng X, Tamai K, Doble B, Li ST, Huang H, Habas R, Okamura H, Woodgett J and He X. A dual-kinase mechanism for Wnt co-receptor phosphorylation and activation. *Nature*. 2005; 438(7069):873-877.
76. Ishitani T, Ninomiya-Tsuji J, Nagai S, Nishita M, Meneghini M, Barker N, Waterman M, Bowerman B, Clevers H, Shibuya H and Matsumoto K. The TAK1-NLK-MAPK-related pathway antagonizes signalling between beta-catenin and transcription factor TCF. *Nature*. 1999; 399(6738):798-802.

77. Deryck R and Zhang YE. Smad-dependent and Smad-independent pathways in TGF-beta family signalling. *Nature*. 2003; 425(6958):577-584.
78. Clarke DC and Liu XD. Decoding the quantitative nature of TGF-beta/Smad signaling. *Trends in cell biology*. 2008; 18(9):430-442.
79. Massague J, Blain SW and Lo RS. TGFbeta signaling in growth control, cancer, and heritable disorders. *Cell*. 2000; 103(2):295-309.
80. Massague J. TGF beta signalling in context. *Nature Reviews Molecular Cell Biology*. 2012; 13(10):616-630.
81. Shi WB, Sun CX, He B, Xiong WC, Shi XM, Yao DC and Cao X. GADD34-PP1c recruited by Smad7 dephosphorylates TGF beta type 1 receptor. *Journal of Cell Biology*. 2004; 164(2):291-300.
82. Yamaguchi K, Shirakabe T, Shibuya H, Irie K, Oishi I, Ueno N, Taniguchi T, Nishida E and Matsumoto K. Identification of a Member of the Mapkkk Family as a Potential Mediator of Tgf-Beta Signal-Transduction. *Science*. 1995; 270(5244):2008-2011.
83. Li M, Wang H, Huang T, Wang JY, Ding Y, Li ZF, Zhang JK and Li L. TAB2 Scaffolds TAK1 and NLK in Repressing Canonical Wnt Signaling. *Journal of Biological Chemistry*. 2010; 285(18):13397-13404.
84. Ishitani T, Ninomiya-Tsuji J and Matsumoto K. Regulation of lymphoid enhancer factor 1/T-Cell factor by mitogen-activated protein kinase-related nemo-like kinase-dependent phosphorylation in Wnt/beta-catenin signaling. *Molecular and Cellular Biology*. 2003; 23(4):1379-1389.
85. Yagi K, Furuhashi M, Aoki H, Goto D, Kuwano H, Sugamura K, Miyazono K and Kato M. c-myc is a downstream target of the Smad pathway. *Journal of Biological Chemistry*. 2002; 277(1):854-861.
86. Chen CR, Kang YB, Siegel PM and Massague J. E2F4/5 and p107 as Smad cofactors linking the TGF beta receptor to c-myc repression. *Cell*. 2002; 110(1):19-32.
87. Massague J, Seoane J and Wotton D. Smad transcription factors. *Genes & Development*. 2005; 19(23):2783-2810.
88. Ko TC, Sheng HM, Reisman D, Thompson EA and Beauchamp RD. Transforming Growth-Factor-Beta-1 Inhibits Cyclin D1 Expression in Intestinal Epithelial-Cells. *Oncogene*. 1995; 10(1):177-184.
89. Mithani SK, Balch GC, Shiou SR, Whitehead RH, Datta PK and Beauchamp RD. Smad3 has a critical role in TGF-beta-mediated growth inhibition and apoptosis in colonic epithelial cells. *Journal of Surgical Research*. 2004; 117(2):296-305.

90. Ding ZH, Wu CJ, Chu GC, Xiao YH, Ho D, Zhang JF, Perry SR, Labrot ES, Wu XQ, Lis R, Hoshida Y, Hiller D, Hu BL, Jiang S, Zheng HW, Stegh AH, et al. SMAD4-dependent barrier constrains prostate cancer growth and metastatic progression. *Nature*. 2011; 470(7333):269-+.
91. Lin X, Duan XY, Liang YY, Su Y, Wrighton KH, Long JY, Hu M, Davis CM, Wang JR, Brunicardi FC, Shi YG, Chen YG, Meng AM and Feng XH. PPM1A functions as a Smad phosphatase to terminate TGF beta signaling. *Cell*. 2006; 125(5):915-928.
92. Kohn KW. Molecular interaction map of the mammalian cell cycle control and DNA repair systems. *Mol Biol Cell*. 1999; 10(8):2703-2734.
93. Bracken AP, Ciro M, Cocito A and Helin K. E2F target genes: unraveling the biology. *Trends in Biochemical Sciences*. 2004; 29(8):409-417.
94. Chen HZ, Tsai SY and Leone G. Emerging roles of E2Fs in cancer: an exit from cell cycle control. *Nature Reviews Cancer*. 2009; 9(11):785-797.
95. Swartwout SG and Kinniburgh AJ. C-Myc RNA Degradation in Growing and Differentiating Cells - Possible Alternate Pathways. *Molecular and Cellular Biology*. 1989; 9(1):288-295.
96. Alao JP. The regulation of cyclin D1 degradation: roles in cancer development and the potential for therapeutic invention. *Molecular Cancer*. 2007; 6.

Supplementary Table 1.2 - Glossary (referred to the MIM Fig. 1 and Supplementary Fig. 1.3)

In our MIM network we have represented 15 kinase-related cartouches (kinases can act on more than one protein), 7 known phosphatases have been described independently, and 14 additional phosphatases (each kinase activity has to be equilibrated with a corresponding phosphatase activity) have been grouped together (n. 44 in the Glossary), 1 phospholipase (PLC γ), 31 signaling/adaptor-proteins-related cartouches (for TGF β , WNT and EGF, in each case we have indicated a single molecule as a representative of a family of molecules), 6 small molecules as small rectangular cartouches, 8 white transcription-related cartouches. In the Glossary, we have grouped together three ErbB-family receptors (n. 27 in the Glossary). PIP2 and PIP3 have been grouped together (n. 48 in the Glossary), and GDP and GTP have been grouped together (n. 35 in the Glossary). In conclusion, the Glossary, which includes all the molecules represented in our MIM (colored + white cartouches), only contains 69 numbered items. A total of 85 cartouches are represented in our MIM.

In the signaling network region depicted in our MIM only pathway-involved basic species are represented, not the 447 reactants (complexes) involved in ODEs.

In the Glossary:

Signaling proteins/ adaptor proteins: in **bold**

Kinases/GTPase: underlined

Phosphatases: in **bold italics**

Small Molecules: in italics and underlined

white transcription-related cartouches: in *italics*

phospholipase: **bold** and underlined

1	APC	Adenomatous polyposis coli protein is a tumor suppressor. Promotes rapid degradation of β-Catenin and participates in Wnt signaling as a negative regulator.	MIM's coord. 4,F
2	<u>Akt</u>	The Akt family proteins, also known as protein kinases B (PKB), are serine-threonine protein kinases: they mediate many of the downstream effects of PI3K.	MIM's coord. 2,M
3	AP1	The mammalian Activating Protein-1 proteins are homodimers and heterodimers composed of basic region-leucine zipper (bZIP) proteins that belong to the Jun (c-Jun, JunB and JunD), Fos (c-Fos, FosB, Fra-1 and Fra-2), Jun dimerization partners (JDP1 and JDP2) and the closely related activating transcription factors (ATF2, LRF1/ ATF3 and B-ATF) subfamilies. The AP-1 transcription factors control cell proliferation, survival and death.	MIM's coord. 6, I
4	ARF	The gene CDKN2A (cyclin-dependent kinase inhibitor 2A) generates several transcript variants which differ in their first exons. Three alternatively spliced variants encoding distinct proteins have been reported: two of which, p15INK4b and p16INK4a , encode structurally related isoforms. The remaining transcript includes an alternate first exon located 20 Kb upstream of the remainder of the gene; this transcript contains an alternate open reading frame (ARF) that specifies a protein which is structurally unrelated to the products of the other variants. This ARF product functions as a stabilizer of the tumor suppressor protein p53 as it can interact with, and sequester, the E3 ubiquitin-protein ligase MDM2, a protein responsible for the degradation of p53. Tumor suppressor gene.	MIM's coord. 4, L-M
5	Axin	A scaffold protein that binds directly to many proteins involved in the Wnt signaling pathway and facilitates the phosphorylation of β-Catenin and APC, by GSK3β.	MIM's coord. 4,E-F
6	<u>BRAF</u>	The protein isoform (otherwise known as B-Raf) is a MAP kinase kinase kinase (MAP3K), which functions downstream of the RAS family of membrane associated proteins to which it binds directly.	MIM's coord. 4,I
7	β-catenin	A regulatory protein that integrates cell surface signals with the actin cytoskeleton and transcription factors involved in cell proliferation.	MIM's coord. 5,D-E
8	Cdc25c	The cell division cycle 25 homolog C is a tyrosine phosphatase and belongs to the Cdc25 phosphatase family. When activated dephosphorylates EGFR and is required to control cyclin-dependent kinase (CdK) dephosphorylation and activation..	MIM's coord. 6,G
9	<u>Cdk2</u>	Monomeric CDK is catalytically inactive and require both cyclin association and phosphorylation for full activity. Cyclin-dependent kinase (CDK) forms heterodimers consisting of a proline-directed serine/threonine kinase and a regulatory cyclin subunit. CDK2 is one the major regulators of cell cycle, contributing to induction and/or progression at S phase.	MIM's coord. 7,M-N

10	<u>Cdk4</u>	Cyclin-dependent kinase (CDK) forms heterodimers consisting of a proline-directed serine/threonine kinase and a regulatory cyclin subunit. CDK4 is one of the major regulators of the cell cycle, contributing to induction and/or progression at G1/S transition.	MIM's coord. 6,7,M-N
11	<i>TFBS_{TCF7L2} CCND1/MYC transcription factors binding site</i>	DNA binding sites for transcription factors TCF7L2_BetaCatenin (activating), TCF7L2_BetaCateninY654 (activating), TCF7L2_SMAD4 (activating) and TCF7L2_GROUCHO (inhibitory).	MIM's coord. 9,C
12	<i>TFBS_{SMAD} CCND1/MYC transcription factors binding site</i>	DNA binding sites for transcription factors SMADII-P:SMAD4 (inhibitory) and SMADIPII-P:SMAD4 (inhibitory).	MIM's coord. 9,B-C
13	<i>TFBS_{API} CCND1/MYC transcription factors binding site</i>	DNA binding sites for transcription factors AP1 (activating) and AP1P (activating).	MIM's coord. 9,D-E
14	<i>TFBS_{TP53} CCND1/MYC transcription factors binding site</i>	DNA binding sites for transcription factor TP53(inhibitory).	MIM's coord. 9,E
15	<i>TFBS_{E2F-DP1} CCND1/MYC transcription factors binding site</i>	DNA binding sites for transcription factors E2F:DP1 (activating) and E2F:DP1:pRB (inhibitory).	MIM's coord. 9,F
16	Cyclin D	D-type of cyclins (cyclins D1, D2, and D3) promote cell progression from G1 - S phase by interacting with CDK4 and CDK6.	MIM's coord. 6,M-N
17	<i>CCND1/MYC DNA coding region</i>	RNApol II elongation complex elongates CCND1/MYC mRNA sliding over this region.	MIM's coord. 9,G
18	<i>CCND1/MYC mRNA</i>	CCND1 is a key regulator of G1-to-S phase progression of the cell cycle. The cyclin D1 protein levels are largely controlled at the transcriptional level and by ubiquitin-mediated degradation. cyclin D1 is important for the development and progression of several cancers: it is frequently overexpressed in human cancers. MYC plays a role in cell cycle progression, apoptosis and cellular transformation. It functions as a transcription factor that regulates transcription of specific target genes.	MIM's coord. 9,H-I
19	Cyclin E	cyclin E is a member of the cyclin family which forms a complex with cyclin-dependent kinase (CDK2). Cyclin E/CDK2 regulates multiple cellular processes by phosphorylating numerous downstream proteins.	MIM's coord. 8,M-N

20	<u>DAG</u>	D iacylglycerol functions as a second messenger signaling lipid. DAG stays inside the membrane.	MIM's coord. 2,N-O
21	DP1	Transcription factor Dimerization partner 1. Component of the E2F/DP transcription factor complex. Forms heterodimers with E2F family members, binds DNA cooperatively with E2F family members through the E2 recognition site.	MIM's coord. 8,P
22	Dvl	D ishevelled are scaffold proteins which relays Wnt signals from receptors to downstream effectors.	MIM's coord. 2,E-F
23	E2F	E2F are a family of transcription factors: they play a crucial role in the control of cell cycle. The protein include a DNA binding domain, a dimerization domain which determines interaction with the differentiation regulated transcription factor proteins (DP), a transactivation domain enriched in acidic amino acids, and a tumor suppressor protein association domain which is embedded within the transactivation domain. E2F1-E2F3, have an additional cyclin binding domain.	MIM's coord. 7,P
24	E-Cadherin	Epithelial-Cadherin (Calcium dependent adhesion molecules) is a subclass of type-1 trans- membrane proteins. It plays important roles in cell adhesion.	MIM's coord.1-2,D
25	EGF	Epidermal Growth Factor; belongs to EGF family factors.	MIM's coord. 1,G
26	<i>Elongation complex RNA Pol II</i>	A fully activated RNAPol II complex elongates mRNA.	MIM's coord. 8,G
27	<u>ErbB family receptors</u>	A family of receptor tyrosine kinases (RTKs): ErbB1(v-erb-b1 avian erythroblastic leukemia viral oncogene homolog 1)/EGFR1(Epidermal growth factor receptor 1) is a well known dominant proto-onco-protein; ErbB2/Her2 (Human Epidermal growth factor Receptor 2) /neu (neuro/glioblastoma derived oncogene homolog 2) lacks the capacity to interact with a ligand; ErbB3 is kinase-defective; ErbB4 shares features with ErbB1(not included in the model).	MIM's coord.1-2,G
28	<u>ERK</u>	Extracellular signal-Regulated Kinase or MAPK1 (mitogen-activated protein kinase 1). The activation of this kinase requires its phosphorylation by upstream kinases. Upon activation, this kinase translocates to the nucleus of the stimulated cells, where it phosphorylates nuclear targets.	MIM's coord. 6,I
29	Frz	The F rizzled proteins are seven-pass transmembrane domain cell surface receptors for Wnt ligands, that belong phylogenetically to the large family of G protein-coupled receptors (GPCRs). The mammalian genome harbors 10 frizzled genes.	MIM's coord. 1-2, E

30	GAB1	Belongs to the family of Grb2-associated binder (GAB) adaptor proteins.	MIM's coord. 2,I
31	<u>GAP</u>	A generic GTPase-activating protein (RAS-GAPs) that drastically promotes the weak intrinsic ability of KRAS to hydrolyze GTP and become inactive.	MIM's coord. 3,H-I
32	Grb2	Growth factor receptor-binding protein 2 is an adaptor protein: it plays key roles in signaling downstream of ErbB family receptors.	MIM's coord. 2,G
33	GROUCHO	The protein is the prototype for a large family of co-repressors. As transcriptional co-repressors, Groucho/TLE proteins do not bind to DNA directly, but rather are recruited by DNA-bound repressor proteins.	MIM's coord. 5,C
34	<u>GSK3β</u>	The Glycogen synthase kinase-3 (GSK-3) protein family was originally characterized as a serine/threonine kinase that phosphorylates and inactivates glycogen synthase; it is now implicated in the regulation of several physiological responses in mammalian cells through phosphorylation of many substrates.	MIM's coord. 4,G
35	<u>GTP, GDP</u>	Guanosine-5'-triphosphate is essential to signal transduction, especially with G-proteins, in second-messenger mechanisms where it is converted to guanosine diphosphate) through the action of GTPases	MIM's coord. 2,I
36	<u>IP₃</u>	Inositol trisphosphate together with diacylglycerol (DAG), is a secondary messenger molecule used in signal transduction and lipid signaling in biological cells. IP3 is soluble and diffuses through the cell.	MIM's coord. 2,N
37	KRAS	Small G protein which transmits signals via different effector proteins. RAS-family proteins are well known dominant proto-onco-proteins.	MIM's coord. 2,I
38	LRP5/6	<i>LDL receptor related protein 5 and 6 are co-receptor with Frz in Wnt pathway.</i>	MIM's coord. 2,F
39	MDM2	MDM2 (mouse double-minute 2) belongs to the family of E3 ubiquitin ligases that contain a RING domain and serves as the major E3 ubiquitin ligase for p53 degradationan. MDM2 has potentially oncogenic activity.	MIM's coord. 4,M
40	<u>MEK</u>	MEK kinase or MAP3K (mitogen-activated protein kinase kinase kinase) is a serine/threonine kinase.	MIM's coord. 5,I

41	<i>MKP3</i>	MKP3 is a member of MKPs (MAP Kinase phosphatases), a class of phosphatases with dual-specificity activity toward threonine and tyrosine residues that dephosphorylates and inactivates the MAP kinases.	MIM's coord. 5,H-I
42	<u>NLK</u>	Nemo like kinase is an atypical mitogen-activated protein kinase (MAPK), that belongs to the proline-directed serine/threonine protein kinase superfamily. It phosphorylates several transcription factors: suppresses the transcriptional activity of β -catenin/T-cell factor complex through phosphorylation of TCF/LEF.	MIM's coord. 4,C
43	P16	The gene CDKN2A (cyclin-dependent kinase inhibitor 2A) generates several transcript variants which differ in their first exons. Three alternatively spliced variants encoding distinct proteins have been reported: two of which, p15INK4b and p16INK4a , encode structurally related isoforms known to function as inhibitors of CDK4 kinase.	MIM's coord. 6,N
44	<i>P-ase 1-14</i>	Unknown phosphatases. The effect of a P-kinase has to be balanced by a phosphatase, to avoid shifting of phosphorylated proteins toward a complete and unbalanced phosphorylation.	MIM's coord. 2-6, C-P
45	<u>PDK1</u>	3-phosphoinositide-dependent protein kinase (PDPK) is required for full activation of Akt.	MIM's coord. 3,N
46	<i>PHLPP</i>	The protein phosphatase PHLPP (PH domain leucine-rich repeat protein phosphatase), especially dephosphorylates Akt.	MIM's coord. 2,N
47	<u>PI3K</u>	Phosphoinositide 3-kinases are a family of intracellular lipid kinases that phosphorylate the 3'-hydroxyl group of phosphatidylinositol and phosphoinositides. PI3Ks are classified into classes I, II, and III, based on structure and substrate specificity. Class I PI3Ks phosphorylate phosphatidylinositol-4,5-bisphosphate (PIP_2) to generate phosphatidylinositol-3,4,5-trisphosphate (PIP_3); Class IA PI3Ks are activated by growth factor receptor tyrosine kinases (RTKs) and are heterodimers (regulatory subunit + catalytic subunit).	MIM's coord. 2,L
48	<u>PIP₂, PIP₃</u>	Phosphatidylinositol-3,4-bisphosphate (PtdIns-4,5-P ₂); Phosphatidylinositol 3,4,5-trisphosphate (PtdIns-3,4,5-P ₃). They are defined as second messengers. The concentrations of PIP ₃ and PIP ₂ are regulated at the inner cellular membrane by PI3K and PTEN.	MIM's coord. 2,M-N
49	<i>PK Inactivator</i>	The complex inactivation of PI3K was synthesized as a PK Inactivator function.	MIM's coord. 3,L-M
50	<u>PKC</u>	Protein kinase C is a family of serine- and threonine-specific protein kinases that can be activated by calcium and the second messenger diacylglycerol. PKC family members phosphorylates a wide variety of protein targets and are known to be involved in diverse cellular signaling pathways.	MIM's coord. 2-3,O

51	<i>PLCγ</i>	Phospholipase C gamma binds directly the ErbB family receptors and is activated by their kinase activity: it is implicated in the formation of inositol 1,4,5-triphosphate and generation of a Ca^{2+} response.	MIM's coord. 2,O
52	<i>PPIC</i>	Protein Phosphatase 1C works as a phosphatase of TGF β R-I	MIM's coord. 2,C
53	<i>PPM1A</i>	Protein Phosphatase 1A is a member of the PPM family of monomeric, metal ion-dependent protein serine/threonine phosphatase; it acts as a phosphatase for TGF- β -activated Smad2 and Smad3.	MIM's coord. 5,A
54	<i>pRb</i>	The retinoblastoma protein is a member of the pRB family. The protein is a negative regulator of the cell cycle. The active, hypo-phosphorylated form of the protein binds transcription factor E2F1. Tumor suppressor gene.	MIM's coord. 7,N-O
55	<i>PTEN</i>	Phosphatase and tensin homologue, is a lipid phosphatase and is a ubiquitous regulator of the cellular PI3K signaling pathway. The gene is located on chromosome 10, it can be mutated by deletion, but it can also be hypo-expressed.	MIM's coord. 3,N
56	<i>PTP1B</i>	Protein Tyrosine Phospatase 1B is activated as a hetero-dimer with Cadherin and works as a phosphatase of Y654 of β -catenin.	MIM's coord. 2,D
57	<i>PTPe</i>	Protein tyrosine phosphatase e belongs to a structurally diverse superfamily containing several dozens of membrane-bound or unbound enzymes.	MIM's coord. 3,G
58	<i>Shc</i>	Src homology and collagen-containing protein is an adaptor protein: it plays key roles in signaling downstream of Erb family receptors.	MIM's coord. 3,G
59	<i>Smad2</i>	Belong to a subclass of Smads called receptor regulated Smads (R-Smad) and are transcription factors; these serve principally as substrates for the TGF β receptors. The name Smad (mothers against decapentaplegic homolog) was coined in reference to identification of Smad1 and its sequence similarity to the Sma (the orthologs in <i>C. elegans</i>) and Mad (the orthologs in <i>Drosophila</i>) proteins.	MIM's coord. 2-3,A-B
60	<i>Smad3</i>	Belong to a subclass of Smads called receptor regulated Smads (R-Smad) and are transcription factors; these serve principally as substrates for the TGF β receptors. The name Smad (mothers against decapentaplegic homolog) was coined in reference to identification of Smad1 and its sequence similarity to the Sma (the orthologs in <i>C. elegans</i>) and Mad (the orthologs in <i>Drosophila</i>) proteins.	MIM's coord. 2-3,A-B

61	Smad4	Belongs to a subclass of Smads called co-mediator-Smad (co-Smad) and is a transcription factors.	MIM's coord. 2,C
62	SOS	Son of Sevenless drosophila homolog protein; is a guanine nucleotide exchange factor (GEF) that facilitates dissociation and exchange of bound nucleotides from KRAS. It typically favors the transition from KRAS-GDP to KRAS-GTP.	MIM's coord. 2-3,H
63	TAB2	TAK1-binding protein 2 is a scaffold protein required in several TAK-1 functions.	MIM's coord. 3,D
64	<u>TAK-1</u>	TGF- β activated kinase 1, also known as MEKK7, is a mitogen- activated protein-kinase-kinase kinase (MAP3K). It was originally identified as a kinase involved in TGF- β signaling.	MIM's coord. 3,C
65	TCF7L2	TCF7L2 (transcription factor 7-like 2 (T-cell specific, HMG-box)) also known as TCF4 is a protein acting as a transcription factor. TCF7L2 influencing the transcription of several genes thereby exerting a large variety of functions within the cell.	MIM's coord. 5,C-D
66	TGFβ	The Transforming Growth Factor Beta is a member of the TGF β superfamily of more 30 factors of multifunctional cytokine that regulates biological responses as cell growth, cell cycle progression, differentiation, adhesion, migration and death of target cells, in a developmental context-dependent and cell type-specific manner. Dysfunction of TGF β signaling has been implicated in cancer progression: Because TGF β signaling generally has a negative effect on cell growth, inactivation of this pathway contributes to tumorigenesis.	MIM's coord. 1,B-C
67	<u>TGFβR-I/ TGFβR-II</u>	The effects of TGF β are mediated through type I and type II receptors, which are transmembrane proteins possessing cytoplasmic serine/threonine kinase domains for signal propagation.	MIM's coord. 1-2,B-C
68	TP53	TP53 is a transcription factor whose protein levels and post-translational modification state alter in response to cellular stress. Acts as a tumor suppressor in many tumor types; induces growth arrest or apoptosis depending on the physiological circumstances and cell type.	MIM's coord. 5, N
69	Wnt	<i>Wingless/Int-1</i> (Wnt) is a large family of 19 human highly conserved secreted glycoproteins that play fundamental roles in controlling cell proliferation, cell-fate determination, and differentiation during embryonic development and adult homeostasis.	MIM's coord. 1, E

Oncoprotein inhibitors		
	AZAKENPAULLONE	1-Azakenpaullone is a selective inhibitor of glycogen synthase kinase 3 β (GSK3 β) with 100-fold less cross-reactivity against CDKs.
	CI-1040	CI-1040 (PD184352) is an ATP non-competitive MEK1/2 inhibitor. CI-1040 is a highly specific, small-molecule inhibitor of one of the key components of the MAPK pathway (MEK1/MEK2), and thereby effectively blocks the phosphorylation of ERK and continued signal transduction through this pathway.
	PERIFOSINE	Perifosine is an alkyl-phosphocholine compound which greatly hampers translocation of Akt to the cell membrane, where Thr308- and Ser473-directed kinases normally activate Akt. Perifosine is undergoing its Phase III clinical trials for the treatment of refractory multiple myeloma, in combination with a placebo, and is in Phase II trials for several other cancers.
	PI103	PI-103 is a potent, ATP-competitive PI3K inhibitor of DNA-PK, p110 α , mTORC1, PI3KC2 β , p110 δ , mTORC2, p110 β , and p110 γ .
	XAV939	XAV939 is a trifluoromethylphenylpyrimidine derivative. XAV939 can prolong the half-life of axin and promote β -catenin degradation through inhibiting tankyrase. TNKS1 and TNKS2 modify axin substrate through the addition of several ADP-ribose units, referred to as poly-ADP-ribosylation (PARsylation).

<http://www.ncbi.nlm.nih.gov/gene/>

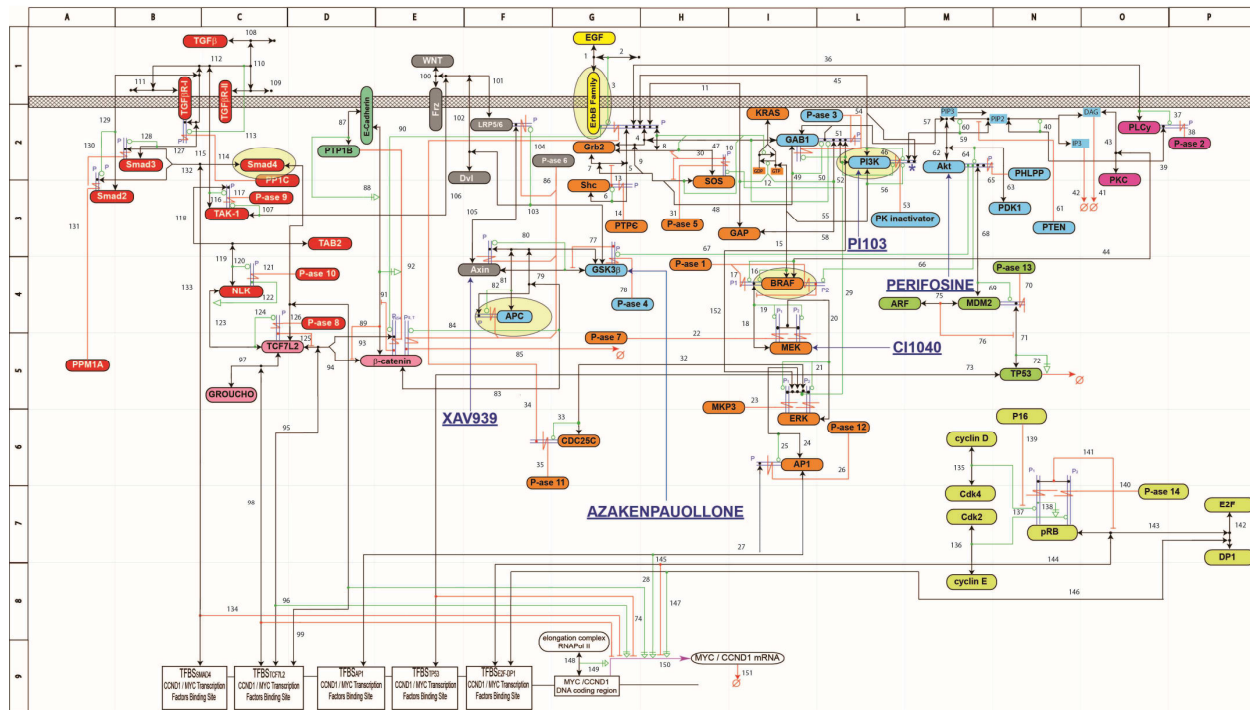
<http://www.genecards.org/>

<http://www.uniprot.org>

Fact Sheet of the inhibitor drugs

References in the Annotation List

Supplementary Figure 1.3 – Molecular Interaction Map (MIM) referred to HT29



Supplementary Fig. (1.3): Molecular Interaction Map (MIM) referred to HT29. Molecular Interaction Map (MIM) referring to the pathways downstream of the TGF β -family, WNT-family and EGF-family proteins, pathways which are relevant in colorectal cancer. The cartouches of mutated / altered signaling-proteins in the HT29 cell line have been surrounded by an oval.

Supplementary Table 1.4 - Pathways present in our MIMs	
1	ErbB-family receptors – PI3K – PTEN – Akt – GSK3 β – APC – β -catenin – TCF7L2 — TFBS _{TCF7L2} (TCF7L2 binding site), transcription agonist
2	ErbB-family receptors – Grb2 – Shc – SOS– GAP– KRAS – BRAF – MEK – ERK- AP1 – AP1 binding site – TFBS _{AP1} , transcription agonist
3	ErbB-family receptors-E-Cadherin (Cadherin/Catenin adhesive complex);
4	ErbB-family receptors – PLC γ – PIP2 – PKC – BRAF – MEK – ERK - AP1– TFBS _{AP1} (AP1 binding sites), transcription agonist, (the terminal parts of pathway 2 and 4 are the same)
5	WNT – Frz/LRP5/6 – Dvl – AXIN – APC – GSK3 β – β -catenin – TCF7L2 — TFBS _{TCF7L2}
6	TGF β -receptors – SMAD2/3 – SMAD4 – TFBS _{SMAD4} (SMAD4 binding site), transcription antagonist
7	TGF β -receptors – TAK-1 – TAB2 – NLK – TCF7L2 –TFBS _{TCF7L2} , converging with 8
8	WNT – Frz/LRP5/6 – TAK-1 – TAB2 – NLK – TCF7L2 — TFBS _{TCF7L2} , converging with 7
9	Akt – MDM2 – TP53 – TFBS _{TP53} (TP53 binding site)
10	Cyclin (D/E) / CDK (2/4) – pRB – E2F:DP – TFBS _{E2F:DP1} (E2F:DP1 binding site).

Supplementary Table 1.4: Simplified description of the pathways involved in our MIMs

Supplementary Table 2.1 - Reaction list

Supplementary Table 2.1 shows a list of 348 protein-protein-interaction reactions (348 association reactions + 348 dissociation reactions) and 174 catalytic reactions, rate-constants included, which represent the complete set of our dynamic simulations. $348 + 348 + 174$ gives a total of 870 reactions.

We derived our list of reactions from the literature. The references associated with the Supplementary Material 1.1 - Annotation List give information about all the interactions described in our MIM. These references were utilized for preliminary extrapolations of kinetic parameters, in a patient patchwork of readjustments, to reconstruct a reasonable global dynamic behavior. The references associated with the Annotation List are the main direct / indirect source of the concentrations and reactions data involved in training the modeling of our MIM. Additional references are listed below.

	Chemical Reactions	Kinetic costants	Reaction Rates	Kinetic costant values	Units	Extrapolations from Annotation List References (SI.I) + Notes / Ref. listed below
1	R + EGF \leftrightarrow RI	c1f	c1f*R*EGF - c1r*RI	0.01	nM ⁻¹ .s ⁻¹	1 - 3 (SI.I) + [1-8]
2	R + EGF \leftrightarrow RI	c1r		1	s ⁻¹	1 - 3 (SI.I) + [1-8]
3	RI + RI \leftrightarrow RI2	c2f	c2f*RI*RI - c2r*RI2	0.01	nM ⁻¹ .s ⁻¹	1 - 3 (SI.I) + [1-8]
4	RI + RI \leftrightarrow RI2	c2r		0.1	s ⁻¹	1 - 3 (SI.I) + [1-8]
5	RI2 \rightarrow RI2P	c3f	c3f*RI2	1	s ⁻¹	1 - 3 (SI.I) + [1-8]
6	RP + PLCy \leftrightarrow RP_PL	c5f	c5f*RP*PLCy - c5r*RP_PL	0.06	nM ⁻¹ .s ⁻¹	1 - 3 (SI.I) + [1-8]
7	RP + PLCy \leftrightarrow RP_PL	c5r		0.2	s ⁻¹	1 - 3 (SI.I) + [1-8]
8	RP_PL \rightarrow RP_PLP	c6f	c6f*RP_PL	1	s ⁻¹	1 - 3 (SI.I) + [1-8]
9	RP_PLP \leftrightarrow RP + PLCyP	c7f		0.3	s ⁻¹	1 - 3 (SI.I) + [1-8]
10	RP_PLP \leftrightarrow RP + PLCyP	c7r	c7f*RP_PLP - c7r*RP*PLCyP	0.006	nM ⁻¹ .s ⁻¹	1 - 3 (SI.I) + [1-8]
11	RP + Grb \leftrightarrow RP_G	c10f	c10f*RP*Grb - c10r*RP_G	0.0015	nM ⁻¹ .s ⁻¹	1 - 5 (SI.I) + [1-9]
12	RP + Grb \leftrightarrow RP_G	c10r		0.2	s ⁻¹	1 - 5 (SI.I) + [1-9]
13	RP_G + SOS \leftrightarrow RP_G_S	c11f	c11f*RP_G*SOS - c11r*RP_G_S	0.01	nM ⁻¹ .s ⁻¹	1 - 6 (SI.I) + [1-9]
14	RP_G + SOS \leftrightarrow RP_G_S	c11r		0.06	s ⁻¹	1 - 6 (SI.I) + [1-9]
15	RP_G_S \leftrightarrow RP + G_S	c12f	c12f*RP_G_S - c12r*RP*G_S	0.15	s ⁻¹	1 - 6 (SI.I) + [1-9]

16	RP_G_S <-> RP + G_S	c12r		0.0028	nM ⁻¹ .s ⁻¹	1 - 6 (SI.I) + [1-9]
17	G_S <-> Grb + SOS	c13f	c13f*G_S - c13r*Grb*SOS	0.0015	s ⁻¹	1 - 6 (SI.I) + [1-9]
18	G_S <-> Grb + SOS	c13r		0.0001	nM ⁻¹ .s ⁻¹	1 - 6 (SI.I) + [1-9]
19	RP + Shc <-> RP_Sh	c14f	c14f*RP*Shc - c14r*RP_Sh	0.09	nM ⁻¹ .s ⁻¹	1 - 5 (SI.I) + [1-9]
20	RP + Shc <-> RP_Sh	c14r		0.6	s ⁻¹	1 - 5 (SI.I) + [1-9]
21	RP_Sh -> RP_ShP	c15	c15*RP_Sh	6	s ⁻¹	1 - 5 (SI.I) + [1-9]
22	RP_ShP <-> ShP + RP	c16f		0.3	s ⁻¹	1 - 5 (SI.I) + [1-9]
23	RP_ShP <-> ShP + RP	c16r	c16f*RP_ShP - c16r*ShP*RP	0.0009	nM ⁻¹ .s ⁻¹	1 - 5 (SI.I) + [1-9]
24	RP_ShP + Grb <-> RP_ShP_G	c17f	c17f*RP_ShP*Grb - c17r*RP_ShP_G	0.003	nM ⁻¹ .s ⁻¹	1 - 5 (SI.I) + [1-9]
25	RP_ShP + Grb <-> RP_ShP_G	c17r		0.1	s ⁻¹	1 - 5 (SI.I) + [1-9]
26	RP_ShP_G <-> RP + ShP_G	c18f	c18f*RP_ShP_G - c18r*RP*ShP_G	0.3	s ⁻¹	1 - 5 (SI.I) + [1-9]
27	RP_ShP_G <-> RP + ShP_G	c18r		0.0009	nM ⁻¹ .s ⁻¹	1 - 5 (SI.I) + [1-9]
28	RP_ShP_G + SOS <-> RP_ShP_G_S	c19f	c19f*RP_ShP_G*SOS - c19r*RP_ShP_G_S	0.01	nM ⁻¹ .s ⁻¹	1 - 6 (SI.I) + [1-9]
29	RP_ShP_G + SOS <-> RP_ShP_G_S	c19r		0.0214	s ⁻¹	1 - 6 (SI.I) + [1-9]
30	RP_ShP_G_S <-> ShP_G_S + RP	c20f	c20f*RP_ShP_G_S - c20r*ShP_G_S*RP	0.12	s ⁻¹	1 - 6 (SI.I) + [1-9]
31	RP_ShP_G_S <-> ShP_G_S + RP	c20r		0.00024	nM ⁻¹ .s ⁻¹	1 - 6, 9 (SI.I) + [1-9]
32	ShP_G + SOS <-> ShP_G_S	c21f	c21f*ShP_G*SOS - c21r*ShP_G_S	0.03	nM ⁻¹ .s ⁻¹	4 - 6, 9, 24 (SI.I) + [1-9]
33	ShP_G + SOS <-> ShP_G_S	c21r		0.064	s ⁻¹	4 - 6, 9, 24 (SI.I) + [1-9]
34	ShP + Grb <-> ShP_G	c22f	c22f*ShP*Grb - c22r*ShP_G	0.003	nM ⁻¹ .s ⁻¹	4 - 6, 9, 24 (SI.I) + [1-9]
35	ShP + Grb <-> ShP_G	c22r		0.1	s ⁻¹	4 - 6, 9, 24 (SI.I) + [1-9]
36	ShP_G_S <-> ShP + G_S	c24f	c24f*ShP_G_S - c24r*ShP*G_S	0.1	s ⁻¹	4 - 6, 9, 24 (SI.I) + [1-9]
37	ShP_G_S <-> ShP + G_S	c24r		0.021	nM ⁻¹ .s ⁻¹	4 - 6, 9, 24 (SI.I) + [1-9]
38	RP_ShP + G_S <-> RP_ShP_G_S	c25f	c25f*RP_ShP*G_S - c25r*RP_ShP_G_S	0.009	nM ⁻¹ .s ⁻¹	1 - 6, 9, 24 (SI.I) + [1-9]
39	RP_ShP + G_S <-> RP_ShP_G_S	c25r		0.0429	s ⁻¹	1 - 6, 9, 24 (SI.I) + [1-9]
40	Ras_GDP <-> Ras + GDP	c26f	c26f*Ras_GDP - c26r*Ras*GDP	0.0000054	s ⁻¹	1 - 8 (SI.I) + [1-11]
41	Ras_GDP <-> Ras + GDP	c26r		0.00027	nM ⁻¹ .s ⁻¹	1 - 8 (SI.I) + [1-11]
42	Ras + GTP <-> Ras_GTP	c27f	c27f*Ras*GTP - c27r*Ras_GTP	0.078	nM ⁻¹ .s ⁻¹	1 - 8 (SI.I) + [1-11]
43	Ras + GTP <-> Ras_GTP	c27r		0.00078	s ⁻¹	1 - 8 (SI.I) + [1-11]
44	Ras_GTP -> Ras_GDP	c28	c28*Ras_GTP	0.00001	s ⁻¹	1 - 8 (SI.I) + [1-11]
45	RP_ShP_G_S + Ras_GDP <-> RP_ShP_G_S_Ras_GDP	c29f	c29f*RP_ShP_G_S*Ras_GDP - c29r*RP_ShP_G_S_Ras_GDP	0.00475	nM ⁻¹ .s ⁻¹	1 - 8 (SI.I) + [1-11]

46	RP_ShP_G_S + Ras_GDP <-> RP_ShP_G_S_Ras_GDP	c29r		0.76	s ⁻¹	1 - 8 (SI.I) + [1-11]
47	RP_ShP_G_S_Ras_GDP <-> RP_ShP_G_S_Ras + GDP	c30f	c30f*RP_ShP_G_S_Ras_GDP - c30r*RP_ShP_G_S_Ras*GDP	46.5	s ⁻¹	1 - 8 (SI.I) + [1-11]
48	RP_ShP_G_S_Ras_GDP <-> RP_ShP_G_S_Ras + GDP	c30r		0.093	nM ⁻¹ .s ⁻¹	1 - 8 (SI.I) + [1-11]
49	RP_ShP_G_S_Ras + GTP <-> RP_ShP_G_S_Ras GTP	c31f	c31f*RP_ShP_G_S_Ras*GTP - c31r*RP_ShP_G_S_Ras_GTP	0.003	nM ⁻¹ .s ⁻¹	1 - 8 (SI.I) + [1-11]
50	RP_ShP_G_S_Ras + GTP <-> RP_ShP_G_S_Ras GTP	c31r		2.4	s ⁻¹	1 - 8 (SI.I) + [1-11]
51	RP_ShP_G_S_Ras_GTP <-> RP_ShP_G_S + Ras_GTP	c32f	c32f*RP_ShP_G_S_Ras_GTP - c32r*RP_ShP_G_S*Ras_GTP	806.4	s ⁻¹	1 - 8 (SI.I) + [1-11]
52	RP_ShP_G_S_Ras_GTP <-> RP_ShP_G_S + Ras_GTP	c32r		1.575	nM ⁻¹ .s ⁻¹	1 - 8 (SI.I) + [1-11]
53	RP_ShP_G_S + Ras <-> RP_ShP_G_S_Ras	c33f	c33f*RP_ShP_G_S*Ras - c33r*RP_ShP_G_S_Ras	0.15625	nM ⁻¹ .s ⁻¹	1 - 8 (SI.I) + [1-11]
54	RP_ShP_G_S + Ras <-> RP_ShP_G_S_Ras	c33r		0.001	s ⁻¹	1 - 8 (SI.I) + [1-11]
55	RP_G_S + Ras_GDP <-> RP_G_S_Ras_GDP	c34f	c34f*RP_G_S*Ras_GDP - c34r*RP_G_S_Ras_GDP	0.0075	nM ⁻¹ .s ⁻¹	1 - 8 (SI.I) + [1-11]
56	RP_G_S + Ras_GDP <-> RP_G_S_Ras_GDP	c34r		1.2	s ⁻¹	1 - 8 (SI.I) + [1-11]
57	RP_G_S_Ras_GDP <-> RP_G_S_Ras + GDP	c35f	c35f*RP_G_S_Ras_GDP - c35r*RP_G_S_Ras*GDP	50	s ⁻¹	1 - 8 (SI.I) + [1-11]
58	RP_G_S_Ras_GDP <-> RP_G_S_Ras + GDP	c35r		0.1	nM ⁻¹ .s ⁻¹	1 - 8 (SI.I) + [1-11]
59	RP_G_S_Ras + GTP <-> RP_G_S_Ras_GTP	c36f	c36f*RP_G_S_Ras*GTP - c36r*RP_G_S_Ras_GTP	0.1	nM ⁻¹ .s ⁻¹	1 - 8 (SI.I) + [1-11]
60	RP_G_S_Ras + GTP <-> RP_G_S_Ras_GTP	c36r		80	s ⁻¹	1 - 8 (SI.I) + [1-11]
61	RP_G_S_Ras_GTP <-> RP_G_S + Ras_GTP	c37f	c37f*RP_G_S_Ras_GTP - c37r*RP_G_S*Ras_GTP	640	s ⁻¹	1 - 8 (SI.I) + [1-11]
62	RP_G_S_Ras_GTP <-> RP_G_S + Ras_GTP	c37r		1.25	nM ⁻¹ .s ⁻¹	1 - 8 (SI.I) + [1-11]
63	RP_G_S + Ras <-> RP_G_S_Ras	c38f	c38f*RP_G_S*Ras - c38r*RP_G_S_Ras	0.25	nM ⁻¹ .s ⁻¹	1 - 8 (SI.I) + [1-11]
64	RP_G_S + Ras <-> RP_G_S_Ras	c38r		0.0016	s ⁻¹	1 - 8 (SI.I) + [1-11]
65	Raf + Ras_GTP <-> Raf_Ras_GTP	c39f	c39f*Raf*Ras_GTP - c39r*Raf_Ras_GTP	0.01	nM ⁻¹ .s ⁻¹	6 - 8, 11 - 14 (SI.I) + [1-11]
66	Raf + Ras_GTP <-> Raf_Ras_GTP	c39r		0.0053	s ⁻¹	6 - 8, 11 - 14 (SI.I) + [1-11]
67	Raf_Ras_GTP -> [Raf] + Ras_GTP	c40f	c40f*Raf_Ras_GTP	1	s ⁻¹	6 - 8, 11 - 14 (SI.I) + [1-11]
68	[Raf] + Pase1 <-> [Raf_Pase1]	c41f	c41f*[Raf*]*Pase1 - c41r*[Raf*__Pase1)	0.0717	nM ⁻¹ .s ⁻¹	11 - 14 (SI.I) + [1,4-9]
69	[Raf] + Pase1 <-> [Raf_Pase1]	c41r		0.2	s ⁻¹	11 - 14 (SI.I) + [1,4-9]
70	[Raf_Pase1] -> Raf + Pase1	c42	c42*[Raf*__Pase1)	1	s ⁻¹	11 - 14 (SI.I) + [1,4-9]
71	MEK + [Raf] <-> [MEK_Raf]	c43f		0.01	nM ⁻¹ .s ⁻¹	11 - 14 (SI.I) + [1,4-9]

72	MEK + [Raf] <-> [MEK_Raf]	c43r	c43f*MEK*[Raf*] - c43r*[MEK_Raf*]	0.1	s ⁻¹	11 – 14 (SI.I) + [1,4-9]
73	[MEK_Raf] -> [Raf] + MEKP	c44	c44*[MEK_Raf*)	1	s ⁻¹	11 – 14 (SI.I) + [1,4-9]
74	MEKP + [Raf] <-> [MEKP_Raf]	c45f	c45f*MEKP*[Raf*] - c45r*[MEKP_Raf*)	0.01	nM ^{-1.s⁻¹}	11 – 14 (SI.I) + [1,4-9]
75	MEKP + [Raf] <-> [MEKP_Raf]	c45r		0.1	s ⁻¹	11 – 14 (SI.I) + [1,4-9]
76	[MEKP_Raf] -> MEKPP + [Raf]	c46	c46*[MEKP_Raf*)	1	s ⁻¹	11 – 14 (SI.I) + [1,4-9]
77	MEKPP + Pase2 <-> MEKPP_Pase2	c47f	c47f*MEKPP*Pase2 - c47r*MEKPP_Pase2	0.01	nM ^{-1.s⁻¹}	11 – 14 (SI.I) + [1,4-9]
78	MEKPP + Pase2 <-> MEKPP_Pase2	c47r		0.1	s ⁻¹	11 – 14 (SI.I) + [1,4-9]
79	MEKPP_Pase2 -> MEKP + Pase2	c48	c48*MEKPP_Pase2	0.1	s ⁻¹	11 – 14 (SI.I) + [1,4-9]
80	MEKP + Pase2 <-> MEKP_Pase2	c49f	c49f*MEKP*Pase2 - c49r*MEKP_Pase2	0.01	nM ^{-1.s⁻¹}	11 – 14 (SI.I) + [1,4-9]
81	MEKP + Pase2 <-> MEKP_Pase2	c49r		0.1	s ⁻¹	11 – 14 (SI.I) + [1,4-9]
82	MEKP_Pase2 -> MEK + Pase2	c50	c50*MEKP_Pase2	0.1	s ⁻¹	11 – 14 (SI.I) + [1,4-9]
83	ERK + MEKPP <-> ERK_MEKPP	c51f	c51f*ERK*MEKPP - c51r*ERK_MEKPP	0.01	nM ^{-1.s⁻¹}	11 – 14 (SI.I) + [1,4-9]
84	ERK + MEKPP <-> ERK_MEKPP	c51r		0.0033	s ⁻¹	11 – 14 (SI.I) + [1,4-9]
85	ERK_MEKPP -> ERKP + MEKPP	c52	c52*ERK_MEKPP	16	s ⁻¹	11 – 14 (SI.I) + [1,4-9]
86	ERKP + MEKPP <-> ERKP_MEKPP	c53f	c53f*ERKP*MEKPP - c53r*ERKP_MEKPP	0.01	nM ^{-1.s⁻¹}	11 – 14 (SI.I) + [1,4-9]
87	ERKP + MEKPP <-> ERKP_MEKPP	c53r		0.0033	s ⁻¹	11 – 14 (SI.I) + [1,4-9]
88	ERKP_MEKPP -> ERKPP + MEKPP	c54	c54*ERKP_MEKPP	5.7	s ⁻¹	11 – 14 (SI.I) + [1,4-9]
89	ERKPP + Pase3 <-> ERKPP_Pase3	c55f	c55f*ERKPP*Pase3 - c55r*ERKPP_Pase3	0.0145	nM ^{-1.s⁻¹}	11 – 14 (SI.I) + [1,4-9]
90	ERKPP + Pase3 <-> ERKPP_Pase3	c55r		0.6	s ⁻¹	11 – 14 (SI.I) + [1,4-9]
91	ERKPP_Pase3 -> ERKP + Pase3	c56	c56*ERKPP_Pase3	0.27	s ⁻¹	11 – 14 (SI.I) + [1,4-9]
92	ERKP + Pase3 <-> ERKP_Pase3	c57f	c57f*ERKP*Pase3 - c57r*ERKP_Pase3	0.05	nM ^{-1.s⁻¹}	11 – 14 (SI.I) + [1,4-9]
93	ERKP + Pase3 <-> ERKP_Pase3	c57r		0.5	s ⁻¹	11 – 14 (SI.I) + [1,4-9]
94	ERKP_Pase3 -> ERK + Pase3	c58	c58*ERKP_Pase3	0.3	s ⁻¹	11 – 14 (SI.I) + [1,4-9]
95	GAP + RP <-> RP_GAP	c59f	c59f*GAP*RP - c59r*RP_GAP	0.083	nM ^{-1.s⁻¹}	6 - 8 (SI.I) + [1,5,11]
96	GAP + RP <-> RP_GAP	c59r		0.15	s ⁻¹	6 - 8 (SI.I) + [1,5,11]
97	Ras_GTP + RP_GAP <-> RP_GAP_Ras_GTP	c60f	c60f*Ras_GTP*RP_GAP - c60r*RP_GAP_Ras_GTP	0.01	nM ^{-1.s⁻¹}	6 - 8 (SI.I) + [1,5,11]
98	Ras_GTP + RP_GAP <-> RP_GAP_Ras_GTP	c60r		0.03	s ⁻¹	6 - 8 (SI.I) + [1,5,11]
99	RP_GAP_Ras_GTP -> RP_GAP + Ras_GDP	c61	c61*RP_GAP_Ras_GTP	1.494	s ⁻¹	6 - 8 (SI.I) + [1,5,11]
100	RP_ShP_G_S + ERKPP <-> RP_ShP_G_S_ERKPP	c70f	c70f*RP_ShP_G_S*ERKPP - c70r*RP_ShP_G_S_ERKPP	0.01	nM ^{-1.s⁻¹}	11, 24, 25 (SI.I) + [1,5,12-13]

101	RP_ShP_G_S + ERKPP <-> RP_ShP_G_S_ERKPP	c70r		0.033	s ⁻¹	11, 24, 25 (SI.I) + [1,5,12-13]
102	RP_ShP_G_S_ERKPP -> RP_ShP_G + ERKPP + SOSP	c71	c71*RP_ShP_G_S_ERKPP	1	s ⁻¹	11, 24, 25 (SI.I) + [1,5,12-13]
103	RP_G_S + ERKPP <-> RP_G_S_ERKPP	c72f	c72f*RP_G_S*ERKPP - c72r*RP_G_S_ERKPP	0.01	nM ⁻¹ .s ⁻¹	11, 24, 25 (SI.I) + [1,5,12-13]
104	RP_G_S + ERKPP <-> RP_G_S_ERKPP	c72r		0.033	s ⁻¹	11,24, 25 (SI.I) + [1,5,12-13]
105	RP_G_S_ERKPP -> RP_G + SOSP + ERKPP	c73	c73*RP_G_S_ERKPP	1	s ⁻¹	11, 24, 25 (SI.I) + [1,5,12-13]
106	SOSP + Pase5 <-> SOSP_Pase5	c74f	c74f*SOSP*Pase5 - c74r*SOSP_Pase5	0.01	nM ⁻¹ .s ⁻¹	11, 24 - 25 (SI.I) + [1,5,13]
107	SOSP + Pase5 <-> SOSP_Pase5	c74r		0.1	s ⁻¹	11, 24 - 25 (SI.I) + [12-13]
108	SOSP_Pase5 -> SOS + Pase5	c75	c75*SOSP_Pase5	1	s ⁻¹	11, 24 - 25 (SI.I) + [12-13]
109	RP_G + GAB <-> RP_G_GAB	c76f	c76f*RP_G*GAB - c76r*RP_G_GAB	0.01	nM ⁻¹ .s ⁻¹	33 (SI.I) + [1,9]
110	RP_G + GAB <-> RP_G_GAB	c76r		1	s ⁻¹	33 (SI.I) + [1,9]
111	RP_ShP_G + GAB <-> RP_ShP_G_GAB	c77f	c77f*RP_ShP_G*GAB - c77r*RP_ShP_G_GAB	0.01	nM ⁻¹ .s ⁻¹	33 (SI.I) + [1,9]
112	RP_ShP_G + GAB <-> RP_ShP_G_GAB	c77r		1	s ⁻¹	33 (SI.I) + [1,9]
113	RP_G_GAB -> RP_G_GABP	c78	c78*RP_G_GAB	0.05	s ⁻¹	33 (SI.I) + [1,9]
114	RP_ShP_G_GAB -> RP_ShP_G_GABP	c79	c79*RP_ShP_G_GAB	0.05	s ⁻¹	33 (SI.I) + [1,9]
115	RP_G_GABP + PI3K <-> RP_G_GABP_PK	c80f	c80f*RP_G_GABP*PI3K - c80r*RP_G_GABP_PK	0.01	nM ⁻¹ .s ⁻¹	31 - 33 (SI.I) + [1,9]
116	RP_G_GABP + PI3K <-> RP_G_GABP_PK	c80r		1	s ⁻¹	31 - 33 (SI.I) + [12-13]
117	RP_G_GABP_PK -> RP_G_GABP_PKP	c82	c82*RP_G_GABP_PK	1	s ⁻¹	31 - 33 (SI.I) + [12-13]
118	RP_ShP_G_GABP + PI3K <-> RP_ShP_G_GABP_PK	c81f	c81f*RP_ShP_G_GABP*PI3K - c81r*RP_ShP_G_GABP_PK	0.01	nM ⁻¹ .s ⁻¹	31 - 33 (SI.I) + [12-13]
119	RP_ShP_G_GABP + PI3K <-> RP_ShP_G_GABP_PK	c81r		1	s ⁻¹	31 - 33 (SI.I) + [12-13]
120	RP_ShP_G_GABP_PK -> RP_ShP_G_GABP_PKP	c83	c83*RP_ShP_G_GABP_PK	1	s ⁻¹	31 - 33 (SI.I) + [12-13]
121	RP_ShP_G_GABP + GAP <-> RP_ShP_G_GABP_GAP	c84f	c84f*RP_ShP_G_GABP*GAP - c84r*RP_ShP_G_GABP_GAP	0.083	nM ⁻¹ .s ⁻¹	33 (SI.I) + [12-13]
122	RP_ShP_G_GABP + GAP <-> RP_ShP_G_GABP_GAP	c84r		0.15	s ⁻¹	33 (SI.I) + [1,5,11]
123	RP_G_GABP + GAP <-> RP_G_GABP_GAP	c85f	c85f*RP_G_GABP*GAP - c85r*RP_G_GABP_GAP	0.083	nM ⁻¹ .s ⁻¹	33 (SI.I) + [1,5,11]
124	RP_G_GABP + GAP <-> RP_G_GABP_GAP	c85r		0.15	s ⁻¹	33 (SI.I) + [1,5,11]

125	RP_G_GABP_GAP + Ras_GTP <-> RP_G_GABP_GAP_Ras_GTP	c86f	c86f*RP_G_GABP_GAP*Ras_GTP - c86r*RP_G_GABP_GAP_Ras_GTP	0.6225	nM ⁻¹ .s ⁻¹	7, 8, 33 (SI.I) + [1,5,11]
126	RP_G_GABP_GAP + Ras_GTP <-> RP_G_GABP_GAP_Ras_GTP	c86r		0.3	s ⁻¹	7, 8, 33 (SI.I) + [1,5,11]
127	RP_G_GABP_GAP_Ras_GTP -> RP_G_GABP_GAP + Ras_GDP	c87	c87*RP_G_GABP_GAP_Ras_GTP	1.494	s ⁻¹	7, 8, 33 (SI.I) + [1,5,11]
128	RP_ShP_G_GABP_GAP + Ras_GTP <-> RP_ShP_G_GABP_GAP_Ras_GTP	c88f	c88f*RP_ShP_G_GABP_GAP*Ras_GTP - c88r*RP_ShP_G_GABP_GAP_Ras_GTP	0.6225	nM ⁻¹ .s ⁻¹	7, 8, 33 (SI.I) + [1,5,11]
129	RP_ShP_G_GABP_GAP + Ras_GTP <-> RP_ShP_G_GABP_GAP_Ras_GTP	c88r		0.3	s ⁻¹	7, 8, 33 (SI.I) + [1,5,11]
130	RP_ShP_G_GABP_GAP_Ras_GTP -> RP_ShP_G_GABP_GAP + Ras_GDP	c89	c89*RP_ShP_G_GABP_GAP_Ras_GTP	1.494	s ⁻¹	7, 8, 33 (SI.I) + [1,5,11]
131	RP + PI3K <-> RP_PK	c90f	c90f*RP*PI3K - c90r*RP_PK	0.01	nM ⁻¹ .s ⁻¹	1 - 3, 31, 32 (SI.I) + [12-13]
132	RP + PI3K <-> RP_PK	c90r		1	s ⁻¹	1 - 3, 31, 32 (SI.I) + [12-13]
133	RP_PK -> RP_PKP	c91	c91*RP_PK	1	s ⁻¹	1 - 3, 31, 32 (SI.I) + [12-13]
134	RP + PKP <-> RP_PKP	c92r	c92f*RP*PKP - c92r*RP_PKP	0.1	s ⁻¹	1 - 3, 31, 32 (SI.I) + [12-13]
135	RP + PKP <-> RP_PKP	c92f		0.01	nM ⁻¹ .s ⁻¹	1 - 3, 31, 32 (SI.I) + [12-13]
136	PIP3 + PTEN <-> PIP3_PTEN	c93f	c93f*PIP3*PTEN - c93r*PIP3_PTEN	0.01	nM ⁻¹ .s ⁻¹	31, 32 (SI.I) + [1-9]
137	PIP3 + PTEN <-> PIP3_PTEN	c93r		0.01	s ⁻¹	31, 32 (SI.I)) + [1-9]
138	PIP3_PTEN -> PIP2 + PTEN	c94	c94*PIP3_PTEN	20	s ⁻¹	31, 32 (SI.I) + [1-9]
139	PKP + PIP2 <-> PKP_PIP2	c95f	c95f*PKP*PIP2 - c95r*PKP_PIP2	0.01	nM ⁻¹ .s ⁻¹	31, 32 (SI.I) + [1-9]
140	PKP + PIP2 <-> PKP_PIP2	c95r		0.035	s ⁻¹	31, 32 (SI.I) + [1-9]
141	PKP_PIP2 -> PKP + PIP3	c96	c96*PKP_PIP2	2.5	s ⁻¹	31, 32 (SI.I) + [1-9]
142	RP_ShP_G_GABP + PhoA <-> RP_ShP_G_GABP_PhоА	c98f	c98f*RP_ShP_G_GABP*PhoA - c98r*RP_ShP_G_GABP_PhоА	0.001	nM ⁻¹ .s ⁻¹	33 (SI.I) + [1-9]
143	RP_ShP_G_GABP + PhoA <-> RP_ShP_G_GABP_PhоА	c98r		0.1	s ⁻¹	33 (SI.I) + [1-9]
144	RP_ShP_G_GABP_PhоA -> RP_ShP_G_GAB + PhoA	c100	c100*RP_ShP_G_GABP_PhоA	0.03	s ⁻¹	33 (SI.I) + [1-9]
145	RP_G_GABP + PhoA <-> RP_G_GABP_PhоA	c99f	c99f*RP_G_GABP*PhoA - c99r*RP_G_GABP_PhоA	0.001	nM ⁻¹ .s ⁻¹	33 (SI.I) + [1-9]
146	RP_G_GABP + PhoA <-> RP_G_GABP_PhоA	c99r		0.1	s ⁻¹	33 (SI.I) + [1-9]
147	RP_G_GABP_PhоA -> RP_G_GAB + PhoA	c101	c101*RP_G_GABP_PhоA	0.03	s ⁻¹	33 (SI.I) + [1-9]

148	RP_G_GABP_PKP + PIP2 <-> RP_G_GABP_PKP_PIP2	c102f	c102f*RP_G_GABP_PKP*PIP2 - c102r*RP_G_GABP_PKP_PIP2	6.25	nM ⁻¹ .s ⁻¹	33 (SI.I) + [1-9]
149	RP_G_GABP_PKP + PIP2 <-> RP_G_GABP_PKP_PIP2	c102r		3.5	s ⁻¹	33 (SI.I) + [1-9]
150	RP_ShP_G_GABP_PKP + PIP2 <-> RP_ShP_G_GABP_PKP_PIP2	c103f	c103f*RP_ShP_G_GABP_PKP*PIP2 - c103r*RP_ShP_G_GABP_PKP_PIP2	6.25	nM ⁻¹ .s ⁻¹	33 (SI.I) + [1-9]
151	RP_ShP_G_GABP_PKP + PIP2 <-> RP_ShP_G_GABP_PKP_PIP2	c103r		3.5	s ⁻¹	33 (SI.I) + [1-9]
152	RP_G_GABP_PKP_PIP2 -> RP_G_GABP_PKP + PIP3	c104	c104*RP_G_GABP_PKP_PIP2	25	s ⁻¹	33 (SI.I) + [1-9]
153	RP_ShP_G_GABP_PKP_PIP2 -> RP_ShP_G_GABP_PKP + PIP3	c105	c105*RP_ShP_G_GABP_PKP_PIP2	25	s ⁻¹	33 (SI.I) + [1-9]
154	RP_ShP_G + GABP <-> RP_ShP_G_GABP	c110r	c110f*RP_ShP_G*GABP - c110r*RP_ShP_G_GABP	1	s ⁻¹	33 (SI.I) + [1-9]
155	RP_ShP_G + GABP <-> RP_ShP_G_GABP	c110f		0.01	nM ⁻¹ .s ⁻¹	33 (SI.I) + [1-9]
156	RP_G + GABP <-> RP_G_GABP	c111r	c111f*RP_G*GABP - c111r*RP_G_GABP	1	s ⁻¹	33 (SI.I) + [1-9]
157	RP_G + GABP <-> RP_G_GABP	c111f		0.01	nM ⁻¹ .s ⁻¹	33 (SI.I) + [1-9]
158	GABP + PhoA <-> GABP_PhоА	c112f	c112f*GABP*PhoA - c112r*GABP_PhоА	0.001	nM ⁻¹ .s ⁻¹	33 (SI.I) + [1-9]
159	GABP + PhoA <-> GABP_PhоА	c112r		0.1	s ⁻¹	33 (SI.I) + [1-9]
160	GABP_PhоА -> GAB + PhoA	c113	c113*GABP_PhоА	0.03	s ⁻¹	33 (SI.I) + [1-9]
161	AKT + PIP3 <-> AKT_PIP3	c114f	c114f*AKT*PIP3 - c114r*AKT_PIP3	0.01	nM ⁻¹ .s ⁻¹	31, 32, 37 (SI.I) + [1-9]
162	AKT + PIP3 <-> AKT_PIP3	c114r		10	s ⁻¹	31, 32, 37 (SI.I) + [1-9]
163	GAB + PIP3 <-> GAB_PIP3	c115f	c115f*GAB*PIP3 - c115r*GAB_PIP3	0.01	nM ⁻¹ .s ⁻¹	33 (SI.I) + [1-9]
164	GAB + PIP3 <-> GAB_PIP3	c115r		3	s ⁻¹	33 (SI.I) + [1-9]
165	GABP + PIP3 <-> GABP_PIP3	c116f	c116f*GABP*PIP3 - c116r*GABP_PIP3	0.01	nM ⁻¹ .s ⁻¹	33 (SI.I) + [1-9]
166	GABP + PIP3 <-> GABP_PIP3	c116r		3	s ⁻¹	33 (SI.I) + [1-9]
167	RP_G + GAB_PIP3 <-> RP_G_GAB_PIP3	c117f	c117f*RP_G*GAB_PIP3 - c117r*RP_G_GAB_PIP3	2.5	nM ⁻¹ .s ⁻¹	33 (SI.I) + [1-9]
168	RP_G + GAB_PIP3 <-> RP_G_GAB_PIP3	c117r		1	s ⁻¹	33 (SI.I) + [1-9]
169	RP_ShP_G + GAB_PIP3 <-> RP_ShP_G_GAB_PIP3	c119r	c119f*RP_ShP_G*GAB_PIP3 - c119r*RP_ShP_G_GAB_PIP3	1	s ⁻¹	33 (SI.I) + [1-9]
170	RP_ShP_G + GAB_PIP3 <-> RP_ShP_G_GAB_PIP3	c119f		2.5	nM ⁻¹ .s ⁻¹	33 (SI.I) + [1-9]
171	RP_ShP_G_GAB_PIP3 -> RP_ShP_G_GABP + PIP3	c120	c120*RP_ShP_G_GAB_PIP3	0.01	s ⁻¹	33 (SI.I) + [1-9]
172	AKT_PIP3 + PDK1 <-> AKT_PIP3_PDK1	c124f	c124f*AKT_PIP3*PDK1 - c124r*AKT_PIP3_PDK1	0.01	nM ⁻¹ .s ⁻¹	31, 32, 37 (SI.I) + [1-9]
173	AKT_PIP3 + PDK1 <-> AKT_PIP3_PDK1	c124r		0.1	s ⁻¹	31, 32, 37 (SI.I) + [1-9]
174	AKT_PIP3_PDK1 -> AKTP + PIP3 + PDK1	c123	c123*AKT_PIP3_PDK1	5	s ⁻¹	31, 32, 37 (SI.I) + [1-9]

175	AKTP + TAKT <-> AKTP_TAKT	c129f	c129f*AKTP*TAKT - c129r*AKTP_TAKT	0.01	nM ⁻¹ .s ⁻¹	31, 32, 37 (SI.I) + [1-9]
176	AKTP + TAKT <-> AKTP_TAKT	c129r		1	s ⁻¹	31, 32, 37 (SI.I) + [1-9]
177	AKTP_TAKT -> AKT + TAKT	c130	c130*AKTP_TAKT	1	s ⁻¹	31, 32, 37 (SI.I) + [1-9]
178	PKP + PhoB <-> PKP_Phob	c135f	c135f*PKP*PhoB - c135r*PKP_Phob	0.01	nM ⁻¹ .s ⁻¹	31, 32, 37 (SI.I) + [1-9]
179	PKP + PhoB <-> PKP_Phob	c135r		1	s ⁻¹	31, 32, 37 (SI.I) + [1-9]
180	PKP_Phob -> PI3K + PhoB	c136	c136*PKP_Phob	0.5	s ⁻¹	31, 32, 37 (SI.I) + [1-9]
181	RP_G_GABP_PKP + PhoB <-> RP_G_GABP_PKP_Phob	c137f	c137f*RP_G_GABP_PKP*PhoB - c137r*RP_G_GABP_PKP_Phob	0.001	nM ⁻¹ .s ⁻¹	33 (SI.I) + [1-9]
182	RP_G_GABP_PKP + PhoB <-> RP_G_GABP_PKP_Phob	c137r		0.038	s ⁻¹	33 (SI.I) + [1-9]
183	RP_G_GABP_PKP_Phob -> RP_G_GABP_PKP + PhoB	c138	c138*RP_G_GABP_PKP_Phob	0.595	s ⁻¹	33 (SI.I) + [1-9]
184	RP_ShP_G_GABP_PKP + PhoB <-> RP_ShP_G_GABP_PKP_Phob	c139f	c139f*RP_ShP_G_GABP_PKP*PhoB - c139r*RP_ShP_G_GABP_PKP_Phob	0.001	nM ⁻¹ .s ⁻¹	33 (SI.I) + [1-9]
185	RP_ShP_G_GABP_PKP + PhoB <-> RP_ShP_G_GABP_PKP_Phob	c139r		0.038	s ⁻¹	33 (SI.I) + [1-9]
186	RP_ShP_G_GABP_PKP_Phob -> RP_ShP_G_GABP_PKP + PhoB	c140	c140*RP_ShP_G_GABP_PKP_Phob	0.595	s ⁻¹	33 (SI.I) + [1-9]
187	RP_ShP_G_GAB + PIP3 <-> RP_ShP_G_GAB_PIP3	c143f	c143f*RP_ShP_G_GAB*PIP3 - c143r*RP_ShP_G_GAB_PIP3	2.5	nM ⁻¹ .s ⁻¹	33 (SI.I) + [1-9]
188	RP_ShP_G_GAB + PIP3 <-> RP_ShP_G_GAB_PIP3	c143r		1	s ⁻¹	33 (SI.I) + [1-9]
189	RP_PKP + PIP2 <-> RP_PKP_PIP2	c146f	c146f*RP_PKP*PIP2 - c146r*RP_PKP_PIP2	6.25	nM ⁻¹ .s ⁻¹	31, 32 (SI.I) + [1-9]
190	RP_PKP + PIP2 <-> RP_PKP_PIP2	c146r		3.5	s ⁻¹	31, 32 (SI.I) + [1-9]
191	RP_PKP_PIP2 -> RP_PKP + PIP3	c147f	c147f*RP_PKP_PIP2	2.5	s ⁻¹	31, 32 (SI.I) + [1-9]
192	RP_ShP_G_GABP_PKP <-> RP_ShP_G_GABP + PKP	c148f	c148f*RP_ShP_G_GABP_PKP - c148r*RP_ShP_G_GABP*PKP	5	s ⁻¹	33 (SI.I) + [1-9]
193	RP_ShP_G_GABP_PKP <-> RP_ShP_G_GABP + PKP	c148r		0.05	nM ⁻¹ .s ⁻¹	33 (SI.I) + [1-9]
194	RP_G_GABP_PKP <-> RP_G_GABP + PKP	c149f	c149f*RP_G_GABP_PKP - c149r*RP_G_GABP*PKP	5	s ⁻¹	33 (SI.I) + [1-9]
195	RP_G_GABP_PKP <-> RP_G_GABP + PKP	c149r		0.05	nM ⁻¹ .s ⁻¹	33 (SI.I) + [1-9]
196	RP_G_GAB_PIP3 -> RP_G_GAB + PIP3	c150	c150*RP_G_GAB_PIP3	0.01	s ⁻¹	33 (SI.I) + [1-9]
197	GSKP + PhoC <-> GSKP_Phoc	c151f	c151f*GSKP*PhoC - c151r*GSKP_Phoc	0.01	nM ⁻¹ .s ⁻¹	46 - 50 (SI.I) + [12-13]
198	GSKP + PhoC <-> GSKP_Phoc	c151r		5	s ⁻¹	46 - 50 (SI.I) + [12-13]
199	GSKP_Phoc -> GSK + PhoC	c152	c152*GSKP_Phoc	0.1	s ⁻¹	46 - 50 (SI.I) + [12-13]
200	RP_G_GAB + PIP3 <-> RP_G_GAB_PIP3	c156f	c156f*RP_G_GAB*PIP3 - c156r*RP_G_GAB_PIP3	1	nM ⁻¹ .s ⁻¹	31, 33 (SI.I) + [1-9]

201	RP_G_GAB + PIP3 <-> RP_G_GAB_PIP3	c156r		2.5	s ⁻¹	31, 33 (SI.I) + [1-9]
202	[Raf] + AKTP <-> [Raf_AKTP]	c157f	c157f*[Raf*]*AKTP - c157r*[Raf*_AKTP)	0.01	nM ⁻¹ .s ⁻¹	38 (SI.I) + [11,13]
203	[Raf] + AKTP <-> [Raf_AKTP]	c157r		0.033	s ⁻¹	38 (SI.I) + [11,13]
204	[Raf_AKTP] -> [Raf] + AKTP	c158	c158*[Raf*_AKTP)	5.7	s ⁻¹	38 (SI.I) + [11,13]
205	[Raf] + Pase1 <-> [Raf_Pase1]	c159f	c159f*[Raf**]*Pase1 - c159r*[Raf**_Pase1)	0.0717	nM ⁻¹ .s ⁻¹	12 – 14 (1SI.I) + [11,13]
206	[Raf] + Pase1 <-> [Raf_Pase1]	c159r		0.2	s ⁻¹	12 – 14 (1SI.I) + [11,13]
207	[Raf_Pase1] -> [Raf] + Pase1	c160	c160*[Raf**_Pase1)	1	s ⁻¹	12 – 14 (1SI.I) + [11,13]
208	AKTP + GSK <-> [AKTP_GSK)	c170f	c170f*AKTP*GSK - c170r*[AKTP_GSK)	0.01	nM ⁻¹ .s ⁻¹	31 - 32, 44 - 49 (1SI.I) + [12-13]
209	AKTP + GSK <-> [AKTP_GSK)	c170r		0.1	s ⁻¹	31 - 32, 44 - 49 (1SI.I) + [12-13]
210	[AKTP_GSK] -> AKTP + GSKP	c171	c171*[AKTP_GSK)	1	s ⁻¹	31 - 32, 44 - 49 (1SI.I) + [12-13]
211	R + R <-> R_R	c181f		0.0001	nM ⁻¹ .s ⁻¹	1 - 3 (SI.I) + [1-9,12-16]
212	R + R <-> R_R	c181r	c181f*R*R - c181r*R_R	0.1	s ⁻¹	1 - 3 (SI.I) + [1-9,12-16]
213	EGF + R_R <-> RI_R	c182f	c182f*EGF*R_R - c182r*RI_R	0.0001	nM ⁻¹ .s ⁻¹	1 - 3 (SI.I) + [1-9,12-16]
214	EGF + R_R <-> RI_R	c182r		1	s ⁻¹	1 - 3 (SI.I) + [1-9,12-16]
215	RI + R <-> RI_R	c183f	c183f*RI*R - c183r*RI_R	0.001	nM ⁻¹ .s ⁻¹	1 - 3 (SI.I) + [1-9,12-16]
216	RI + R <-> RI_R	c183r		0.1	s ⁻¹	1 - 3 (SI.I) + [1-9,12-16]
217	RI_R -> RIP_RP	c184f	c184f*RI_R	1	s ⁻¹	1 - 3 (SI.I) + [1-9,12-16]
218	RIP_RP <-> EGF + RP_RP	c185f	c185f*RIP_RP - c185r*EGF*RP_RP	0.1	s ⁻¹	1 - 3 (SI.I) + [1-9,12-16]
219	RIP_RP <-> EGF + RP_RP	c185r		0.01	nM ⁻¹ .s ⁻¹	1 - 3 (SI.I) + [1-9,12-16]
220	RP_RP <-> RP + RP	c186f	c186f*RP_RP - c187r*RP*RP	0.1	s ⁻¹	1 - 3 (SI.I) + [1-9,12-16]
221	RP_RP <-> RP + RP	c187r	c187f*RP_R	0.01	nM ⁻¹ .s ⁻¹	1 - 3 (SI.I) + [1-9,12-16]
222	RP_R -> RP_RP	c187f		1	s ⁻¹	1 - 3 (SI.I) + [1-9,12-16]
223	RP + R <-> RP_R	c189f	c189f*RP*R - c189r*RP_R	0.001	nM ⁻¹ .s ⁻¹	1 - 3 (SI.I) + [1-9,12-16]
224	RP + R <-> RP_R	c189r		0.1	s ⁻¹	1 - 3 (SI.I) + [1-9,12-16]
225	CDC25CP + RP <-> CDC25CP_RP	c190f	c190f*CDC25CP*RP - c190r*CDC25CP_RP	0.01	nM ⁻¹ .s ⁻¹	26, 27 (SI.I) + [12-13]
226	CDC25CP + RP <-> CDC25CP_RP	c190r		0.1	s ⁻¹	26, 27 (SI.I) + [12-13]
227	CDC25CP_RP -> CDC25CP + R	c191f	c191f*CDC25CP_RP	1	s ⁻¹	26, 27 (SI.I) + [12-13]
228	CDC25CP + RP_RP <-> CDC25CP_RP_RP	c192f		0.01	nM ⁻¹ .s ⁻¹	26, 27 (SI.I) + [12-13]
229	CDC25CP + RP_RP <-> CDC25CP_RP_RP	c192r	c192f*CDC25CP*RP_RP - c192r*CDC25CP_RP_RP	0.1	s ⁻¹	26, 27 (SI.I) + [12-13]

230	CDC25CP_RP_RP -> CDC25CP + R_R	c193f	c193f*CDC25CP_RP_RP	0.5	s ⁻¹	26, 27 (SI.I) + [12-13]
231	R + ERB <-> R_ERB	c194f	c194f*R*ERB - c194r*R_ERB	0.001	nM ⁻¹ .s ⁻¹	1 - 3 (SI.I) + [1,6,13-16]
232	R + ERB <-> R_ERB	c194r		0.1	s ⁻¹	1 - 3 (SI.I) + [1,6,13-16]
233	R_ERB + EGF <-> RI_ERB	c195f	c195f*R_ERB*EGF - c195r*RI_ERB	0.01	nM ⁻¹ .s ⁻¹	1 - 3 (SI.I) + [1,6,13-16]
234	R_ERB + EGF <-> RI_ERB	c195r		0.1	s ⁻¹	1 - 3 (SI.I) + [1,6,13-16]
235	RI_ERB -> RIP_ERBP	c196f	c196f*RI_ERB	1	s ⁻¹	1 - 3 (SI.I) + [1,6,13-16]
236	RIP_ERBP <-> EGF + RP_ERBP	c197f	c197f*RIP_ERBP - c197r*EGF*RP_ERBP	0.1	s ⁻¹	1 - 3 (SI.I) + [1,6,13-16]
237	RIP_ERBP <-> EGF + RP_ERBP	c197r		0.01	nM ⁻¹ .s ⁻¹	1 - 3 (SI.I) + [1,6,13-16]
238	RP_ERBP <-> RP + ERBP	c198f	c198f*RP_ERBP - c198r*RP*ERBP	0.1	s ⁻¹	1 - 3 (SI.I) + [1,6,13-16]
239	RP_ERBP <-> RP + ERBP	c198r		0.01	nM ⁻¹ .s ⁻¹	1 - 3 (SI.I) + [1,6,13-16]
240	RI + ERB <-> RI_ERB	c199f	c199f*RI*ERB - c199r*RI_ERB	0.01	nM ⁻¹ .s ⁻¹	1 - 3 (SI.I) + [1,6,13-16]
241	RI + ERB <-> RI_ERB	c199r		0.1	s ⁻¹	1 - 3 (SI.I) + [1,6,13-16]
242	R + ERBP <-> R_ERBP	c200f	c200f*R*ERBP - c200r*R_ERBP	0.001	nM ⁻¹ .s ⁻¹	1 - 3 (SI.I) + [1,6,13-16]
243	R + ERBP <-> R_ERBP	c200r		0.1	s ⁻¹	1 - 3 (SI.I) + [1,6,13-16]
244	R_ERBP -> RP_ERBP	c201f	c201f*R_ERBP	1	s ⁻¹	1 - 3 (SI.I) + [1,6,13-16]
245	RIP_ERBP <-> RIP + ERBP	c202f	c202f*RIP_ERBP - c202r*RIP*ERBP	0.1	s ⁻¹	1 - 3 (SI.I) + [1,6,13-16]
246	RIP_ERBP <-> RIP + ERBP	c202r		0.01	nM ⁻¹ .s ⁻¹	1 - 3 (SI.I) + [1,6,13-16]
247	RP + ERB <-> RP_ERB	c203f	c203f*RP*ERB - c203r*RP_ERB	0.01	nM ⁻¹ .s ⁻¹	1 - 3 (SI.I) + [1,6,13-16]
248	RP + ERB <-> RP_ERB	c203r		0.1	s ⁻¹	1 - 3 (SI.I) + [1,6,13-16]
249	RP_ERB -> RP_ERBP	c204f	c204f*RP_ERB	1	s ⁻¹	1 - 3 (SI.I) + [1,6,13-16]
250	ERBP + ERB <-> ERBP_ERB	c205f	c205f*ERBP*ERB - c205r*ERBP_ERB	0.01	nM ⁻¹ .s ⁻¹	1 - 3 (SI.I) + [1,6,13-16]
251	ERBP + ERB <-> ERBP_ERB	c205r		0.1	s ⁻¹	1 - 3 (SI.I) + [1,6,13-16]
252	ERBP_ERBP <-> ERBP + ERBP	c207f	c207f*ERBP_ERBP - c207r*ERBP*ERBP	0.1	s ⁻¹	1 - 3 (SI.I) + [1,6,13-16]
253	ERBP_ERBP <-> ERBP + ERBP	c207r		0.01	nM ⁻¹ .s ⁻¹	1 - 3 (SI.I) + [1,6,13-16]
254	ERB + ERB <-> ERB_ERB	c208f	c208f*ERB*ERB - c209r*ERB_ERB	0.01	nM ⁻¹ .s ⁻¹	1 - 3 (SI.I) + [1,6,13-16]
255	ERB + ERB <-> ERB_ERB	c209r		0.1	s ⁻¹	1 - 3 (SI.I) + [1,6,13-16]
256	ERBP_ERB -> ERBP_ERBP	c206f	c206f*ERBP_ERB	1	s ⁻¹	1 - 3 (SI.I) + [1,6,13-16]
257	CDC25CP + ERBP <-> CDC25CP_ERBP	c207f_n	c207f_n*CDC25CP*ERBP - c208r*CDC25CP_ERBP	0.01	nM ⁻¹ .s ⁻¹	26, 27 (SI.I) + [12-13,16]
258	CDC25CP + ERBP <-> CDC25CP_ERBP	c208r	c208f_n*CDC25CP_ERBP	0.1	s ⁻¹	26, 27 (SI.I) + [12-13,16]
259	CDC25CP_ERBP -> CDC25CP + ERB	c208f_n		0.5	s ⁻¹	26, 27 (SI.I) + [12-13,16]
260	ShP + PTP1E <-> PTP1E_ShP	c210f	c210f*ShP*PTP1E - c210r*PTP1E_ShP	0.01	nM ⁻¹ .s ⁻¹	10 (SI.I) + [1]

261	ShP + PTP1E <-> PTP1E_ShP	c210r		0.1	s ⁻¹	10 (SI.I) + [1]
262	PTP1E_ShP -> PTP1E + Shc	c209f	c209f*PTP1E_ShP	0.005	s ⁻¹	10 (SI.I) + [1]
263	PLCyP + PaseX <-> PLCyP_PaseX	c211f	c211f*PLCyP*PaseX - c211r*PLCyP_PaseX	0.01	nM ⁻¹ .s ⁻¹	1 - 3 (SI.I) + [1]
264	PLCyP + PaseX <-> PLCyP_PaseX	c211r		0.1	s ⁻¹	1 - 3 (SI.I) + [1]
265	PLCyP_PaseX -> PLCy + PaseX	c212f	c212f*PLCyP_PaseX	0.01	s ⁻¹	1 - 3 (SI.I) + [1]
266	RIP2 <-> RIP + RIP	c213f	c213f*RIP2 - c213r*RIP*RIP	0.1	s ⁻¹	1 - 3 (SI.I) + [1,6,13-16]
267	RIP2 <-> RIP + RIP	c213r		0.01	nM ⁻¹ .s ⁻¹	1 - 3 (SI.I) + [1,6,13-16]
268	RIP <-> EGF + RP	c214f	c214f*RIP - c214r*EGF*RP	0.1	s ⁻¹	1 - 3 (SI.I) + [1,6,13-16]
269	RIP <-> EGF + RP	c214r		0.01	nM ⁻¹ .s ⁻¹	1 - 3 (SI.I) + [1,6,13-16]
270	CDC25CP + ERBP_ERBP <-> CDC25CP_ERBP_ERBP	c215f	c215f*CDC25CP*ERBP_ERBP - c215r*CDC25CP_ERBP_ERBP	0.01	nM ⁻¹ .s ⁻¹	26, 27 (SI.I) + [12-13,16]
271	CDC25CP + ERBP_ERBP <-> CDC25CP_ERBP_ERBP	c215r		0.1	s ⁻¹	26, 27 (SI.I) + [12-13,16]
272	CDC25CP_ERBP_ERBP -> CDC25CP + ERB_ERB	c216f	c216f*CDC25CP_ERBP_ERBP	0.5	s ⁻¹	26, 27 (SI.I) + [12-13,16]
273	ERBP + PLCy <-> ERBP_PL	c_a_185f	c_a_185f*ERBP*PLCy - c_a_185r*ERBP_PL	0.06	nM ⁻¹ .s ⁻¹	2, 3 (SI.I) + [1-9,16]
274	ERBP + PLCy <-> ERBP_PL	c_a_185r		0.2	s ⁻¹	2, 3 (SI.I) + [1-9,16]
275	ERBP_PL -> ERBP_PLP	c_a_186f	c_a_186f*ERBP_PL	1	s ⁻¹	2, 3 (SI.I) + [1-9,16]
276	ERBP_PLP <-> ERBP + PLCyP	c_a_187f	c_a_187f*ERBP_PLP - c_a_187r*ERBP*PLCyP	0.3	s ⁻¹	2, 3 (SI.I) + [1-9,16]
277	ERBP_PLP <-> ERBP + PLCyP	c_a_187r		0.006	nM ⁻¹ .s ⁻¹	2, 3 (SI.I) + [1-9,16]
278	ERBP + Grb <-> ERBP_G	c_a_190f	c_a_190f*ERBP*Grb - c_a_190r*ERBP_G	0.0015	nM ⁻¹ .s ⁻¹	2, 3 (SI.I) + [1-9,16]
279	ERBP + Grb <-> ERBP_G	c_a_190r		0.2	s ⁻¹	2, 3 (SI.I) + [1-9,16]
280	ERBP_G + SOS <-> ERBP_G_S	c_a_191f	c_a_191f*ERBP_G*SOS - c_a_191r*ERBP_G_S	0.01	nM ⁻¹ .s ⁻¹	2, 3 (SI.I) + [1-9,16]
281	ERBP_G + SOS <-> ERBP_G_S	c_a_191r		0.06	s ⁻¹	2, 3 (SI.I) + [1-9,16]
282	ERBP_G_S <-> ERBP + G_S	c_a_192f	c_a_192f*ERBP_G_S - c_a_192r*ERBP*G_S	0.15	s ⁻¹	2, 3 (SI.I) + [1-9,16]
283	ERBP_G_S <-> ERBP + G_S	c_a_192r		0.0028	nM ⁻¹ .s ⁻¹	2, 3 (SI.I) + [1-9,16]
284	ERBP + Shc <-> ERBP_Sh	c_a_194f	c_a_194f*ERBP*Shc - c_a_194r*ERBP_Sh	0.09	nM ⁻¹ .s ⁻¹	2, 3 (SI.I) + [1-9,16]
285	ERBP + Shc <-> ERBP_Sh	c_a_194r		0.6	s ⁻¹	2, 3 (SI.I) + [1-9,16]
286	ERBP_Sh -> ERBP_ShP	c_a_195	c_a_195*ERBP_Sh	6	s ⁻¹	2, 3 (SI.I) + [1-9,16]
287	ERBP_ShP <-> ShP + ERBP	c_a_196f	c_a_196f*ERBP_ShP - c_a_196r*ShP*ERBP	0.3	s ⁻¹	2, 3 (SI.I) + [1-9,16]
288	ERBP_ShP <-> ShP + ERBP	c_a_196r		0.0009	nM ⁻¹ .s ⁻¹	2, 3 (SI.I) + [1-9,16]
289	ERBP_ShP + Grb <-> ERBP_ShP_G	c_a_197f	c_a_197f*ERBP_ShP*Grb - c_a_197r*ERBP_ShP_G	0.003	nM ⁻¹ .s ⁻¹	2, 3 (SI.I) + [1-9,16]
290	ERBP_ShP + Grb <-> ERBP_ShP_G	c_a_197r		0.1	s ⁻¹	2, 3 (SI.I) + [1-9,16]

291	ERBP_ShP_G <-> ERBP + ShP_G	c_a_198f	c_a_198f*ERBP_ShP_G - c_a_198r*ERBP*ShP_G	0.3	s ⁻¹	2, 3 (SI.I) + [1-9,16]
292	ERBP_ShP_G <-> ERBP + ShP_G	c_a_198r		0.0009	nM ⁻¹ .s ⁻¹	2, 3 (SI.I) + [1-9,16]
293	ERBP_ShP_G + SOS <-> ERBP_ShP_G_S	c_a_199f	c_a_199f*ERBP_ShP_G*SOS - c_a_199r*ERBP_ShP_G_S	0.01	nM ⁻¹ .s ⁻¹	2, 3 (SI.I) + [1-9,16]
294	ERBP_ShP_G + SOS <-> ERBP_ShP_G_S	c_a_199r		0.0214	s ⁻¹	2, 3 (SI.I) + [1-9,16]
295	ERBP_ShP_G_S <-> ShP_G_S + ERBP	c_a_200f	c_a_200f*ERBP_ShP_G_S - c_a_200r*ShP_G_S*ERBP	0.12	s ⁻¹	2, 3 (SI.I) + [1-9,16]
296	ERBP_ShP_G_S <-> ShP_G_S + ERBP	c_a_200r		0.00024	nM ⁻¹ .s ⁻¹	2, 3 (SI.I) + [1-9,16]
297	ERBP_ShP_G_S + Ras_GDP <->	c_a_205f	c_a_205f*ERBP_ShP_G_S - c_a_205r*ERBP_ShP_G_S	0.009	nM ⁻¹ .s ⁻¹	2, 3 (SI.I) + [1-9,16]
298	ERBP_ShP_G_S + Ras_GDP <-> ERBP_ShP_G_S	c_a_205r		0.0429	s ⁻¹	2, 3 (SI.I) + [1-9,16]
299	ERBP_ShP_G_S + Ras_GDP <-> ERBP_ShP_G_S Ras_GDP	c_a_209f	c_a_209f*ERBP_ShP_G_S*Ras_GDP - c_a_209r*ERBP_ShP_G_S_Ras_GDP	0.00475	nM ⁻¹ .s ⁻¹	2, 3 (SI.I) + [1-9,16]
300	ERBP_ShP_G_S + Ras_GDP <-> ERBP_ShP_G_S Ras_GDP	c_a_209r		0.76	s ⁻¹	2, 3 (SI.I) + [1-9,16]
301	ERBP_ShP_G_S Ras_GDP <-> ERBP_ShP_G_S Ras + GDP	c_a_210f	c_a_210f*ERBP_ShP_G_S_Ras_GDP - c_a_210r*ERBP_ShP_G_S_Ras*GDP	46.5	s ⁻¹	2, 3 (SI.I) + [1-9,16]
302	ERBP_ShP_G_S Ras_GDP <-> ERBP_ShP_G_S Ras + GDP	c_a_210r		0.093	nM ⁻¹ .s ⁻¹	2, 3 (SI.I) + [1-9,16]
303	ERBP_ShP_G_S Ras + GTP <-> ERBP_ShP_G_S Ras_GTP	c_a_211f	c_a_211f*ERBP_ShP_G_S_Ras*GTP - c_a_211r*ERBP_ShP_G_S_Ras_GTP	0.003	nM ⁻¹ .s ⁻¹	2, 3 (SI.I) + [1-9,16]
304	ERBP_ShP_G_S Ras + GTP <-> ERBP_ShP_G_S Ras_GTP	c_a_211r		2.4	s ⁻¹	2, 3 (SI.I) + [1-9,16]
305	ERBP_ShP_G_S Ras_GTP <-> ERBP_ShP_G_S + Ras_GTP	c_a_212f	c_a_212f*ERBP_ShP_G_S_Ras_GTP - c_a_212r*ERBP_ShP_G_S*Ras_GTP	806.4	s ⁻¹	2, 3 (SI.I) + [1-9,16]
306	ERBP_ShP_G_S Ras_GTP <-> ERBP_ShP_G_S + Ras_GTP	c_a_212r		1.575	nM ⁻¹ .s ⁻¹	2, 3 (SI.I) + [1-9,16]
307	ERBP_ShP_G_S + Ras <-> ERBP_ShP_G_S Ras	c_a_213f	c_a_213f*ERBP_ShP_G_S*Ras - c_a_213r*ERBP_ShP_G_S_Ras	0.15625	nM ⁻¹ .s ⁻¹	2, 3 (SI.I) + [1-9,16]
308	ERBP_ShP_G_S + Ras <-> ERBP_ShP_G_S Ras	c_a_213r		0.001	s ⁻¹	2, 3 (SI.I) + [1-9,16]
309	ERBP_G_S + Ras_GDP <-> ERBP_G_S Ras_GDP	c_a_214f	c_a_214f*ERBP_G_S*Ras_GDP - c_a_214r*ERBP_G_S_Ras_GDP	0.0075	nM ⁻¹ .s ⁻¹	2, 3 (SI.I) + [1-9,16]
310	ERBP_G_S + Ras_GDP <-> ERBP_G_S Ras_GDP	c_a_214r		1.2	s ⁻¹	2, 3 (SI.I) + [1-9,16]
311	ERBP_G_S Ras_GDP <-> ERBP_G_S Ras + GDP	c_a_215f	c_a_215f*ERBP_G_S_Ras_GDP - c_a_215r*ERBP_G_S_Ras*GDP	50	s ⁻¹	2, 3 (SI.I) + [1-9,16]
312	ERBP_G_S Ras_GDP <-> ERBP_G_S Ras + GDP	c_a_215r		0.1	nM ⁻¹ .s ⁻¹	2, 3 (SI.I) + [1-9,16]

313	ERBP_G_S_Ras + GTP <-> ERBP_G_S_Ras_GTP	c_a_216f	c_a_216f*ERBP_G_S_Ras*GTP - c_a_216r*ERBP_G_S_Ras_GTP	0.1	nM ⁻¹ .s ⁻¹	2, 3 (SI.I) + [1-9,16]
314	ERBP_G_S_Ras + GTP <-> ERBP_G_S_Ras_GTP	c_a_216r		80	s ⁻¹	2, 3 (SI.I) + [1-9,16]
315	ERBP_G_S_Ras_GTP <-> ERBP_G_S + Ras_GTP	c_a_217f	c_a_217f*ERBP_G_S_Ras_GTP - c_a_217r*ERBP_G_S*Ras_GTP	640	s ⁻¹	2, 3 (SI.I) + [1-9,16]
316	ERBP_G_S_Ras_GTP <-> ERBP_G_S + Ras_GTP	c_a_217r		1.25	nM ⁻¹ .s ⁻¹	2, 3 (SI.I) + [1-9,16]
317	ERBP_G_S + Ras <-> ERBP_G_S_Ras	c_a_218f	c_a_218f*ERBP_G_S*Ras - c_a_218r*ERBP_G_S_Ras	0.25	nM ⁻¹ .s ⁻¹	2, 3 (SI.I) + [1-9,16]
318	ERBP_G_S + Ras <-> ERBP_G_S_Ras	c_a_218r		0.0016	s ⁻¹	2, 3 (SI.I) + [1-10,16]
319	GAP + ERBP <-> ERBP_GAP	c_a_239f	c_a_239f*GAP*ERBP - c_a_239r*ERBP_GAP	0.083	nM ⁻¹ .s ⁻¹	2, 3 (SI.I) + [1-10,16]
320	GAP + ERBP <-> ERBP_GAP	c_a_239r		0.15	s ⁻¹	2, 3 (SI.I) + [1-10,16]
321	Ras_GTP + ERBP_GAP <-> ERBP_GAP_Ras_GTP	c_a_240f	c_a_240f*Ras_GTP*ERBP_GAP - c_a_240r*ERBP_GAP_Ras_GTP	0.01	nM ⁻¹ .s ⁻¹	2, 3 (SI.I) + [1-10,16]
322	Ras_GTP + ERBP_GAP <-> ERBP_GAP_Ras_GTP	c_a_240r		0.03	s ⁻¹	2, 3 (SI.I) + [1-10,16]
323	ERBP_GAP_Ras_GTP -> ERBP_GAP + Ras_GDP	c_a_241	c_a_241*ERBP_GAP_Ras_GTP	1.494	s ⁻¹	2, 3 (SI.I) + [1-10,16]
324	ERBP_ShP_G_S + ERKPP <-> ERBP_ShP_G_S_ERKPP	c_a_250f	c_a_250f*ERBP_ShP_G_S*ERKPP - c_a_250r*ERBP_ShP_G_S_ERKPP	0.01	nM ⁻¹ .s ⁻¹	11, 24 - 25 (SI.I) + [1,16]
325	ERBP_ShP_G_S + ERKPP <-> ERBP_ShP_G_S_ERKPP	c_a_250r		0.033	s ⁻¹	11, 24 - 25 (SI.I) + [1,16]
326	ERBP_ShP_G_S_ERKPP -> ERBP_ShP_G + ERKPP + SOSP	c_a_251	c_a_251*ERBP_ShP_G_S_ERKPP	1	s ⁻¹	11, 24 - 25 (SI.I) + [1,16]
327	ERBP_G_S + ERKPP <-> ERBP_G_S_ERKPP	c_a_252f	c_a_252f*ERBP_G_S*ERKPP - c_a_252r*ERBP_G_S_ERKPP	0.01	nM ⁻¹ .s ⁻¹	11, 24 - 25 (SI.I) + [1,16]
328	ERBP_G_S + ERKPP <-> ERBP_G_S_ERKPP	c_a_252r		0.033	s ⁻¹	11, 24 - 25 (SI.I) + [1,16]
329	ERBP_G_S_ERKPP -> ERBP_G + SOSP + ERKPP	c_a_253	c_a_253*ERBP_G_S_ERKPP	1	s ⁻¹	11, 24 - 25 (SI.I) + [1,16]
330	ERBP_G + GAB <-> ERBP_G_GAB	c_a_256f	c_a_256f*ERBP_G*GAB - c_a_256r*ERBP_G_GAB	0.01	nM ⁻¹ .s ⁻¹	33 (SI.I) + [1,16]
331	ERBP_G + GAB <-> ERBP_G_GAB	c_a_256r		1	s ⁻¹	33 (SI.I) + [1,16]
332	ERBP_ShP_G + GAB <-> ERBP_ShP_G_GAB	c_a_257f	c_a_257f*ERBP_ShP_G*GAB - c_a_257r*ERBP_ShP_G_GAB	0.01	nM ⁻¹ .s ⁻¹	33 (SI.I) + [1,16]
333	ERBP_ShP_G + GAB <-> ERBP_ShP_G_GAB	c_a_257r		1	s ⁻¹	33 (SI.I) + [1,16]
334	ERBP_G_GAB -> ERBP_G_GABP	c_a_258	c_a_258*ERBP_G_GAB	0.05	s ⁻¹	33 (SI.I) + [1,16]

335	ERBP_ShP_G_GAB -> ERBP_ShP_G_GABP	c_a_259	c_a_259*ERBP_ShP_G_GAB	0.05	s ⁻¹	33 (SI.I) + [1,16]
336	ERBP_G_GABP + PI3K <-> ERBP_G_GABP_PK	c_a_260f	c_a_260f*ERBP_G_GABP*PI3K - c_a_260r*ERBP_G_GABP_PK	0.01	nM ⁻¹ .s ⁻¹	31 - 33 (SI.I) + [12-13,16]
337	ERBP_G_GABP + PI3K <-> ERBP_G_GABP_PK	c_a_260r		1	s ⁻¹	31 - 33 (SI.I) + [12-13,16]
338	ERBP_G_GABP_PK -> ERBP_G_GABP_PKP	c_a_262	c_a_262*ERBP_G_GABP_PK	1	s ⁻¹	31 - 33 (SI.I) + [12-13,16]
339	ERBP_ShP_G_GABP + PI3K <-> ERBP_ShP_G_GABP_PK	c_a_261f	c_a_261f*ERBP_ShP_G_GABP*PI3K - c_a_261r*ERBP_ShP_G_GABP_PK	0.01	nM ⁻¹ .s ⁻¹	31 - 33 (SI.I) + [12-13,16]
340	ERBP_ShP_G_GABP + PI3K <-> ERBP_ShP_G_GABP_PK	c_a_261r		1	s ⁻¹	31 - 33 (SI.I) + [12-13,16]
341	ERBP_ShP_G_GABP_PK -> ERBP_ShP_G_GABP_PKP	c_a_263	c_a_263*ERBP_ShP_G_GABP_PK	1	s ⁻¹	31 - 33 (SI.I) + [12-13,16]
342	ERBP_ShP_G_GABP + GAP <-> ERBP_ShP_G_GABP_GAP	c_a_264f	c_a_264f*ERBP_ShP_G_GABP*GAP - c_a_264r*ERBP_ShP_G_GABP_GAP	0.083	nM ⁻¹ .s ⁻¹	33 (SI.I) + [1,16]
343	ERBP_ShP_G_GABP + GAP <-> ERBP_ShP_G_GABP_GAP	c_a_264r		0.15	s ⁻¹	33 (SI.I) + [1,16]
344	ERBP_G_GABP + GAP <-> ERBP_G_GABP_GAP	c_a_265f	c_a_265f*ERBP_G_GABP*GAP - c_a_265r*ERBP_G_GABP_GAP	0.083	nM ⁻¹ .s ⁻¹	33 (SI.I) + [1,16]
345	ERBP_G_GABP + GAP <-> ERBP_G_GABP_GAP	c_a_265r		0.15	s ⁻¹	33 (SI.I) + [1,16]
346	ERBP_G_GABP_GAP + Ras_GTP <-> ERBP_G_GABP_GAP_Ras_GTP	c_a_266f	c_a_266f*ERBP_G_GABP_GAP*Ras_GTP - c_a_266r*ERBP_G_GABP_GAP_Ras_GTP	0.6225	nM ⁻¹ .s ⁻¹	7, 8, 33 (SI.I) + [1,16]
347	ERBP_G_GABP_GAP + Ras_GTP <-> ERBP_G_GABP_GAP_Ras_GTP	c_a_266r		0.3	s ⁻¹	7, 8, 33 (SI.I) + [1,16]
348	ERBP_G_GABP_GAP_Ras_GTP -> ERBP_G_GABP_GAP + Ras_GDP	c_a_267	c_a_267*ERBP_G_GABP_GAP_Ras_GTP	1.494	s ⁻¹	7, 8, 33 (SI.I) + [1,16]
349	ERBP_ShP_G_GABP_GAP + Ras_GTP <-> ERBP_ShP_G_GABP_GAP_Ras_GTP	c_a_268f	c_a_268f*ERBP_ShP_G_GABP_GAP*Ras_GTP - c_a_268r*ERBP_ShP_G_GABP_GAP_Ras_GTP	0.6225	nM ⁻¹ .s ⁻¹	7, 8, 33 (SI.I) + [1,16]
350	ERBP_ShP_G_GABP_GAP + Ras_GTP <-> ERBP_ShP_G_GABP_GAP_Ras_GTP	c_a_268r		0.3	s ⁻¹	7, 8, 33 (SI.I) + [1,16]
351	ERBP_ShP_G_GABP_GAP_Ras_GTP -> ERBP_ShP_G_GABP_GAP + Ras_GDP	c_a_269	c_a_269*ERBP_ShP_G_GABP_GAP_Ras_GTP	1.494	s ⁻¹	7, 8, 33 (SI.I) + [1,16]
352	ERBP + PI3K <-> ERBP_PK	c_a_270f	c_a_270f*ERBP*PI3K - c_a_270r*ERBP_PK	0.01	nM ⁻¹ .s ⁻¹	1 - 3, 31, 32 (SI.I) + [1,16]
353	ERBP + PI3K <-> ERBP_PK	c_a_270r		1	s ⁻¹	1 - 3, 31, 32 (SI.I) + [1,16]
354	ERBP_PK -> ERBP_PKP	c_a_271f	c_a_271f*ERBP_PK	1	s ⁻¹	1 - 3, 31, 32 (SI.I) + [1,16]
355	ERBP + PKP <-> ERBP_PKP	c_a_272r	c_a_272r*ERBP*PKP - c_a_272f*ERBP_PKP	0.01	nM ⁻¹ .s ⁻¹	1 - 3, 31, 32 (SI.I) + [1,16]
356	ERBP + PKP <-> ERBP_PKP	c_a_272f		0.1	s ⁻¹	1 - 3, 31, 32 (SI.I) + [1,16]

357	ERBP_ShP_G_GABP + PhoA <-> ERBP_ShP_G_GABP_PhоА	c_a_278f	c_a_278f*ERBP_ShP_G_GABP*PhoA - c_a_278r*ERBP_ShP_G_GABP_PhоА	0.001	nM ⁻¹ .s ⁻¹	33 (SI.I) + [1,16]
358	ERBP_ShP_G_GABP + PhoA <-> ERBP_ShP_G_GABP_PhоА	c_a_278r		0.1	s ⁻¹	33 (SI.I) + [1,16]
359	ERBP_ShP_G_GABP_PhоА -> ERBP_ShP_G_GAB + PhoA	c_a_280	c_a_280*ERBP_ShP_G_GABP_PhоА	0.03	s ⁻¹	33 (SI.I) + [1,16]
360	ERBP_G_GABP + PhoA <-> ERBP_G_GABP_PhоА	c_a_279f	c_a_279f*ERBP_G_GABP*PhoA - c_a_279r*ERBP_G_GABP_PhоА	0.001	nM ⁻¹ .s ⁻¹	33 (SI.I) + [1,16]
361	ERBP_G_GABP + PhoA <-> ERBP_G_GABP_PhоА	c_a_279r		0.1	s ⁻¹	33 (SI.I) + [1,16]
362	ERBP_G_GABP_PhоА -> ERBP_G_GAB + PhoA	c_a_281	c_a_281*ERBP_G_GABP_PhоА	0.03	s ⁻¹	33 (SI.I) + [1,16]
363	ERBP_G_GABP_PKP + PIP2 <-> ERBP_G_GABP_PKP_PIP2	c_a_282f	c_a_282f*ERBP_G_GABP_PKP*PIP2 - c_a_282r*ERBP_G_GABP_PKP_PIP2	6.25	nM ⁻¹ .s ⁻¹	1 - 3, 31 - 33 (SI.I) + [1,16]
364	ERBP_G_GABP_PKP + PIP2 <-> ERBP_G_GABP_PKP_PIP2	c_a_282r		3.5	s ⁻¹	1 - 3, 31 - 33 (SI.I) + [1,16]
365	ERBP_ShP_G_GABP_PKP + PIP2 <-> ERBP_ShP_G_GABP_PKP_PIP2	c_a_283f	c_a_283f*ERBP_ShP_G_GABP_PKP*PIP2 - c_a_283r*ERBP_ShP_G_GABP_PKP_PIP2	6.25	nM ⁻¹ .s ⁻¹	1 - 3, 31 - 33 (SI.I) + [1,16]
366	ERBP_ShP_G_GABP_PKP + PIP2 <-> ERBP_ShP_G_GABP_PKP_PIP2	c_a_283r		3.5	s ⁻¹	1 - 3, 31 - 33 (SI.I) + [1,16]
367	ERBP_G_GABP_PKP_PIP2 -> ERBP_G_GABP_PKP + PIP3	c_a_284	c_a_284*ERBP_G_GABP_PKP_PIP2	25	s ⁻¹	1 - 3, 31 - 33 (SI.I) + [1,16]
368	ERBP_ShP_G_GABP_PKP_PIP2 -> ERBP_ShP_G_GABP_PKP + PIP3	c_a_285	c_a_285*ERBP_ShP_G_GABP_PKP_PIP2	25	s ⁻¹	1 - 3, 31 - 33 (SI.I) + [1,16]
369	ERBP_G_GABP_PKP + PIP3 <-> ERBP_G_GABP_PKP_PIP3	c_a_288f	c_a_288f*ERBP_G_GABP_PKP*PIP3 - c_a_288r*ERBP_G_GABP_PKP_PIP3	25	nM ⁻¹ .s ⁻¹	1 - 3, 31 - 33 (SI.I) + [1,16]
370	ERBP_G_GABP_PKP + PIP3 <-> ERBP_G_GABP_PKP_PIP3	c_a_288r		3	s ⁻¹	1 - 3, 31 - 33 (SI.I) + [1,16]
371	ERBP_ShP_G_GABP_PKP + PIP3 <-> ERBP_ShP_G_GABP_PKP_PIP3	c_a_289f	c_a_289f*ERBP_ShP_G_GABP_PKP*PIP3 - c_a_289r*ERBP_ShP_G_GABP_PKP_PIP3	25	nM ⁻¹ .s ⁻¹	1 - 3, 31 - 33 (SI.I) + [1,16]
372	ERBP_ShP_G_GABP_PKP + PIP3 <-> ERBP_ShP_G_GABP_PKP_PIP3	c_a_289r		3	s ⁻¹	1 - 3, 31 - 33 (SI.I) + [1,16]
373	ERBP_ShP_G + GABP <-> ERBP_ShP_G_GABP	c_a_290r	c_a_290r*ERBP_ShP_G*GABP - c_a_290f*ERBP_ShP_G_GABP	0.01	nM ⁻¹ .s ⁻¹	1 - 3, 31 - 33 (SI.I) + [1,16]
374	ERBP_ShP_G + GABP <-> ERBP_ShP_G_GABP	c_a_290f		1	s ⁻¹	1 - 3, 31 - 33 (SI.I) + [1,16]
375	ERBP_G + GABP <-> ERBP_G_GABP	c_a_291r	c_a_291r*ERBP_G*GABP - c_a_291f*ERBP_G_GABP	0.01	nM ⁻¹ .s ⁻¹	1 - 3, 33 (SI.I) + [1,16]
376	ERBP_G + GABP <-> ERBP_G_GABP	c_a_291f		1	s ⁻¹	1 - 3, 33 (SI.I) + [1,16]
377	ERBP_G + GAB_PIP3 <-> ERBP_G_GAB_PIP3	c_a_297f	c_a_297f*ERBP_G*GAB_PIP3 - c_a_297r*ERBP_G_GAB_PIP3	2.5	nM ⁻¹ .s ⁻¹	1 - 3, 33 (SI.I) + [1,16]

378	ERBP_G + GAB_PIP3 <-> ERBP_G_GAB_PIP3	c_a_297r		1	s ⁻¹	1 - 3, 33 (SI.I) + [1,16]
379	ERBP_ShP_G + GAB_PIP3 <-> ERBP_ShP_G_GAB_PIP3	c_a_299r	c_a_299r*ERBP_ShP_G*GAB_PIP3 - c_a_299r*ERBP_ShP_G_GAB_PIP3	2.5	nM ⁻¹ .s ⁻¹	1 - 3, 33 (SI.I) + [1,16]
380	ERBP_ShP_G + GAB_PIP3 <-> ERBP_ShP_G_GAB_PIP3	c_a_299f		1	s ⁻¹	1 - 3, 33 (SI.I) + [1,16]
381	ERBP_ShP_G_GAB_PIP3 -> ERBP_ShP_G_GABP + PIP3	c_a_300	c_a_300*ERBP_ShP_G_GAB_PIP3	0.01	s ⁻¹	1 - 3, 33 (SI.I) + [1,16]
382	ERBP_G_GABP_PKP + PhoB <-> ERBP_G_GABP_PKP_Phob	c_a_317f	c_a_317f*ERBP_G_GABP_PKP*PhoB - c_a_317r*ERBP_G_GABP_PKP_Phob	0.001	nM ⁻¹ .s ⁻¹	1 - 3, 33 (SI.I) + [1,16]
383	ERBP_G_GABP_PKP + PhoB <-> ERBP_G_GABP_PKP_Phob	c_a_317r		0.038	s ⁻¹	1 - 3, 33 (SI.I) + [1,16]
384	ERBP_G_GABP_PKP_Phob -> ERBP_G_GABP_PK_Phob	c_a_318	c_a_318*ERBP_G_GABP_PKP_Phob	0.595	s ⁻¹	1 - 3, 33 (SI.I) + [1,16]
385	ERBP_ShP_G_GABP_PKP + PhoB <-> ERBP_ShP_G_GABP_PKP_Phob	c_a_319f	c_a_319f*ERBP_ShP_G_GABP_PKP*PhoB - c_a_319r*ERBP_ShP_G_GABP_PKP_Phob	0.001	nM ⁻¹ .s ⁻¹	1 - 3, 33 (SI.I) + [1,16]
386	ERBP_ShP_G_GABP_PKP + PhoB <-> ERBP_ShP_G_GABP_PKP_Phob	c_a_319r		0.038	s ⁻¹	1 - 3, 33 (SI.I) + [1,16]
387	ERBP_ShP_G_GABP_PKP_Phob -> ERBP_ShP_G_GABP_PK_Phob	c_a_320	c_a_320*ERBP_ShP_G_GABP_PKP_Phob	0.595	s ⁻¹	1 - 3, 33 (SI.I) + [1,16]
388	ERBP_ShP_G_GAB + PIP3 <-> ERBP_ShP_G_GAB_PIP3	c_a_323f	c_a_323f*ERBP_ShP_G_GAB*PIP3 - c_a_323r*ERBP_ShP_G_GAB_PIP3	2.5	nM ⁻¹ .s ⁻¹	1 - 3, 33 (SI.I) + [1,16]
389	ERBP_ShP_G_GAB + PIP3 <-> ERBP_ShP_G_GAB_PIP3	c_a_323r		1	s ⁻¹	1 - 3, 33 (SI.I) + [1,16]
390	ERBP_PKP + PIP2 <-> ERBP_PKP_PIP2	c_a_326f	c_a_326f*ERBP_PKP*PIP2 - c_a_326r*ERBP_PKP_PIP2	6.25	nM ⁻¹ .s ⁻¹	1 - 3, 31, 32 (SI.I) + [1,16]
391	ERBP_PKP + PIP2 <-> ERBP_PKP_PIP2	c_a_326r		3.5	s ⁻¹	1 - 3, 31, 32 (SI.I) + [1,16]
392	ERBP_PKP_PIP2 -> ERBP_PKP + PIP3	c_a_327f	c_a_327f*ERBP_PKP_PIP2	2.5	s ⁻¹	1 - 3, 31, 32 (SI.I) + [1,16]
393	ERBP_ShP_G_GABP_PKP <-> ERBP_ShP_G_GABP + PKP	c_a_328f	c_a_328f*ERBP_ShP_G_GABP_PKP - c_a_328r*ERBP_ShP_G_GABP*PKP	5	s ⁻¹	1 - 3, 31, 32 (SI.I) + [1,16]
394	ERBP_ShP_G_GABP_PKP <-> ERBP_ShP_G_GABP + PKP	c_a_328r		0.05	nM ⁻¹ .s ⁻¹	1 - 3, 31, 32 (SI.I) + [1,16]
395	ERBP_G_GABP_PKP <-> ERBP_G_GABP + PKP	c_a_329f	c_a_329f*ERBP_G_GABP_PKP - c_a_329r*ERBP_G_GABP*PKP	5	s ⁻¹	1 - 3, 31, 32 (SI.I) + [1,16]
396	ERBP_G_GABP_PKP <-> ERBP_G_GABP + PKP	c_a_329r		0.05	nM ⁻¹ .s ⁻¹	1 - 3, 31, 32 (SI.I) + [1,16]
397	ERBP_G_GAB_PIP3 -> ERBP_G_GABP + PIP3	c_a_330	c_a_330*ERBP_G_GAB_PIP3	0.01	s ⁻¹	1 - 3, 31, 32 (SI.I) + [1,16]

398	ERBP_G_GAB + PIP3 <-> ERBP_G_GAB_PIP3	c_a_336f	c_a_336f*ERBP_G_GAB*PIP3 - c_a_336r*ERBP_G_GAB_PIP3	1	nM ⁻¹ .s ⁻¹	1 – 3, 31, 32 (SI.I) + [1,16]
399	ERBP_G_GAB + PIP3 <-> ERBP_G_GAB_PIP3	c_a_336r		2.5	s ⁻¹	1 – 3, 31, 32 (SI.I) + [1,16]
400	ERB3P + PLCy <-> ERB3P_PL	c_b_185f	c_b_185f*ERB3P*PLCy - c_b_185r*ERB3P_PL	0.06	nM ⁻¹ .s ⁻¹	1 – 3 (SI.I) + [1,16]
401	ERB3P + PLCy <-> ERB3P_PL	c_b_185r		0.2	s ⁻¹	1 – 3 (SI.I) + [1,16]
402	ERB3P_PL > ERB3P_PLP	c_b_186f	c_b_186f*ERB3P_PL	1	s ⁻¹	1 – 3 (SI.I) + [1,16]
403	ERB3P_PLP <-> ERB3P + PLCyP	c_b_187f	c_b_187f*ERB3P_PLP - c_b_187r*ERB3P*PLCyP	0.3	s ⁻¹	1 – 3 (SI.I) + [1,16]
404	ERB3P_PLP <-> ERB3P + PLCyP	c_b_187r		0.006	nM ⁻¹ .s ⁻¹	1 – 3 (SI.I) + [1,16]
405	ERB3P + Grb <-> ERB3P_G	c_b_190f	c_b_190f*ERB3P*Grb - c_b_190r*ERB3P_G	0.0015	nM ⁻¹ .s ⁻¹	1 – 5 (SI.I) + [1,16]
406	ERB3P + Grb <-> ERB3P_G	c_b_190r		0.2	s ⁻¹	1 – 5 (SI.I) + [1,16]
407	ERB3P_G + SOS <-> ERB3P_G_S	c_b_191f	c_b_191f*ERB3P_G*SOS - c_b_191r*ERB3P_G_S	0.01	nM ⁻¹ .s ⁻¹	1 – 5 (SI.I) + [1,16]
408	ERB3P_G + SOS <-> ERB3P_G_S	c_b_191r		0.06	s ⁻¹	1 – 5 (SI.I) + [1,16]
409	ERB3P_G_S <-> ERB3P + G_S	c_b_192f	c_b_192f*ERB3P_G_S - c_b_192r*ERB3P*G_S	0.15	s ⁻¹	1 – 5 (SI.I) + [1,16]
410	ERB3P_G_S <-> ERB3P + G_S	c_b_192r		0.0028	nM ⁻¹ .s ⁻¹	1 – 5 (SI.I) + [1,16]
411	ERB3P + Shc <-> ERB3P_Sh	c_b_194f	c_b_194f*ERB3P*Shc - c_b_194r*ERB3P_Sh	0.09	nM ⁻¹ .s ⁻¹	1 – 5 (SI.I) + [1,16]
412	ERB3P + Shc <-> ERB3P_Sh	c_b_194r		0.6	s ⁻¹	1 – 5 (SI.I) + [1,16]
413	ERB3P_Sh > ERB3P_ShP	c_b_195f	c_b_195f*ERB3P_Sh	6	s ⁻¹	1 – 5 (SI.I) + [1,16]
414	ERB3P_ShP <-> ShP + ERB3P	c_b_196f	c_b_196f*ERB3P_ShP - c_b_196r*ShP*ERB3P	0.3	s ⁻¹	1 – 5 (SI.I) + [1,16]
415	ERB3P_ShP <-> ShP + ERB3P	c_b_196r		0.0009	nM ⁻¹ .s ⁻¹	1 – 5 (SI.I) + [1,16]
416	ERB3P_ShP + Grb <-> ERB3P_ShP_G	c_b_197f	c_b_197f*ERB3P_ShP*Grb - c_b_197r*ERB3P_ShP_G	0.003	nM ⁻¹ .s ⁻¹	1 – 5 (SI.I) + [1,16]
417	ERB3P_ShP + Grb <-> ERB3P_ShP_G	c_b_197r		0.1	s ⁻¹	1 – 5 (SI.I) + [1,16]
418	ERB3P_ShP_G <-> ERB3P + ShP_G	c_b_198f	c_b_198f*ERB3P_ShP_G - c_b_198r*ERB3P*ShP_G	0.3	s ⁻¹	1 – 5 (SI.I) + [1,16]
419	ERB3P_ShP_G <-> ERB3P + ShP_G	c_b_198r		0.0009	nM ⁻¹ .s ⁻¹	1 – 5 (SI.I) + [1,16]
420	ERB3P_ShP_G + SOS <-> ERB3P_ShP_G_S	c_b_199f	c_b_199f*ERB3P_ShP_G*SOS - c_b_199r*ERB3P_ShP_G_S	0.01	nM ⁻¹ .s ⁻¹	1 – 6 (SI.I) + [1,16]
421	ERB3P_ShP_G + SOS <-> ERB3P_ShP_G_S	c_b_199r		0.0214	s ⁻¹	1 – 6 (SI.I) + [1,16]
422	ERB3P_ShP_G_S <-> ShP_G_S + ERB3P	c_b_200f	c_b_200f*ERB3P_ShP_G_S - c_b_200r*ShP_G_S*ERB3P	0.12	s ⁻¹	1 – 6 (SI.I) + [1,16]
423	ERB3P_ShP_G_S <-> ShP_G_S + ERB3P	c_b_200r		0.00024	nM ⁻¹ .s ⁻¹	1 – 6 (SI.I) + [1,16]
424	ERB3P_ShP_G_S <-> ERB3P_ShP_G_S	c_b_205f	c_b_205f*ERB3P_ShP_G_S - c_b_205r*ERB3P_ShP_G_S	0.009	nM ⁻¹ .s ⁻¹	1 – 6 (SI.I) + [1,16]

425	ERB3P_ShP + G_S <-> ERB3P_ShP_G_S	c_b_205r		0.0429	s ⁻¹	1 – 6 (SI.I) + [1,16]
426	ERB3P_ShP_G_S + Ras_GDP <-> ERB3P_Sh_G_S_Ras_GDP	c_b_209f	c_b_209f*ERB3P_ShP_G_S*Ras_GDP - c_b_209r*ERB3P_Sh_G_S_Ras_GDP	0.00475	nM ⁻¹ .s ⁻¹	1 – 8 (SI.I) + [1,16]
427	ERB3P_ShP_G_S + Ras_GDP <-> ERB3P_Sh_G_S_Ras_GDP	c_b_209r		0.76	s ⁻¹	1 – 8 (SI.I) + [1,16]
428	ERB3P_Sh_G_S_Ras_GDP <-> ERB3P_Sh_G_S_Ras + GDP	c_b_210f	c_b_210f*ERB3P_Sh_G_S_Ras_GDP - c_b_210r*ERB3P_Sh_G_S_Ras*GDP	46.5	s ⁻¹	1 – 8 (SI.I) + [1,16]
429	ERB3P_Sh_G_S_Ras_GDP <-> ERB3P_Sh_G_S_Ras + GDP	c_b_210r		0.093	nM ⁻¹ .s ⁻¹	1 – 8 (SI.I) + [1,16]
430	ERB3P_Sh_G_S_Ras + GTP <-> ERB3P_Sh_G_S_Ras_GTP	c_b_211f	c_b_211f*ERB3P_Sh_G_S_Ras*GTP - c_b_211r*ERB3P_Sh_G_S_Ras_GTP	0.003	nM ⁻¹ .s ⁻¹	1 – 8 (SI.I) + [1,16]
431	ERB3P_Sh_G_S_Ras + GTP <-> ERB3P_Sh_G_S_Ras_GTP	c_b_211r		2.4	s ⁻¹	1 – 8 (SI.I) + [1,16]
432	ERB3P_Sh_G_S_Ras_GTP <-> ERB3P_ShP_G_S + Ras_GTP	c_b_212f	c_b_212f*ERB3P_Sh_G_S_Ras_GTP - c_b_212r*ERB3P_ShP_G_S*Ras_GTP	806.4	s ⁻¹	1 – 8 (SI.I) + [1,16]
433	ERB3P_Sh_G_S_Ras_GTP <-> ERB3P_ShP_G_S + Ras_GTP	c_b_212r		1.575	nM ⁻¹ .s ⁻¹	1 – 8 (SI.I) + [1,16]
434	ERB3P_ShP_G_S + Ras <-> ERB3P_Sh_G_S_Ras	c_b_213f	c_b_213f*ERB3P_ShP_G_S*Ras - c_b_213r*ERB3P_Sh_G_S_Ras	0.15625	nM ⁻¹ .s ⁻¹	1 – 8 (SI.I) + [1,16]
435	ERB3P_ShP_G_S + Ras <-> ERB3P_Sh_G_S_Ras	c_b_213r		0.001	s ⁻¹	1 – 8 (SI.I) + [1,16]
436	ERB3P_G_S + Ras_GDP <-> ERB3P_G_S_Ras_GDP	c_b_214f	c_b_214f*ERB3P_G_S*Ras_GDP - c_b_214r*ERB3P_G_S_Ras_GDP	0.0075	nM ⁻¹ .s ⁻¹	1 – 8 (SI.I) + [1,16]
437	ERB3P_G_S + Ras_GDP <-> ERB3P_G_S_Ras_GDP	c_b_214r		1.2	s ⁻¹	1 – 8 (SI.I) + [1,16]
438	ERB3P_G_S_Ras_GDP <-> ERB3P_G_S_Ras + GDP	c_b_215f	c_b_215f*ERB3P_G_S_Ras_GDP - c_b_215r*ERB3P_G_S_Ras*GDP	50	s ⁻¹	1 – 8 (SI.I) + [1,16]
439	ERB3P_G_S_Ras_GDP <-> ERB3P_G_S_Ras + GDP	c_b_215r		0.1	nM ⁻¹ .s ⁻¹	1 – 8 (SI.I) + [1,16]
440	ERB3P_G_S_Ras + GTP <-> ERB3P_G_S_Ras_GTP	c_b_216f	c_b_216f*ERB3P_G_S_Ras*GTP - c_b_216r*ERB3P_G_S_Ras_GTP	0.1	nM ⁻¹ .s ⁻¹	1 – 8 (SI.I) + [1,16]
441	ERB3P_G_S_Ras + GTP <-> ERB3P_G_S_Ras_GTP	c_b_216r		80	s ⁻¹	1 – 8 (SI.I) + [1,16]
442	ERB3P_G_S_Ras_GTP <-> ERB3P_G_S + Ras_GTP	c_b_217f	c_b_217f*ERB3P_G_S_Ras_GTP - c_b_217r*ERB3P_G_S*Ras_GTP	640	s ⁻¹	1 – 8 (SI.I) + [1,16]
443	ERB3P_G_S_Ras_GTP <-> ERB3P_G_S + Ras_GTP	c_b_217r		1.25	nM ⁻¹ .s ⁻¹	1 – 8 (SI.I) + [1,16]
444	ERB3P_G_S + Ras <-> ERB3P_G_S_Ras	c_b_218f	c_b_218f*ERB3P_G_S*Ras - c_b_218r*ERB3P_G_S_Ras	0.25	nM ⁻¹ .s ⁻¹	1 – 8 (SI.I) + [1,16]
445	ERB3P_G_S + Ras <-> ERB3P_G_S_Ras	c_b_218r		0.0016	s ⁻¹	1 – 8 (SI.I) + [1,16]

446	GAP + ERB3P <-> ERB3P_GAP	c_b_239f	c_b_239f*GAP*ERB3P - c_b_239r*ERB3P_GAP	0.083	nM ⁻¹ .s ⁻¹	1 – 8 (SI.I) + [1,16]
447	GAP + ERB3P <-> ERB3P_GAP	c_b_239r		0.15	s ⁻¹	1 – 8 (SI.I) + [1,16]
448	Ras_GTP + ERB3P_GAP <-> ERB3P_GAP_Ras_GTP	c_b_240f	c_b_240f*Ras_GTP*ERB3P_GAP - c_b_240r*ERB3P_GAP_Ras_GTP	0.01	nM ⁻¹ .s ⁻¹	1 – 8 (SI.I) + [1,16]
449	Ras_GTP + ERB3P_GAP <-> ERB3P_GAP_Ras_GTP	c_b_240r		0.03	s ⁻¹	1 – 8 (SI.I) + [1,16]
450	ERB3P_GAP_Ras_GTP -> ERB3P_GAP + Ras_GDP	c_b_241	c_b_241*ERB3P_GAP_Ras_GTP	1.494	s ⁻¹	1 – 8 (SI.I) + [1,16]
451	ERB3P_ShP_G_S + ERKPP <-> ERB3P_Sh_G_S_ERKPP	c_b_250f	c_b_250f*ERB3P_ShP_G_S*ERKPP - c_b_250r*ERB3P_Sh_G_S_ERKPP	0.01	nM ⁻¹ .s ⁻¹	11, 24, 25 (SI.I) + [1,16]
452	ERB3P_ShP_G_S + ERKPP <-> ERB3P_Sh_G_S_ERKPP	c_b_250r		0.033	s ⁻¹	11, 24, 25 (SI.I) + [1,16]
453	ERB3P_Sh_G_S_ERKPP -> ERB3P_ShP_G + ERKPP + SOSP	c_b_251	c_b_251*ERB3P_Sh_G_S_ERKPP	1	s ⁻¹	11, 24, 25 (SI.I) + [1,16]
454	ERB3P_G_S + ERKPP <-> ERB3P_G_S_ERKPP	c_b_252f	c_b_252f*ERB3P_G_S*ERKPP - c_b_252r*ERB3P_G_S_ERKPP	0.01	nM ⁻¹ .s ⁻¹	11, 24, 25 (SI.I) + [1,16]
455	ERB3P_G_S + ERKPP <-> ERB3P_G_S_ERKPP	c_b_252r		0.033	s ⁻¹	11, 24, 25 (SI.I) + [1,16]
456	ERB3P_G_S_ERKPP -> ERB3P_G + SOSP + ERKPP	c_b_253	c_b_253*ERB3P_G_S_ERKPP	1	s ⁻¹	11, 24, 25 (SI.I) + [1,16]
457	ERB3P_G + GAB <-> ERB3P_G_GAB	c_b_256f	c_b_256f*ERB3P_G*GAB - c_b_256r*ERB3P_G_GAB	0.01	nM ⁻¹ .s ⁻¹	33 (SI.I) + [1,16]
458	ERB3P_G + GAB <-> ERB3P_G_GAB	c_b_256r		1	s ⁻¹	33 (SI.I) + [1,16]
459	ERB3P_ShP_G + GAB <-> ERB3P_ShP_G_GAB	c_b_257f	c_b_257f*ERB3P_ShP_G*GAB - c_b_257r*ERB3P_ShP_G_GAB	0.01	nM ⁻¹ .s ⁻¹	33 (SI.I) + [1,16]
460	ERB3P_ShP_G + GAB <-> ERB3P_ShP_G_GAB	c_b_257r		1	s ⁻¹	33 (SI.I) + [1,16]
461	ERB3P_G_GAB -> ERB3P_G_GABP	c_b_258	c_b_258*ERB3P_G_GAB	0.05	s ⁻¹	33 (SI.I) + [1,16]
462	ERB3P_ShP_G_GAB -> ERB3P_ShP_G_GABP	c_b_259	c_b_259*ERB3P_ShP_G_GAB	0.05	s ⁻¹	33 (SI.I) + [1,16]
463	ERB3P_G_GABP + PI3K <-> ERB3P_G_GABP_PK	c_b_260f	c_b_260f*ERB3P_G_GABP*PI3K - c_b_260r*ERB3P_G_GABP_PK	0.01	nM ⁻¹ .s ⁻¹	33 (SI.I) + [12-13,16]
464	ERB3P_G_GABP + PI3K <-> ERB3P_G_GABP_PK	c_b_260r		1	s ⁻¹	33 (SI.I) + [12-13,16]
465	ERB3P_G_GABP_PK -> ERB3P_G_GABP_PKP	c_b_262	c_b_262*ERB3P_G_GABP_PK	1	s ⁻¹	33 (SI.I) + [12-13,16]
466	ERB3P_ShP_G_GABP + PI3K <-> ERB3P_ShP_G_GABP_PK	c_b_261f	c_b_261f*ERB3P_ShP_G_GABP*PI3K - c_b_261r*ERB3P_ShP_G_GABP_PK	0.01	nM ⁻¹ .s ⁻¹	33 (SI.I) + [12-13,16]
467	ERB3P_ShP_G_GABP + PI3K <-> ERB3P_ShP_G_GABP_PK	c_b_261r		1	s ⁻¹	33 (SI.I) + [12-13,16]

468	ERB3P_ShP_G_GABP_PK -> ERB3P_ShP_G_GABP_PKP	c_b_263	c_b_263*ERB3P_ShP_G_GABP_PK	1	s ⁻¹	33 (SI.I) + [12-13,16]
469	ERB3P_ShP_G_GABP + GAP <-> ERB3P_ShP_G_GABP_GAP	c_b_264f	c_b_264f*ERB3P_ShP_G_GABP*GAP - c_b_264r*ERB3P_ShP_G_GABP_GAP	0.083	nM ⁻¹ .s ⁻¹	33 (SI.I) + [1,16]
470	ERB3P_ShP_G_GABP + GAP <-> ERB3P_ShP_G_GABP_GAP	c_b_264r		0.15	s ⁻¹	33 (SI.I) + [12-13,16]
471	ERB3P_G_GABP + GAP <-> ERB3P_G_GABP_GAP	c_b_265f	c_b_265f*ERB3P_G_GABP*GAP - c_b_265r*ERB3P_G_GABP_GAP	0.083	nM ⁻¹ .s ⁻¹	33 (SI.I) + [1,16]
472	ERB3P_G_GABP + GAP <-> ERB3P_G_GABP_GAP	c_b_265r		0.15	s ⁻¹	33 (SI.I) + [12-13,16]
473	ERB3P_G_GABP_GAP + Ras_GTP <-> ERB3P_G_GABP_GAP_Ras_GTP	c_b_266f	c_b_266f*ERB3P_G_GABP_GAP*Ras_GTP - c_b_266r*ERB3P_G_GABP_GAP_Ras_GTP	0.6225	nM ⁻¹ .s ⁻¹	7, 8, 33 (SI.I) + [12-13,16]
474	ERB3P_G_GABP_GAP + Ras_GTP <-> ERB3P_G_GABP_GAP_Ras_GTP	c_b_266r		0.3	s ⁻¹	7, 8, 33 (SI.I) + [12-13,16]
475	ERB3P_G_GABP_GAP_Ras_GTP -> ERB3P_G_GABP_GAP + Ras_GDP	c_b_267f	c_b_267f*ERB3P_G_GABP_GAP_Ras_GTP	1.494	s ⁻¹	7, 8, 33 (SI.I) + [12-13,16]
476	ERB3P_ShP_G_GABP_GAP + Ras_GTP <-> ERB3P_ShP_G_GABP_GAP_Ras_GTP	c_b_268f	c_b_268f*ERB3P_ShP_G_GABP_GAP*Ras_GTP - c_b_268r*ERB3P_ShP_G_GABP_GAP_Ras_GTP	0.6225	nM ⁻¹ .s ⁻¹	7, 8, 33 (SI.I) + [12-13,16]
477	ERB3P_ShP_G_GABP_GAP + Ras_GTP <-> ERB3P_ShP_G_GABP_GAP_Ras_GTP	c_b_268r		0.3	s ⁻¹	7, 8, 33 (SI.I) + [12-13,16]
478	ERB3P_ShP_G_GABP_GAP_Ras_GTP -> ERB3P_ShP_G_GABP_GAP + Ras_GDP	c_b_269	c_b_269*ERB3P_ShP_G_GABP_GAP_Ras_GTP	1.494	s ⁻¹	7, 8, 33 (SI.I) + [12-13,16]
479	ERB3P + PI3K <-> ERB3P_PK	c_b_270f	c_b_270f*ERB3P*PI3K - c_b_270r*ERB3P_PK	0.01	nM ⁻¹ .s ⁻¹	1 - 3, 31 - 32 (SI.I) + [1,16]
480	ERB3P + PI3K <-> ERB3P_PK	c_b_270r		1	s ⁻¹	1 - 3, 31-32 (SI.I) + [12-13,16]
481	ERB3P_PK -> ERB3P_PKP	c_b_271f	c_b_271f*ERB3P_PK	1	s ⁻¹	1 - 3, 31-32 (SI.I) + [12-13,16]
482	ERB3P + PKP <-> ERB3P_PKP	c_b_272r	c_b_272r*ERB3P*PKP - c_b_272f*ERB3P_PKP	0.01	nM ⁻¹ .s ⁻¹	31-32 (SI.I) + [12-13,16]
483	ERB3P + PKP <-> ERB3P_PKP	c_b_272f		0.1	s ⁻¹	31-32 (SI.I) + [12-13,16]
484	ERB3P_ShP_G_GABP + PhoA <-> ERB3P_ShP_G_GABP_PhоА	c_b_278f	c_b_278f*ERB3P_ShP_G_GABP*PhoA - c_b_278r*ERB3P_ShP_G_GABP_PhоА	0.001	nM ⁻¹ .s ⁻¹	33 (SI.I) + [1,13,16]
485	ERB3P_ShP_G_GABP + PhoA <-> ERB3P_ShP_G_GABP_PhоА	c_b_278r		0.1	s ⁻¹	33 (SI.I) + [11,13,16]
486	ERB3P_ShP_G_GABP_PhоА -> ERB3P_ShP_G_GAB + PhoA	c_b_280	c_b_280*ERB3P_ShP_G_GABP_PhоА	0.03	s ⁻¹	33 (SI.I) + [11,13,16]
487	ERB3P_G_GABP + PhoA <-> ERB3P_G_GABP_PhоА	c_b_279f	c_b_279f*ERB3P_G_GABP*PhoA - c_b_279r*ERB3P_G_GABP_PhоА	0.001	nM ⁻¹ .s ⁻¹	33 (SI.I) + [11,13,16]
488	ERB3P_G_GABP + PhoA <-> ERB3P_G_GABP_PhоА	c_b_279r		0.1	s ⁻¹	33 (SI.I) + [11,13,16]

489	ERB3P_G_GABP_PhоА -> ERB3P_G_GAB + PhоА	c_b_281	c_b_281*ERB3P_G_GABP_PhоА	0.03	s ⁻¹	33 (SI.I) + [11,13,16]
490	ERB3P_G_GABP_PKP + PIP2 <-> ERB3P_G_GABP_PKP_PIP2	c_b_282f	c_b_282f*ERB3P_G_GABP_PKP*PIP2 - c_b_282r*ERB3P_G_GABP_PKP_PIP2	6.25	nM ⁻¹ .s ⁻¹	31 - 33 (SI.I) + [11,13,16]
491	ERB3P_G_GABP_PKP + PIP2 <-> ERB3P_G_GABP_PKP_PIP2	c_b_282r		3.5	s ⁻¹	31 - 33 (SI.I) + [11,13,16]
492	ERB3P_ShP_G_GABP_PKP + PIP2 <-> ERB3P_ShP_G_GABP_PKP_PIP2	c_b_283f	c_b_283f*ERB3P_ShP_G_GABP_PKP*PIP2 - c_b_283r*ERB3P_ShP_G_GABP_PKP_PIP2	6.25	nM ⁻¹ .s ⁻¹	31 - 33 (SI.I) + [11,13,16]
493	ERB3P_ShP_G_GABP_PKP + PIP2 <-> ERB3P_ShP_G_GABP_PKP_PIP2	c_b_283r		3.5	s ⁻¹	31 - 33 (SI.I) + [11,13,16]
494	ERB3P_G_GABP_PKP_PIP2 -> ERB3P_G_GABP_PKP + PIP3	c_b_284	c_b_284*ERB3P_G_GABP_PKP_PIP2	25	s ⁻¹	31 - 33 (SI.I) + [11,13,16]
495	ERB3P_ShP_G_GABP_PKP_PIP2 -> ERB3P_ShP_G_GABP_PKP + PIP3	c_b_285	c_b_285*ERB3P_ShP_G_GABP_PKP_PIP2	25	s ⁻¹	31 - 33 (SI.I) + [11,13,16]
496	ERB3P_ShP_G + GABP <-> ERB3P_ShP_G_GABP	c_b_290r	c_b_290r*ERB3P_ShP_G*GABP - c_b_290f*ERB3P_ShP_G_GABP	0.01	nM ⁻¹ .s ⁻¹	33 (SI.I) + [11,13,16]
497	ERB3P_ShP_G + GABP <-> ERB3P_ShP_G_GABP	c_b_290f		1	s ⁻¹	33 (SI.I) + [11,13,16]
498	ERB3P_G + GABP <-> ERB3P_G_GABP	c_b_291r	c_b_291r*ERB3P_G*GABP - c_b_291f*ERB3P_G_GABP	0.01	nM ⁻¹ .s ⁻¹	33 (SI.I) + [11,13,16]
499	ERB3P_G + GABP <-> ERB3P_G_GABP	c_b_291f		1	s ⁻¹	33 (SI.I) + [11,13,16]
500	ERB3P_G + GAB_PIP3 <-> ERB3P_G_GAB_PIP3	c_b_297f	c_b_297f*ERB3P_G*GAB_PIP3 - c_b_297r*ERB3P_G_GAB_PIP3	2.5	nM ⁻¹ .s ⁻¹	33 (SI.I) + [11,13,16]
501	ERB3P_G + GAB_PIP3 <-> ERB3P_G_GAB_PIP3	c_b_297r		1	s ⁻¹	33 (SI.I) + [11,13,16]
502	ERB3P_ShP_G + GAB_PIP3 <-> ERB3P_ShP_G_GAB_PIP3	c_b_299r	c_b_299r*ERB3P_ShP_G*GAB_PIP3 - c_b_299f*ERB3P_ShP_G_GAB_PIP3	2.5	nM ⁻¹ .s ⁻¹	33 (SI.I) + [11,13,16]
503	ERB3P_ShP_G + GAB_PIP3 <-> ERB3P_ShP_G_GAB_PIP3	c_b_299f		1	s ⁻¹	33 (SI.I) + [11,13,16]
504	ERB3P_ShP_G_GAB_PIP3 -> ERB3P_ShP_G_GABP + PIP3	c_b_300	c_b_300*ERB3P_ShP_G_GAB_PIP3	0.01	s ⁻¹	33 (SI.I) + [11,13,16]
505	ERB3P_G_GABP_PKP + PhoB <-> ERB3P_G_GABP_PKP_PhоB	c_b_317f	c_b_317f*ERB3P_G_GABP_PKP*PhoB - c_b_317r*ERB3P_G_GABP_PKP_PhоB	0.001	nM ⁻¹ .s ⁻¹	31 - 33 (SI.I) + [11,13,16]
506	ERB3P_G_GABP_PKP + PhoB <-> ERB3P_G_GABP_PKP_PhоB	c_b_317r		0.038	s ⁻¹	31 - 33 (SI.I) + [11,13,16]
507	ERB3P_G_GABP_PKP_PhоB -> ERB3P_G_GABP_PKP + PhoB	c_b_318	c_b_318*ERB3P_G_GABP_PKP_PhоB	0.595	s ⁻¹	31 - 33 (SI.I) + [11,13,16]
508	ERB3P_ShP_G_GABP_PKP + PhoB <-> ERB3P_ShP_G_GABP_PKP_PhоB	c_b_319f	c_b_319f*ERB3P_ShP_G_GABP_PKP*PhoB - c_b_319r*ERB3P_ShP_G_GABP_PKP_PhоB	0.001	nM ⁻¹ .s ⁻¹	31 - 33 (SI.I) + [11,13,16]
509	ERB3P_ShP_G_GABP_PKP + PhoB <-> ERB3P_ShP_G_GABP_PKP_PhоB	c_b_319r		0.038	s ⁻¹	31 - 33 (SI.I) + [11,13,16]

510	ERB3P_ShP_G_GABP_PKP_Phob -> ERB3P_ShP_G_GABP_PK + Phob	c_b_320	c_b_320*ERB3P_ShP_G_GABP_PKP_Phob	0.595	s ⁻¹	31 - 33 (SI.I) + [11,13,16]
511	ERB3P_ShP_G_GAB + PIP3 <-> ERB3P_ShP_G_GAB_PIP3	c_b_323f	c_b_323f*ERB3P_ShP_G_GAB*PIP3 - c_b_323r*ERB3P_ShP_G_GAB_PIP3	2.5	nM ⁻¹ .s ⁻¹	31 - 33 (SI.I) + [11,13,16]
512	ERB3P_ShP_G_GAB + PIP3 <-> ERB3P_ShP_G_GAB_PIP3	c_b_323r		1	s ⁻¹	31 - 33 (SI.I) + [11,13,16]
513	ERB3P_PKP + PIP2 <-> ERB3P_PKP_PIP2	c_b_326f	c_b_326f*ERB3P_PKP*PIP2 - c_b_326r*ERB3P_PKP_PIP2	6.25	nM ⁻¹ .s ⁻¹	31 - 32 (SI.I) + [11,13,16]
514	ERB3P_PKP + PIP2 <-> ERB3P_PKP_PIP2	c_b_326r		3.5	s ⁻¹	31 - 32 (SI.I) + [11,13,16]
515	ERB3P_PKP_PIP2 -> ERB3P_PKP + PIP3	c_b_327f	c_b_327f*ERB3P_PKP_PIP2	2.5	s ⁻¹	31 - 32 (SI.I) + [11,13,16]
516	ERB3P_ShP_G_GABP_PKP <-> ERB3P_ShP_G_GABP + PKP	c_b_328f	c_b_328f*ERB3P_ShP_G_GABP_PKP - c_b_328r*ERB3P_ShP_G_GABP*PKP	5	s ⁻¹	31 - 33 (SI.I) + [11,13,16]
517	ERB3P_ShP_G_GABP_PKP <-> ERB3P_ShP_G_GABP + PKP	c_b_328r		0.05	nM ⁻¹ .s ⁻¹	31 - 33 (SI.I) + [11,13,16]
518	ERB3P_G_GABP_PKP <-> ERB3P_G_GABP + PKP	c_b_329f	c_b_329f*ERB3P_G_GABP_PKP - c_b_329r*ERB3P_G_GABP*PKP	5	s ⁻¹	31 - 33 (SI.I) + [11,13,16]
519	ERB3P_G_GABP_PKP <-> ERB3P_G_GABP + PKP	c_b_329r		0.05	nM ⁻¹ .s ⁻¹	31 - 33 (SI.I) + [11,13,16]
520	ERB3P_G_GAB_PIP3 -> ERB3P_G_GABP + PIP3	c_b_330	c_b_330*ERB3P_G_GAB_PIP3	0.01	s ⁻¹	31 - 33 (SI.I) + [11,13,16]
521	ERB3P_G_GAB + PIP3 <-> ERB3P_G_GAB_PIP3	c_b_336f	c_b_336f*ERB3P_G_GAB*PIP3 - c_b_336r*ERB3P_G_GAB_PIP3	1	nM ⁻¹ .s ⁻¹	31 - 33 (SI.I) + [11,13,16]
522	ERB3P_G_GAB + PIP3 <-> ERB3P_G_GAB_PIP3	c_b_336r		2.5	s ⁻¹	31 - 33 (SI.I) + [11,13,16]
523	R + ERB3 <-> R_ERB3	c217f	c217f*R*ERB3 - c217r*R_ERB3	0.0001	nM ⁻¹ .s ⁻¹	1 - 3 (SI.I) + [1-9,13,16]
524	R + ERB3 <-> R_ERB3	c217r		0.1	s ⁻¹	1 - 3 (SI.I) + [1-9,13,16]
525	EGF + R_ERB3 <-> RI_ERB3	c218f	c218f*EGF*R_ERB3 - c218r*RI_ERB3	0.0001	nM ⁻¹ .s ⁻¹	1 - 3 (SI.I) + [1-9,13,16]
526	EGF + R_ERB3 <-> RI_ERB3	c218r		0.1	s ⁻¹	1 - 3 (SI.I) + [1-9,13,16]
527	RI_ERB3 -> RIP_ERB3P	c219f	c219f*RI_ERB3	1	s ⁻¹	1 - 3 (SI.I) + [1-9,13,16]
528	RIP_ERB3P <-> EGF + RP_ERB3P	c220f	c220f*RIP_ERB3P - c220r*EGF*RP_ERB3P	0.1	s ⁻¹	1 - 3 (SI.I) + [1-9,13,16]
529	RIP_ERB3P <-> EGF + RP_ERB3P	c220r		0.01	nM ⁻¹ .s ⁻¹	1 - 3 (SI.I) + [1-9,13,16]
530	RP_ERB3P <-> RP + ERB3P	c221f	c221f*RP_ERB3P - c221r*RP*ERB3P	0.1	s ⁻¹	1 - 3 (SI.I) + [1-9,13,16]
531	RP_ERB3P <-> RP + ERB3P	c221r		0.01	nM ⁻¹ .s ⁻¹	1 - 3 (SI.I) + [1-9,13,16]
532	RI + ERB3 <-> RI_ERB3	c223f	c223f*RI*ERB3 - c223r*RI_ERB3	0.001	nM ⁻¹ .s ⁻¹	1 - 3 (SI.I) + [1-9,13,16]
533	RI + ERB3 <-> RI_ERB3	c223r		0.1	s ⁻¹	1 - 3 (SI.I) + [1-9,13,16]
534	ERB3P + R <-> R_ERB3P	c224f	c224f*ERB3P*R - c224r*R_ERB3P	0.001	nM ⁻¹ .s ⁻¹	1 - 3 (SI.I) + [1-9,13,16]

535	ERB3P + R <-> R_ERB3P	c224r		0.1	s ⁻¹	1 - 3 (SI.I) + [1-9,13,16]
536	RIP_ERB3P <-> RIP + ERB3P	c226f	c226f*RIP_ERB3P - c227r_n*RIP*ERB3P	0.1	s ⁻¹	1 - 3 (SI.I) + [1-9,13,16]
537	RIP_ERB3P <-> RIP + ERB3P	c227r_n		0.01	nM ⁻¹ .s ⁻¹	1 - 3 (SI.I) + [1-9,13,16]
538	RP + ERB3 <-> RP_ERB3	c227f	c227f*RP*ERB3 - c227r*RP_ERB3	0.001	nM ⁻¹ .s ⁻¹	1 - 3 (SI.I) + [1-9,13,16]
539	RP + ERB3 <-> RP_ERB3	c227r		0.1	s ⁻¹	1 - 3 (SI.I) + [1-9,13,16]
540	RP_ERB3 -> RP_ERB3P	c228f	c228f*RP_ERB3	1	s ⁻¹	1 - 3 (SI.I) + [1-9,13,16]
541	ERB3 + ERB3 <-> ERB3_ERB3	c229f	c229f*ERB3*ERB3 - c229r*ERB3_ERB3	0.0001	nM ⁻¹ .s ⁻¹	1 - 3 (SI.I) + [1-9,13,16]
542	ERB3 + ERB3 <-> ERB3_ERB3	c229r		0.1	s ⁻¹	1 - 3 (SI.I) + [1-9,13,16]
543	ERB3P + ERB <-> ERB3P_ERB	c230f	c230f*ERB3P*ERB - c230r*ERB3P_ERB	0.01	nM ⁻¹ .s ⁻¹	1 - 3 (SI.I) + [1-9,13,16]
544	ERB3P + ERB <-> ERB3P_ERB	c230r		0.1	s ⁻¹	1 - 3 (SI.I) + [1-9,13,16]
545	ERB3P_ERB3P <-> ERB3P + ERB3P	c232f	c232f*ERB3P_ERB3P - c232r*ERB3P*ERB3P	0.1	s ⁻¹	1 - 3 (SI.I) + [1-9,13,16]
546	ERB3P_ERB3P <-> ERB3P + ERB3P	c232r		0.01	nM ⁻¹ .s ⁻¹	1 - 3 (SI.I) + [1-9,13,16]
547	ERB3 + ERB <-> ERB3_ERB	c233f	c233f*ERB3*ERB - c233r*ERB3_ERB	0.001	nM ⁻¹ .s ⁻¹	1 - 3 (SI.I) + [1-9,13,16]
548	ERB3 + ERB <-> ERB3_ERB	c233r		0.1	s ⁻¹	1 - 3 (SI.I) + [1-9,13,16]
549	EGF + ERB3_ERB <-> EGF_ERB3_ERB	c234f	c234f*EGF*ERB3_ERB - c234r*EGF_ERB3_ERB	0.0001	nM ⁻¹ .s ⁻¹	1 - 3 (SI.I) + [1-9,13,16]
550	EGF + ERB3_ERB <-> EGF_ERB3_ERB	c234r		0.1	s ⁻¹	1 - 3 (SI.I) + [1-9,13,16]
551	ERB3 + ERBP <-> ERB3_ERBP	c235f	c235f*ERB3*ERBP - c235r*ERB3_ERBP	0.001	nM ⁻¹ .s ⁻¹	1 - 3 (SI.I) + [1-9,13,16]
552	ERB3 + ERBP <-> ERB3_ERBP	c235r		0.1	s ⁻¹	1 - 3 (SI.I) + [1-9,13,16]
553	ERB3_ERBP -> ERB3P_ERBP	c236f	c236f*ERB3_ERBP	1	s ⁻¹	1 - 3 (SI.I) + [1-9,13,16]
554	ERB3P_ERBP <-> ERB3P + ERBP	c237f	c237f*ERB3P_ERBP - c237r*ERB3P*ERBP	0.1	s ⁻¹	1 - 3 (SI.I) + [1-9,13,16]
555	ERB3P_ERBP <-> ERB3P + ERBP	c237r		0.001	nM ⁻¹ .s ⁻¹	1 - 3 (SI.I) + [1-9,13,16]
556	EGF + ERB3 <-> EGF_ERB3	c238f	c238f*EGF*ERB3 - c238r*EGF_ERB3	0.0001	nM ⁻¹ .s ⁻¹	1 - 3 (SI.I) + [1-9,13,16]
557	EGF + ERB3 <-> EGF_ERB3	c238r		0.1	s ⁻¹	1 - 3 (SI.I) + [1-9,13,16]
558	EGF_ERB3 + R <-> EGF_ERB3_R	c239f	c239f*EGF_ERB3*R - c239r*EGF_ERB3_R	0.0001	nM ⁻¹ .s ⁻¹	1 - 3 (SI.I) + [1-9,13,16]
559	EGF_ERB3 + R <-> EGF_ERB3_R	c239r		0.1	s ⁻¹	1 - 3 (SI.I) + [1-9,13,16]
560	EGF_ERB3 + RP <-> EGF_ERB3_RP	c240f	c240f*EGF_ERB3*RP - c240r*EGF_ERB3_RP	0.0001	nM ⁻¹ .s ⁻¹	1 - 3 (SI.I) + [1-9,13,16]
561	EGF_ERB3 + RP <-> EGF_ERB3_RP	c240r		0.1	s ⁻¹	1 - 3 (SI.I) + [1-9,13,16]
562	EGF_ERB3_RP -> EGF_ERB3P_RP	c241f	c241f*EGF_ERB3_RP	1	s ⁻¹	1 - 3 (SI.I) + [1-9,13,16]
563	EGF_ERB3P_RP <-> EGF + RP_ERB3P	c242f	c242f*EGF_ERB3P_RP - c242r*EGF*RP_ERB3P	0.1	s ⁻¹	1 - 3 (SI.I) + [1-9,13,16]
564	EGF_ERB3P_RP <-> EGF + RP_ERB3P	c242r		0.0001	nM ⁻¹ .s ⁻¹	1 - 3 (SI.I) + [1-9,13,16]
565	EGF_ERB3P_RP <-> EGF_ERB3P + RP	c243f	c243f*EGF_ERB3P_RP - c243r*EGF_ERB3P*RP	0.1	s ⁻¹	1 - 3 (SI.I) + [1-9,13,16]

566	EGF_ERB3P_RP <-> EGF_ERB3P + RP	c243r		0.0001	nM ⁻¹ .s ⁻¹	1 - 3 (SI.I) + [1-9,13,16]
567	EGF_ERB3 + ERBP <-> EGF_ERB3_ERBP	c244f	c244f*EGF_ERB3*ERBP - c244r*EGF_ERB3_ERBP	0.0001	nM ⁻¹ .s ⁻¹	1 - 3 (SI.I) + [1-9,13,16]
568	EGF_ERB3 + ERBP <-> EGF_ERB3_ERBP	c244r		0.1	s ⁻¹	1 - 3 (SI.I) + [1-9,13,16]
569	EGF_ERB3_ERBP -> EGF_ERB3P_ERBP	c245f	c245f*EGF_ERB3_ERBP	1	s ⁻¹	1 - 3 (SI.I) + [1-9,13,16]
570	EGF_ERB3P_ERBP <-> EGF + ERB3P_ERBP	c246f	c246f*EGF_ERB3P_ERBP - c246r*EGF*ERB3P_ERBP	0.1	s ⁻¹	1 - 3 (SI.I) + [1-9,13,16]
571	EGF_ERB3P_ERBP <-> EGF + ERB3P_ERBP	c246r		0.0001	nM ⁻¹ .s ⁻¹	1 - 3 (SI.I) + [1-9,13,16]
572	EGF_ERB3 + ERB <-> EGF_ERB3_ERB	c247f	c247f*EGF_ERB3*ERB - c247r*EGF_ERB3_ERB	0.0001	nM ⁻¹ .s ⁻¹	1 - 3 (SI.I) + [1-9,13,16]
573	EGF_ERB3 + ERB <-> EGF_ERB3_ERB	c247r		0.1	s ⁻¹	1 - 3 (SI.I) + [1-9,13,16]
574	EGF_ERB3P_ERBP <-> EGF_ERB3P + ERBP	c248f	c248f*EGF_ERB3P_ERBP - c248r*EGF_ERB3P*ERBP	0.1	s ⁻¹	1 - 3 (SI.I) + [1-9,13,16]
575	EGF_ERB3P_ERBP <-> EGF_ERB3P + ERBP	c248r		0.0001	nM ⁻¹ .s ⁻¹	1 - 3 (SI.I) + [1-9,13,16]
576	EGF_ERB3 + ERB3 <-> EGF_ERB3_ERB3	c252f	c252f*EGF_ERB3*ERB3 - c252r*EGF_ERB3_ERB3	0.0001	nM ⁻¹ .s ⁻¹	1 - 3 (SI.I) + [1-9,13,16]
577	EGF_ERB3 + ERB3 <-> EGF_ERB3_ERB3	c252r		0.1	s ⁻¹	1 - 3 (SI.I) + [1-9,13,16]
578	EGF + ERB3_ERB3 <-> EGF_ERB3_ERB3	c253f	c253f*EGF*ERB3_ERB3 - c253r*EGF_ERB3_ERB3	0.0001	nM ⁻¹ .s ⁻¹	1 - 3 (SI.I) + [1-9,13,16]
579	EGF + ERB3_ERB3 <-> EGF_ERB3_ERB3	c253r		0.1	s ⁻¹	1 - 3 (SI.I) + [1-9,13,16]
580	CDC25CP + ERB3P <-> CDC25CP_ERB3P	c254f	c254f*CDC25CP*ERB3P - c254r*CDC25CP_ERB3P	0.01	nM ⁻¹ .s ⁻¹	26, 27 (SI.I) + [12-13,16]
581	CDC25CP + ERB3P <-> CDC25CP_ERB3P	c254r		0.1	s ⁻¹	26, 27 (SI.I) + [12-13,16]
582	CDC25CP_ERB3P -> CDC25CP + ERB3	c255f	c255f*CDC25CP_ERB3P	0.5	s ⁻¹	26, 27 (SI.I) + [12-13,16]
583	CDC25CP + ERB3P_ERB3P <-> CDC25CP_ERB3P_ERB3P	c256f	c256f*CDC25CP*ERB3P_ERB3P - c256r*CDC25CP_ERB3P_ERB3P	0.01	nM ⁻¹ .s ⁻¹	26, 27 (SI.I) + [12-13,16]
584	CDC25CP + ERB3P_ERB3P <-> CDC25CP_ERB3P_ERB3P	c256r		0.1	s ⁻¹	26, 27 (SI.I) + [12-13,16]
585	CDC25CP_ERB3P_ERB3P -> CDC25CP + ERB3_ERB3	c257f	c257f*CDC25CP_ERB3P_ERB3P	0.5	s ⁻¹	26, 27 (SI.I) + [12-13,16]
586	ERB3P + ERB3 <-> ERB3P_ERB3	c258f	c258f*ERB3P*ERB3 - c258r*ERB3P_ERB3	0.001	nM ⁻¹ .s ⁻¹	1 - 3 (SI.I) + [1-9,13,16]
587	ERB3P + ERB3 <-> ERB3P_ERB3	c258r		0.1	s ⁻¹	1 - 3 (SI.I) + [1-9,13,16]
588	R_ERB3P + EGF <-> RI_ERB3P	c259f	c259f*R_ERB3P*EGF - c259r*RI_ERB3P	0.01	nM ⁻¹ .s ⁻¹	1 - 3 (SI.I) + [1-9,13,16]
589	R_ERB3P + EGF <-> RI_ERB3P	c259r		0.1	s ⁻¹	1 - 3 (SI.I) + [1-9,13,16]
590	RI_ERB3P -> RIP_ERB3P	c260f	c260f*RI_ERB3P	1	s ⁻¹	1 - 3 (SI.I) + [1-9,13,16]
591	RP_ERB3P <-> ERB3P + RP	c261f	c261f*RP_ERB3P - c261r*ERB3P*RP	0.1	s ⁻¹	1 - 3 (SI.I) + [1-9,13,16]

592	RP_ERB3P <-> ERB3P + RP	c261r		0.01	nM ⁻¹ .s ⁻¹	1 - 3 (SI.I) + [1-9,13,16]
593	ERBP_PKP + PhoB <-> ERBP_PKP_Phob	c262f	c262f*ERBP_PKP*PhoB - c262r*ERBP_PKP_Phob	0.001	nM ⁻¹ .s ⁻¹	1 - 3, 31, 32 (SI.I) + [11,13,16]
594	ERBP_PKP + PhoB <-> ERBP_PKP_Phob	c262r	c263f*ERBP_PKP_Phob	0.038	s ⁻¹	1 - 3, 31, 32 (SI.I) + [11,13,16]
595	ERBP_PKP_Phob -> ERBP_PK + PhoB	c263f		0.595	s ⁻¹	1 - 3, 31, 32 (SI.I) + [1,16]
596	ERB3P_PKP + PhoB <-> ERB3P_PKP_Phob	c264f	c264f*ERB3P_PKP*PhoB - c264r*ERB3P_PKP_Phob	0.001	nM ⁻¹ .s ⁻¹	1 - 3, 31, 32 (SI.I) + [11,13,16]
597	ERB3P_PKP + PhoB <-> ERB3P_PKP_Phob	c264r		0.038	s ⁻¹	1 - 3, 31, 32 (SI.I) + [11,13,16]
598	ERB3P_PKP_Phob -> ERB3P_PK + PhoB	c265f	c265f*ERB3P_PKP_Phob	0.595	s ⁻¹	1 - 3, 31, 32 (SI.I) + [11,13,16]
599	RP_PKP + PhoB <-> RP_PKP_Phob	c266f	c266f*RP_PKP*PhoB - c266r*RP_PKP_Phob	0.001	nM ⁻¹ .s ⁻¹	1 - 3, 31, 32 (SI.I) + [11,13,16]
600	RP_PKP + PhoB <-> RP_PKP_Phob	c266r		0.038	s ⁻¹	1 - 3, 31, 32 (SI.I) + [11,13,16]
601	RP_PKP_Phob -> RP_PK + PhoB	c267f	c267f*RP_PKP_Phob	0.595	s ⁻¹	1 - 3, 31, 32 (SI.I) + [11,13,16]
602	ERB_ERB -> ERBP_ERBP	c268f	c268f*ERB_ERB	1	s ⁻¹	1 - 3, 31, 32 (SI.I) + [11,13,16]
603	BetaCatenin + Cadh <-> BetaCatenin_Cadh	c269f	c269f*BetaCatenin*Cadh - c269r*BetaCatenin_Cadh	0.01	nM ⁻¹ .s ⁻¹	55, 56 (SI.I) + [1]
604	BetaCatenin + Cadh <-> BetaCatenin_Cadh	c269r		0.01	s ⁻¹	55, 56 (SI.I) + [12-13]
605	BetaCatenin_Cadh + PTP <-> BetaCatenin_Cadh_PTP	c270f	c270f*BetaCatenin_Cadh*PTP - c270r*BetaCatenin_Cadh_PTP	0.01	nM ⁻¹ .s ⁻¹	55, 56 (SI.I) + [11,13]
606	BetaCatenin_Cadh + PTP <-> BetaCatenin_Cadh_PTP	c270r		1	s ⁻¹	55, 56 (SI.I) + [11,13]
607	Cadh + PTP <-> Cadh_PTP	c271f	c271f*Cadh*PTP - c271r*Cadh_PTP	0.01	nM ⁻¹ .s ⁻¹	55, 56 (SI.I) + [11,13]
608	Cadh + PTP <-> Cadh_PTP	c271r		1	s ⁻¹	55, 56 (SI.I) + [11,13]
609	BetaCatenin_Cadh + RP <-> BetaCatenin_Cadh_RP	c272f	c272f*BetaCatenin_Cadh*RP - c272r*BetaCatenin_Cadh_RP	2.5	nM ⁻¹ .s ⁻¹	55, 56 (SI.I) + [11,13,16]
610	BetaCatenin_Cadh + RP <-> BetaCatenin_Cadh_RP	c272r		1	s ⁻¹	55, 56 (SI.I) + [11,13,16]
611	BetaCatenin_Cadh_RP -> BetaCateninY654 + Cadh + RP	c273f	c273f*BetaCatenin_Cadh_RP	1	s ⁻¹	55, 56 (SI.I) + [11,13,16]
612	Cadh_PTP + BetaCateninY654 <-> BetaCateninY654_Cadh_PTP	c274f	c274f*Cadh_PTP*BetaCateninY654 - c274r*BetaCateninY654_Cadh_PTP	0.01	nM ⁻¹ .s ⁻¹	55, 56 (SI.I) + [11,13]
613	Cadh_PTP + BetaCateninY654 <-> BetaCateninY654_Cadh_PTP	c274r		0.1	s ⁻¹	55, 56 (SI.I) + [11,13]

614	BetaCateninY654_Cadh_PTP -> BetaCatenin + Cadh_PTP	c275f	c275f*BetaCateninY654_Cadh_PTP	1	s ⁻¹	55, 56 (SI.I) + [11,13]
615	BetaCatenin_Cadh_PTP <-> BetaCatenin + Cadh_PTP	c276f	c276f*BetaCatenin_Cadh_PTP - [276r)*BetaCatenin*Cadh_PTP	0.1	s ⁻¹	55, 56 (SI.I) + [11,13]
616	BetaCatenin_Cadh_PTP <-> BetaCatenin + Cadh_PTP	276r		0.01	nM ⁻¹ .s ⁻¹	55, 56 (SI.I) + [11,13]
617	BetaCatenin_Cadh + ERBP <-> BetaCatenin_Cadh_ERBP	c277f	c277f*BetaCatenin_Cadh*ERBP - c277r*BetaCatenin_Cadh_ERBP	2.5	nM ⁻¹ .s ⁻¹	55, 56 (SI.I) + [11,13,16]
618	BetaCatenin_Cadh + ERBP <-> BetaCatenin_Cadh_ERBP	c277r		1	s ⁻¹	55, 56 (SI.I) + [11,13,16]
619	BetaCatenin_Cadh_ERBP -> BetaCateninY654 + Cadh + ERBP	c278f	c278f*BetaCatenin_Cadh_ERBP	1	s ⁻¹	55, 56 (SI.I) + [11,13,16]
620	TGF + TGF <-> DIMTGF	c480f	c480f*TGF*TGF - c480r*DIMTGF	0.01	nM ⁻¹ .s ⁻¹	77 - 80 (SI.I) + [12-13,17-19]
621	TGF + TGF <-> DIMTGF	c480r		0.01	s ⁻¹	77 - 80 (SI.I) + [12-13,17-19]
622	DIMTGF + DIMTBRII <-> DIMTGF_DIMTBRII	C481F	C481F*DIMTGF*DIMTBRII - C481R*DIMTGF_DIMTBRII	0.01	nM ⁻¹ .s ⁻¹	77 - 80 (SI.I) + [12-13,17-19]
623	DIMTGF + DIMTBRII <-> DIMTGF_DIMTBRII	C481R		0.03	s ⁻¹	77 - 80 (SI.I) + [12-13,17-19]
624	DIMTGF_DIMTBRII + DIMTBRI <-> DIMTGF_DIMTBRII_DIMTBRI	C482F	C482F*DIMTGF_DIMTBRII*DIMTBRI - C482R*DIMTGF_DIMTBRII_DIMTBRI	0.01	nM ⁻¹ .s ⁻¹	77 - 80 (SI.I) + [12-13,17-19]
625	DIMTGF_DIMTBRII + DIMTBRI <-> DIMTGF_DIMTBRII_DIMTBRI	C482R		0.01	s ⁻¹	77 - 80 (SI.I) + [12-13,17-19]
626	DIMTGF_DIMTBRII_DIMTBRI -> DIMTGF_DIMTBRII_DIMTBRIIP	C483	C483*DIMTGF_DIMTBRII_DIMTBRI	0.1	s ⁻¹	77 - 80 (SI.I) + [12-13,17-19]
627	DIMTGF_DIMTBRII_DIMTBRIIP + SMADII <-> DIMTGF_DIMTBRII_DIMTBRIIP_SMADII	C486F	C486F*DIMTGF_DIMTBRII_DIMTBRIIP*SMADII - C486R*DIMTGF_DIMTBRII_DIMTBRIIP_SMADII	0.01	nM ⁻¹ .s ⁻¹	77 - 80 (SI.I) + [12-13,17-19]
628	DIMTGF_DIMTBRII_DIMTBRIIP + SMADII <-> DIMTGF_DIMTBRII_DIMTBRIIP_SMADII	C486R		10	s ⁻¹	77 - 80 (SI.I) + [12-13,17-19]
629	TBRI + TBRI <-> DIMTBRI	C487F	C487F*TBRI*TBRI - C487R*DIMTBRI	0.01	nM ⁻¹ .s ⁻¹	77 - 80 (SI.I) + [12-13,17-19]
630	TBRI + TBRI <-> DIMTBRI	C487R		0.1	s ⁻¹	77 - 80 (SI.I) + [12-13,17-19]
631	TBRII + TBRII <-> DIMTBRII	C488F	C488F*TBRII*TBRII - C488R*DIMTBRII	0.01	nM ⁻¹ .s ⁻¹	77 - 80 (SI.I) + [12-13,17-19]
632	TBRII + TBRII <-> DIMTBRII	C488R		0.1	s ⁻¹	77 - 80 (SI.I) + [12-13,17-19]

633	DIMTGF_DIMTBRII_DIMTBRIP_SMADII -> DIMTGF_DIMTBRII_DIMTBRIP + SMADIIP	C489	C489*DIMTGF_DIMTBRII_DIMTBRIP_SMADII	1	s ⁻¹	77 - 80 (SI.I) + [12-13,17-19]
634	DIMTGF_DIMTBRII_DIMTBRIP + SMADIII <-> DIMTGF_DIMTBRII_DIMTBRIP_SMADIII	C490F	C490F*DIMTGF_DIMTBRII_DIMTBRIP*SMADIII - C490R*DIMTGF_DIMTBRII_DIMTBRIP_SMADIII	0.01	nM ⁻¹ .s ⁻¹	77 - 80 (SI.I) + [12-13,17-19]
635	DIMTGF_DIMTBRII_DIMTBRIP + SMADIII <-> DIMTGF_DIMTBRII_DIMTBRIP_SMADIII	C490R		10	s ⁻¹	77 - 80 (SI.I) + [12-13,17-19]
636	DIMTGF_DIMTBRII_DIMTBRIP_SMADIII -> DIMTGF_DIMTBRII_DIMTBRIP + SMADIIP	C491	C491*DIMTGF_DIMTBRII_DIMTBRIP_SMADIII	1	s ⁻¹	77 - 80 (SI.I) + [12-13], 17 - 19
637	DIMTGF_DIMTBRII_DIMTBRIP + TAK <-> DIMTGF_DIMTBRII_DIMTBRIP_TAK	C492F	C492F*DIMTGF_DIMTBRII_DIMTBRIP*TAK - C492R*DIMTGF_DIMTBRII_DIMTBRIP_TAK	0.01	nM ⁻¹ .s ⁻¹	82 - 84 (SI.I) + [12-13]
638	DIMTGF_DIMTBRII_DIMTBRIP + TAK <-> DIMTGF_DIMTBRII_DIMTBRIP_TAK	C492R		0.01	s ⁻¹	82 - 84 (SI.I) + [12-13]
639	DIMTGF_DIMTBRII_DIMTBRIP_TAK -> DIMTGF_DIMTBRII_DIMTBRIP + TAKP	C493	C493*DIMTGF_DIMTBRII_DIMTBRIP_TAK	10	s ⁻¹	82 - 84 (SI.I) + [12-13]
640	NLKP + TCFLEF <-> NLKP_TCFLEF	C496F	C496F*NLPK*TCFLEF - C496R*NLPK_TCFLEF	0.01	nM ⁻¹ .s ⁻¹	82 - 84 (SI.I) + [12-13]
641	NLKP + TCFLEF <-> NLKP_TCFLEF	C496R		1	s ⁻¹	82 - 84 (SI.I) + [12-13]
642	NLKP_TCFLEF -> NLKP + TCFLEFP	C497	C497*NLPK_TCFLEF	1	s ⁻¹	82 - 84 (SI.I) + [12-13]
643	TCFLEFP + Pase8 <-> TCFLEFP_Pase8	C498F	C498F*TCFLEFP*Pase8 - C498R*TCFLEFP_Pase8	0.01	nM ⁻¹ .s ⁻¹	82 - 84 (SI.I) + [12-13]
644	TCFLEFP + Pase8 <-> TCFLEFP_Pase8	C498R		1	s ⁻¹	82 - 84 (SI.I) + [12-13]
645	TCFLEFP_Pase8 -> TCFLEF + Pase8	C499	C499*TCFLEFP_Pase8	0.1	s ⁻¹	82 - 84 (SI.I) + [12-13]
646	TAKP + Pase9 <-> TAKP_Pase9	C500F	C500F*TAKP*Pase9 - C500R*TAKP_Pase9	0.01	nM ⁻¹ .s ⁻¹	82 - 84 (SI.I) + [12-13]
647	TAKP + Pase9 <-> TAKP_Pase9	C500R		1	s ⁻¹	82 - 84 (SI.I) + [12-13]
648	TAKP_Pase9 -> TAK + Pase9	C501	C501*TAKP_Pase9	0.1	s ⁻¹	82 - 84 (SI.I) + [12-13]
649	NLKP + Pase10 <-> NLKP_Pase10	C502F	C502F*NLPK*Pase10 - C502R*NLPK_Pase10	0.01	nM ⁻¹ .s ⁻¹	82 - 84 (SI.I) + [12-13]
650	NLKP + Pase10 <-> NLKP_Pase10	C502R		1	s ⁻¹	82 - 84 (SI.I) + [12-13]
651	NLKP_Pase10 -> NLK + Pase10	C503	C503*NLPK_Pase10	0.1	s ⁻¹	82 - 84 (SI.I) + [12-13]
652	SMADIIP + SMAD4 <-> SMADIIP_SMAD4	C504F	C504F*SMADIIP*SMAD4 - C504R*SMADIIP_SMAD4	0.01	nM ⁻¹ .s ⁻¹	77 - 80 (SI.I) + [12-13,17-19]
653	SMADIIP + SMAD4 <-> SMADIIP_SMAD4	C504R		0.01	s ⁻¹	77 - 80 (SI.I) + [12-13,17-19]
654	SMADIIP + SMAD4 <-> SMADIIP_SMAD4	C505F	C505F*SMADIIP*SMAD4 - C505R*SMADIIP_SMAD4	0.01	nM ⁻¹ .s ⁻¹	77 - 80 (SI.I) + [12-13,17-19]
655	SMADIIP + SMAD4 <-> SMADIIP_SMAD4	C505R		0.01	s ⁻¹	77 - 80 (SI.I) + [12-13,17-19]

656	TCFLEF + BetaCatenin <-> TCFLEF_BetaCatenin	C510F	C510F*TCFLEF*BetaCatenin - C510R*TCFLEF_BetaCatenin	0.01	nM ⁻¹ .s ⁻¹	60 (SI.I) + [12-13]
657	TCFLEF + BetaCatenin <-> TCFLEF_BetaCatenin	C510R		10	s ⁻¹	60 (SI.I) + [12-13]
658	SMADIIP + PP1A <-> SMADIIP_PP1A	C511F	C511F*SMADIIP*PP1A - C511R*SMADIIP_PP1A	0.01	nM ⁻¹ .s ⁻¹	91 (SI.I) + [12-13,17-19]
659	SMADIIP + PP1A <-> SMADIIP_PP1A	C511R		10	s ⁻¹	91 (SI.I) + [12-13,17-19]
660	SMADIIP_PP1A -> SMADIII + PP1A	C512	C512*SMADIIP_PP1A	0.1	s ⁻¹	91 (SI.I) + [12-13,17-19]
661	SMADIIP + PP1A <-> SMADIIP_PP1A	C513F	C513F*SMADIIP*PP1A - C514R*SMADIIP_PP1A	0.01	nM ⁻¹ .s ⁻¹	91 (SI.I) + [12-13,17-19]
662	SMADIIP + PP1A <-> SMADIIP_PP1A	C514R	C514*SMADIIP_PP1A	10	s ⁻¹	91 (SI.I) + [12-13,17-19]
663	SMADIIP_PP1A -> SMADII + PP1A	C514		0.1	s ⁻¹	91 (SI.I) + [12-13,17-19]
664	TCFLEF + BetaCateninY654 <-> TCFLEF_BetaCateninY654	C515F	C515F*TCFLEF*BetaCateninY654 - C515R*TCFLEF_BetaCateninY654	0.01	nM ⁻¹ .s ⁻¹	55 - 65 (SI.I) + [12-13]
665	TCFLEF + BetaCateninY654 <-> TCFLEF_BetaCateninY654	C515R		10	s ⁻¹	55 - 65 (SI.I) + [12-13]
666	TCFLEF_BetaCateninY654 + TFBS <-> TCFLEF_BetaCateninY654_TFBS	C516F	C516F*TCFLEF_BetaCateninY654*TFBS - C516R*TCFLEF_BetaCateninY654_TFBS	0.01	nM ⁻¹ .s ⁻¹	55 - 65 (SI.I) + [12-13]
667	TCFLEF_BetaCateninY654 + TFBS <-> TCFLEF_BetaCateninY654_TFBS	C516R		0.01	s ⁻¹	55 - 65 (SI.I) + [12-13]
668	TCFLEF_BetaCatenin + TFBS <-> TCFLEF_BetaCatenin_TFBS	C517F	C517F*TCFLEF_BetaCatenin*TFBS - C517R*TCFLEF_BetaCatenin_TFBS	0.01	nM ⁻¹ .s ⁻¹	55 - 65 (SI.I) + [12-13]
669	TCFLEF_BetaCatenin + TFBS <-> TCFLEF_BetaCatenin_TFBS	C517R		0.02	s ⁻¹	55 - 65 (SI.I) + [12-13]
670	DIMTGF_DIMTBRII + DIMTBRIP <-> DIMTGF_DIMTBRII_DIMTBRIP	C518F	C518F*DIMTGF_DIMTBRII*DIMTBRIP - C518R*DIMTGF_DIMTBRII_DIMTBRIP	0.01	nM ⁻¹ .s ⁻¹	77 - 80 (SI.I) + [12-13]
671	DIMTGF_DIMTBRII + DIMTBRIP <-> DIMTGF_DIMTBRII_DIMTBRIP	C518R		0.1	s ⁻¹	77 - 80 (SI.I) + [12-13]
672	DIMTBRIP + PP1C <-> DIMTBRIP_PP1C	C519F	C519F*DIMTBRIP*PP1C - C519R*DIMTBRIP_PP1C	0.01	nM ⁻¹ .s ⁻¹	81 (SI.I) + [12-13]
673	DIMTBRIP + PP1C <-> DIMTBRIP_PP1C	C519R		1	s ⁻¹	81 (SI.I) + [12-13]
674	DIMTBRIP_PP1C -> DIMTBRI + PP1C	C520	C520*DIMTBRIP_PP1C	0.5	s ⁻¹	81 (SI.I) + [12-13]
675	SMADIIP_SMAD4 + TFBSI <-> SMADIIP_SMAD4_TFBST	C521F	C521F*SMADIIP_SMAD4*TFBSI - C521R*SMADIIP_SMAD4_TFBST	0.01	nM ⁻¹ .s ⁻¹	85 - 90 (SI.I) + [12-13]
676	SMADIIP_SMAD4 + TFBSI <-> SMADIIP_SMAD4_TFBST	C521R		0.1	s ⁻¹	85 - 90 (SI.I) + [12-13]
677	SMADIIP_SMAD4 + TFBSI <-> SMADIIP_SMAD4_TFBST	C522F	C522F*SMADIIP_SMAD4*TFBSI - C522R*SMADIIP_SMAD4_TFBST	0.01	nM ⁻¹ .s ⁻¹	85 - 90 (SI.I) + [12-13]
678	SMADIIP_SMAD4 + TFBSI <-> SMADIIP_SMAD4_TFBST	C522R		0.1	s ⁻¹	85 - 90 (SI.I) + [12-13]

679	Ras_GTP + PI3K <-> Ras_GTP_PK	C523F	C523F*Ras_GTP*PI3K - C523R*Ras_GTP_PK	0.001	nM ⁻¹ .s ⁻¹	34 (SI.I) + [12-13]
680	Ras_GTP + PI3K <-> Ras_GTP_PK	C523R		15	s ⁻¹	34 (SI.I) + [12-13]
681	Ras_GTP_PK -> Ras_GTP_PKP	C524	C524*Ras_GTP_PK	0.1	s ⁻¹	34 (SI.I) + [12-13]
682	Ras_GTP_PKP <-> Ras_GTP + PKP	C525R	C525R*Ras_GTP_PKP - C525F*Ras_GTP*PKP	15	s ⁻¹	34 (SI.I) + [12-13]
683	Ras_GTP_PKP <-> Ras_GTP + PKP	C525F		0.001	nM ⁻¹ .s ⁻¹	34 (SI.I) + [12-13]
684	Ras_GTP_PKP + PIP2 <-> Ras_GTP_PKP_PIP2	C526F	C526F*Ras_GTP_PKP*PIP2 - C526R*Ras_GTP_PKP_PIP2	0.625	nM ⁻¹ .s ⁻¹	31, 32, 34 (SI.I) + [12-13]
685	Ras_GTP_PKP + PIP2 <-> Ras_GTP_PKP_PIP2	C526R		10	s ⁻¹	31, 32, 34 (SI.I) + [12-13]
686	Ras_GTP_PKP + PhoB <-> Ras_GTP_PKP_Phob	C528F	C528F*Ras_GTP_PKP*PhoB - C528R*Ras_GTP_PKP_Phob	0.01	nM ⁻¹ .s ⁻¹	31, 32, 34 (SI.I) + [12-13]
687	Ras_GTP_PKP + PhoB <-> Ras_GTP_PKP_Phob	C528R		1	s ⁻¹	31, 32, 34 (SI.I) + [12-13]
688	Ras_GTP_PKP_Phob -> Ras_GTP + PI3K + PhoB	C528	C528*Ras_GTP_PKP_Phob	0.5	s ⁻¹	31, 32, 34 (SI.I) + [12-13]
689	Ras_GTP_PKP_PIP2 -> Ras_GTP_PKP + PIP3	C527	C527*Ras_GTP_PKP_PIP2	2.5	s ⁻¹	31, 32, 34 (SI.I) + [12-13]
690	ERKPP + AP1 <-> ERKPP_AP1	c528f	c528f*ERKPP*AP1 - c528r*ERKPP_AP1	0.01	nM ⁻¹ .s ⁻¹	15 - 23 (SI.I) + [12-13]
691	ERKPP + AP1 <-> ERKPP_AP1	c528r		10	s ⁻¹	15 - 23 (SI.I) + [12-13]
692	ERKPP_AP1 -> ERKPP + AP1P	c529	c529*ERKPP_AP1	1	s ⁻¹	15 - 23 (SI.I) + [12-13]
693	AP1P + Pase12 <-> AP1P_Pase12	c530f	c530f*AP1P*Pase12 - c530r*AP1P_Pase12	0.01	nM ⁻¹ .s ⁻¹	15 - 23 (SI.I) + [12-13]
694	AP1P + Pase12 <-> AP1P_Pase12	c530r		0.1	s ⁻¹	15 - 23 (SI.I) + [12-13]
695	AP1P_Pase12 -> AP1 + Pase12	c531	c531*AP1P_Pase12	1	s ⁻¹	15 - 23 (SI.I) + [12-13]
696	AP1 + TFBSII <-> AP1_TFBSII	c532f	c532f*AP1*TFBSII - c532r*AP1_TFBSII	0.01	nM ⁻¹ .s ⁻¹	15 - 23 (SI.I) + [12-13]
697	AP1 + TFBSII <-> AP1_TFBSII	c532r		7	s ⁻¹	15 - 23 (SI.I) + [12-13]
698	AP1P + TFBSII <-> AP1P_TFBSII	c533f	c533f*AP1P*TFBSII - c533r*AP1P_TFBSII	0.01	nM ⁻¹ .s ⁻¹	15 - 23 (SI.I) + [12-13]
699	AP1P + TFBSII <-> AP1P_TFBSII	c533r		0.35	s ⁻¹	15 - 23 (SI.I) + [12-13]
700	WNT + FRZ <-> WNT_FRZ	c534f	c534f*WNT*FRZ - c534r*WNT_FRZ	0.01	nM ⁻¹ .s ⁻¹	49, 70 - 75 (SI.I) + [12-13]
701	WNT + FRZ <-> WNT_FRZ	c534r		0.04	s ⁻¹	49, 70 - 75 (SI.I) + [12-13]
702	WNT_FRZ + LRP6 <-> WNT_FRZ_LRP6	c535f	c535f*WNT_FRZ*LRP6 - c535r*WNT_FRZ_LRP6	0.01	nM ⁻¹ .s ⁻¹	49, 70 - 75 (SI.I) + [12-13]
703	WNT_FRZ + LRP6 <-> WNT_FRZ_LRP6	c535r		0.04	s ⁻¹	49, 70 - 75 (SI.I) + [12-13]
704	WNT_FRZ_LRP6 + DVL <-> WNT_FRZ_LRP6_DVL	c536f	c536f*WNT_FRZ_LRP6*DVL - c536r*WNT_FRZ_LRP6_DVL	0.01	nM ⁻¹ .s ⁻¹	49, 70 - 75 (SI.I) + [12-13]

705	WNT_FRZ_LRP6 + DVL <-> WNT_FRZ_LRP6_DVL	c536r		0.04	s ⁻¹	49, 70 - 75 (SI.I) + [12-13]
706	AXN + GSK <-> AXN_GSK	c537f	c537f*AXN*GSK - c537r*AXN_GSK	0.01	nM ⁻¹ .s ⁻¹	49, 70 - 75 (SI.I) + [12-13,20]
707	AXN + GSK <-> AXN_GSK	c537r		0.1	s ⁻¹	48 - 55 (SI.I) + [12-13,20]
708	AXN_GSK -> AXNP_GSK	c538	c538*AXN_GSK	1	s ⁻¹	48 - 55 (SI.I) + [12-13,20]
709	AXNP_GSK + APC <-> AXNP_GSK_APPC	c539f	c539f*AXNP_GSK*APC - c539r*AXNP_GSK_APPC	0.01	nM ⁻¹ .s ⁻¹	48 - 55 (SI.I) + [12-13,20]
710	AXNP_GSK + APC <-> AXNP_GSK_APPC	c539r		0.1	s ⁻¹	48 - 55 (SI.I) + [12-13,20]
711	AXNP_GSK_APPC -> AXNP_GSK_APPCP	c540	c540*AXNP_GSK_APPC	1	s ⁻¹	48 - 55 (SI.I) + [12-13,20]
712	WNT_FRZ_LRP6_DVL + GSK <-> WNT_FRZ_LRP6_DVL_GSK	c541f		0.01	nM ⁻¹ .s ⁻¹	49, 70 - 75 (SI.I) + [12-13]
713	WNT_FRZ_LRP6_DVL + GSK <-> WNT_FRZ_LRP6_DVL_GSK	c541r	c541f*WNT_FRZ_LRP6_DVL*GSK - c541r*WNT_FRZ_LRP6_DVL_GSK	0.04	s ⁻¹	49, 70 - 75 (SI.I) + [12-13]
714	WNT_FRZ_LRP6_DVL_GSK -> WNT_FRZ_LRP6P_DVL_GSK	c542	c542*WNT_FRZ_LRP6_DVL_GSK	1	s ⁻¹	49, 70 - 75 (SI.I) + [12-13]
715	WNT_FRZ_LRP6P_DVL_GSK + AXN <-> WNT_FRZ_LRP6P_DVL_GSK_AXN	c543f	c543f*WNT_FRZ_LRP6P_DVL_GSK*AXN - c543r*WNT_FRZ_LRP6P_DVL_GSK_AXN	0.01	v	49, 70 - 75 (SI.I) + [12-13]
716	WNT_FRZ_LRP6P_DVL_GSK + AXN <-> WNT_FRZ_LRP6P_DVL_GSK_AXN	c543r		0.04	s ⁻¹	49, 70 - 75 (SI.I) + [12-13]
717	AXNP_GSK_APPC + BetaCatenin <-> AXNP_GSK_APPC_BetaCatenin	c544f	c544f*AXNP_GSK_APPC*BetaCatenin - c544r*AXNP_GSK_APPC_BetaCatenin	0.01	nM ⁻¹ .s ⁻¹	48 - 55 (SI.I) + [12-13,20]
718	AXNP_GSK_APPC + BetaCatenin <-> AXNP_GSK_APPC_BetaCatenin	c544r		0.1	s ⁻¹	48 - 55 (SI.I) + [12-13,20]
719	AXNP_GSK_APPC_BetaCatenin -> AXNP_GSK_APPC_BetaCateninP	c545	c545*AXNP_GSK_APPC_BetaCatenin	1	s ⁻¹	48 - 55 (SI.I) + [12-13,20]
720	BetaCateninP -> BetaCateninU	c546	c546*BetaCateninP	1	s ⁻¹	49 , 53 (SI.I) + [20,21]
721	BetaCatenin_generator -> BetaCatenin	c547	c547*BetaCatenin_generator	0.05	s ⁻¹	49 , 53 (SI.I) + [20,21]
722	WNT_FRZ_LRP6P_DVL_GSK + PhoE <-> WNT_FRZ_LRP6P_DVL_GSK_PhоЕ	c548f	c548f*WNT_FRZ_LRP6P_DVL_GSK*PhoE - c548r*WNT_FRZ_LRP6P_DVL_GSK_PhоЕ	0.01	nM ⁻¹ .s ⁻¹	49, 70 - 75 (SI.I) + [12-13]
723	WNT_FRZ_LRP6P_DVL_GSK + PhoE <-> WNT_FRZ_LRP6P_DVL_GSK_PhоЕ	c548r		0.1	s ⁻¹	49, 70 - 75 (SI.I) + [12-13]
724	WNT_FRZ_LRP6P_DVL_GSK_PhоE -> WNT_FRZ_LRP6_DVL + GSK + PhoE	c549	c549*WNT_FRZ_LRP6P_DVL_GSK_PhоE	0.5	s ⁻¹	49, 70 - 75 (SI.I) + [12-13]
725	AXNP_GSK + PhoE <-> AXNP_GSK_PhоE	c550f	c550f*AXNP_GSK*PhoE - c550r*AXNP_GSK_PhоE	0.01	nM ⁻¹ .s ⁻¹	48 - 55 (SI.I) + [12-13,20]
726	AXNP_GSK + PhoE <-> AXNP_GSK_PhоE	c550r		0.1	s ⁻¹	48 - 55 (SI.I) + [12-13,20]
727	AXNP_GSK_PhоE -> AXN + GSK + PhoE	c551	c551*AXNP_GSK_PhоE	0.5	s ⁻¹	48 - 55 (SI.I) + [12-13,20]

728	BetaCateninP + PhoE <-> BetaCateninP_PhоЕ	c552f	c552f*BetaCateninP*PhoE - c552r*BetaCateninP_PhоЕ	0.01	nM ⁻¹ .s ⁻¹	48 - 55 (SI.I) + [12-13,20]
729	BetaCateninP + PhoE <-> BetaCateninP_PhоЕ	c552r		0.1	s ⁻¹	48 - 55 (SI.I) + [12-13,20]
730	BetaCateninP_PhоЕ -> BetaCatenin + PhoE	c553	c553*BetaCateninP_PhоЕ	1	s ⁻¹	48 - 55 (SI.I) + [12-13,20]
731	AXNP_GSK <-> AXNP + GSK	c554r	c554r*AXNP_GSK - c554f*AXNP*GSK	0.1	s ⁻¹	48 - 55 (SI.I) + [12-13,20]
732	AXNP_GSK <-> AXNP + GSK	c554f		0.01	nM ⁻¹ .s ⁻¹	48 - 55 (SI.I) + [12-13,20]
733	AXNP + PhoE <-> AXNP_PhоЕ	c555f	c555f*AXNP*PhoE - c555r*AXNP_PhоЕ	0.01	nM ⁻¹ .s ⁻¹	48 - 55 (SI.I) + [12-13,20]
734	AXNP + PhoE <-> AXNP_PhоЕ	c555r		0.1	s ⁻¹	48 - 55 (SI.I) + [12-13,20]
735	AXNP_PhоЕ -> AXN + PhoE	c556	c556*AXNP_PhоЕ	1	s ⁻¹	48 - 55 (SI.I) + [12-13,20]
736	AXNP_GSK_APCP <-> AXNP_GSK + APCP	c557r	c557r*AXNP_GSK_APCP - c557f*AXNP_GSK*APCP	0.1	s ⁻¹	48 - 55 (SI.I) + [12-13,20]
737	AXNP_GSK_APCP <-> AXNP_GSK + APCP	c557f		0.01	nM ⁻¹ .s ⁻¹	48 - 55 (SI.I) + [12-13,20]
738	APCP + PhoE <-> APCP_PhоЕ	c558f	c558f*APCP*PhoE - c558r*APCP_PhоЕ	0.01	nM ⁻¹ .s ⁻¹	48 - 55 (SI.I) + [12-13,20]
739	APCP + PhoE <-> APCP_PhоЕ	c558r		0.1	s ⁻¹	48 - 55 (SI.I) + [12-13,20]
740	APCP_PhоЕ -> APC + PhoE	c559	c559*APCP_PhоЕ	1	s ⁻¹	48 - 55 (SI.I) + [12-13,20]
741	PIP2_Gen -> PIP2	c560	c560*PIP2_Gen	10	s ⁻¹	32, 37 (SI.I) + [12-13,21]
742	PIP2 + PLCyP <-> PIP2_PLCyP	c561f	c561f*PIP2*PLCyP - c561r*PIP2_PLCyP	0.01	nM ⁻¹ .s ⁻¹	28, 29 (SI.I) + [12-13]
743	PIP2 + PLCyP <-> PIP2_PLCyP	c561r		10	s ⁻¹	28, 29 (SI.I) + [12-13]
744	PIP2_PLCyP -> IP3 + DAG + PLCyP	c562	c562*PIP2_PLCyP	0.001	s ⁻¹	28, 29 (SI.I) + [12-13]
745	DAG + PKC <-> DAG_PKC	c563f	c563f*DAG*PKC - c563r*DAG_PKC	0.01	nM ⁻¹ .s ⁻¹	28, 29 (SI.I) + [12-13],
746	DAG + PKC <-> DAG_PKC	c563r		0.1	s ⁻¹	28, 29 (SI.I) + [12-13],
747	IP3 -> IP3D	c565	c565*IP3	0.00001	s ⁻¹	28, 29 (SI.I) + [12-13,21]
748	DAG -> DAGD	c566	c566*DAG	0.00001	s ⁻¹	28, 29 (SI.I) + [12-13,21]
749	DAG_PKC + Raf <-> DAG_PKC_Raf	c567f	c567f*DAG_PKC*Raf - c567r*DAG_PKC_Raf	0.01	nM ⁻¹ .s ⁻¹	30 (SI.I) + [12-13]
750	DAG_PKC + Raf <-> DAG_PKC_Raf	c567r		0.1	s ⁻¹	30 (SI.I) + [12-13]
751	DAG_PKC_Raf -> DAG + PKC + [Raf]	c568	c568*DAG_PKC_Raf	10	s ⁻¹	30 (SI.I) + [12-13]
752	WNT_FRZ_LRP6 + TAK <-> WNT_FRZ_LRP6_TAK	c569f	c569f*WNT_FRZ_LRP6*TAK - c569r*WNT_FRZ_LRP6_TAK	0.01	nM ⁻¹ .s ⁻¹	76, 83, 84 (SI.I) + [12-13]
753	WNT_FRZ_LRP6 + TAK <-> WNT_FRZ_LRP6_TAK	c569r		10	s ⁻¹	76, 83, 84 (SI.I) + [12-13]
754	WNT_FRZ_LRP6_TAK -> WNT_FRZ_LRP6 + TAKP	c570	c570*WNT_FRZ_LRP6_TAK	0.1	s ⁻¹	76, 83, 84 (SI.I) + [12-13]
755	TAKP + TAB <-> TAKP_TAB	c571f	c571f*TAKP*TAB - c571r*TAKP_TAB	0.01	nM ⁻¹ .s ⁻¹	76, 83, 84 (SI.I) + [12-13]

756	TAKP + TAB <-> TAKP_TAB	c571r		10	s ⁻¹	76, 83, 84 (SI.I) + [12-13]
757	TAKP_TAB + NLK <-> TAKP_TAB_NLK	c572f	c572f*TAKP_TAB*NLK - c572r*TAKP_TAB_NLK	0.01	nM ⁻¹ .s ⁻¹	76, 83, 84 (SI.I) + [12-13]
758	TAKP_TAB + NLK <-> TAKP_TAB_NLK	c572r		10	s ⁻¹	76, 83, 84 (SI.I) + [12-13]
759	TAKP_TAB_NLK -> TAKP_TAB + NLKP	c573	c573*TAKP_TAB_NLK	1	s ⁻¹	76, 83, 84 (SI.I) + [12-13]
760	GROUCHO + TCFLEF <-> GROUCHO_TCFLEF	c578f	c578f*GROUCHO*TCFLEF - c578r*GROUCHO_TCFLEF	0.01	nM ⁻¹ .s ⁻¹	68, 69 (SI.I) + [12-13]
761	GROUCHO + TCFLEF <-> GROUCHO_TCFLEF	c578r		10	s ⁻¹	68, 69 (SI.I) + [12-13]
762	GROUCHO_TCFLEF + TFBS <-> GROUCHO_TCFLEF_TFBS	c579f	c579f*GROUCHO_TCFLEF*TFBS - c579r*GROUCHO_TCFLEF_TFBS	0.01	nM ⁻¹ .s ⁻¹	68, 69 (SI.I) + [12-13]
763	GROUCHO_TCFLEF + TFBS <-> GROUCHO_TCFLEF_TFBS	c579r		1	s ⁻¹	68, 69 (SI.I) + [12-13]
764	APC + BetaCatenin <-> APC_BetaCatenin	c581f	c581f*APC*BetaCatenin - c581r*APC_BetaCatenin	0.01	nM ⁻¹ .s ⁻¹	48 - 55 (SI.I) + [12-13,20]
765	APC + BetaCatenin <-> APC_BetaCatenin	c581r		12	s ⁻¹	48 - 55 (SI.I) + [12-13,20]
766	SMAD4 + TCFLEF <-> SMAD4_TCFLEF	c582f	c582f*SMAD4*TCFLEF - c582r*SMAD4_TCFLEF	0.01	nM ⁻¹ .s ⁻¹	69 (SI.I) + [13,14]
767	SMAD4 + TCFLEF <-> SMAD4_TCFLEF	c582r		1	s ⁻¹	69 (SI.I) + [13,14]
768	SMAD4_TCFLEF + TFBS <-> SMAD4_TCFLEF_TFBS	c583f	c583f*SMAD4_TCFLEF*TFBS - c583r*SMAD4_TCFLEF_TFBS	0.01	nM ⁻¹ .s ⁻¹	69 (SI.I) + [13,14]
769	SMAD4_TCFLEF + TFBS <-> SMAD4_TCFLEF_TFBS	c583r		1	s ⁻¹	69 (SI.I) + [13,14]
770	PIP2 -> PIP2deg	c584	c584*PIP2	0.0004	s ⁻¹	32, 37 (SI.I) + [12-13,21]
771	[Raf] + Raf_inhibitor <-> [Raf_Raf_inhibitor]	c585f	c585f*[Raf]*Raf_inhibitor - c585r*[Raf_Raf_inhibitor]	0.01	nM ⁻¹ .s ⁻¹	[23]
772	[Raf] + Raf_inhibitor <-> [Raf_Raf_inhibitor]	c585r		0.001	s ⁻¹	[23]
773	PKP + PI3K_inhibitor <-> PKP_PI3K_inhibitor	c586f	c586f*PKP*PI3K_inhibitor - c586r*PKP_PI3K_inhibitor	0.01	nM ⁻¹ .s ⁻¹	[23]
774	PKP + PI3K_inhibitor <-> PKP_PI3K_inhibitor	c586r		1.5	s ⁻¹	[23]
775	BetaCatenin -> BetaCateninDeg	c587	c587*BetaCatenin	0.0000001	s ⁻¹	49, 53 (SI.I) + [20,21]
776	RP + PanERB <-> RP_PanERB	c588f	c588f*RP*PanERB - c588r*RP_PanERB	0.01	nM ⁻¹ .s ⁻¹	[23]
777	RP + PanERB <-> RP_PanERB	c588r		0.00001	s ⁻¹	[23]
778	ERBP + PanERB <-> ERBP_PanERB	c589f	c589f*ERBP*PanERB - c589r*ERBP_PanERB	0.01	nM ⁻¹ .s ⁻¹	[23]
779	ERBP + PanERB <-> ERBP_PanERB	c589r		0.00001	s ⁻¹	[23]
780	ERB3P + PanERB <-> ERB3P_PanERB	c590f	c590f*ERB3P*PanERB - c590r*ERB3P_PanERB	0.01	nM ⁻¹ .s ⁻¹	[23]
781	ERB3P + PanERB <-> ERB3P_PanERB	c590r		0.00001	s ⁻¹	[23]

782	PIP3 -> PIP3Deg	c591	c591*PIP3	0.0001	s ⁻¹	[23]
783	AKT + AKT_inhibi <-> AKT_AKT_inhibi	c592f	c592f*AKT*AKT_inhibi - c592r*AKT_AKT_inhibi	0.01	nM ⁻¹ .s ⁻¹	[23]
784	AKT + AKT_inhibi <-> AKT_AKT_inhibi	c592r		48	s ⁻¹	[23]
785	AXNP_GSK + BetaCatenin <-> AXNP_GSK_BetaCatenin	c593f	c593f*AXNP_GSK*BetaCatenin - c593r*AXNP_GSK_BetaCatenin	0.01	nM ⁻¹ .s ⁻¹	48 - 55 (SI.I) + [12-13,20]
786	AXNP_GSK + BetaCatenin <-> AXNP_GSK_BetaCatenin	c593r		10000	s ⁻¹	48 - 55 (SI.I) + [12-13,20]
787	AXNP_GSK_BetaCatenin -> AXNP_GSK + BetaCateninP	c594	c594*AXNP_GSK_BetaCatenin	1	s ⁻¹	48 - 55 (SI.I) + [12-13,20]
788	MEKPP + MEK_inhi <-> MEKPP_MEK_inhi	c595f	c595f*MEKPP*MEK_inhi - c595r*MEKPP_MEK_inhi	0.01	nM ⁻¹ .s ⁻¹	[23]
789	MEKPP + MEK_inhi <-> MEKPP_MEK_inhi	c595r		3	s ⁻¹	[23]
790	G_S + ERKPP <-> G_S_ERKPP	c596f	c596f*G_S*ERKPP - c596r*G_S_ERKPP	0.01	nM ⁻¹ .s ⁻¹	11, 24, 25 (SI.I) + [12-13]
791	G_S + ERKPP <-> G_S_ERKPP	c596r		0.033	s ⁻¹	11, 24, 25 (SI.I) + [12-13]
792	G_S_ERKPP -> Grb + SOSP + ERKPP	c597	c597*G_S_ERKPP	1	s ⁻¹	11, 24, 25 (SI.I) + [12-13]
793	AKTP + MDM2 <-> AKTP_MDM2	c598f	c598f*AKTP*MDM2 - c598r*AKTP_MDM2	0.01	nM ⁻¹ .s ⁻¹	40 (SI.I) + [12-13]
794	AKTP + MDM2 <-> AKTP_MDM2	c598r		0.1	s ⁻¹	40 (SI.I) + [12-13]
795	AKTP_MDM2 -> AKTP + MDM2P	c599	c599*AKTP_MDM2	0.1	s ⁻¹	40 (SI.I) + [12-13]
796	MDM2P + TP53 <-> MDM2P_TP53	c600f	c600f*MDM2P*TP53 - c600r*MDM2P_TP53	0.01	nM ⁻¹ .s ⁻¹	40, 41 (SI.I) + [12-13]
797	MDM2P + TP53 <-> MDM2P_TP53	c600r		0.1	s ⁻¹	40, 41 (SI.I) + [12-13]
798	MDM2P_TP53 -> MDM2P + TP53U	c601	c601*MDM2P_TP53	1	s ⁻¹	40, 41 (SI.I) + [12-13]
799	TP53gen -> TP53	c602	c602*TP53gen	0.05	s ⁻¹	(12,13,21)
800	MDM2P + Pho13 <-> MDM2P_Ph013	c603f	c603f*MDM2P*Pho13 - c603r*MDM2P_Ph013	0.01	nM ⁻¹ .s ⁻¹	40 (SI.I) + [12-13]
801	MDM2P + Pho13 <-> MDM2P_Ph013	c603r		0.1	s ⁻¹	40 (SI.I) + [12-13]
802	MDM2P_Ph013 -> MDM2 + Pho13	c604	c604*MDM2P_Ph013	1	s ⁻¹	40 (SI.I) + [12-13]
803	TP53 + TFBSIV <-> TP53_TFBSIV	c605f	c605f*TP53*TFBSIV - c605r*TP53_TFBSIV	0.01	nM ⁻¹ .s ⁻¹	40 - 43 (SI.I) + [12-13]
804	TP53 + TFBSIV <-> TP53_TFBSIV	c605r		0.1	s ⁻¹	40 - 43 (SI.I) + [12-13]
805	RP_ShP_G_GABP + ERKPP <-> RP_ShP_G_GABP_ERKPP	c606f	c606f*RP_ShP_G_GABP*ERKPP - c606r*RP_ShP_G_GABP_ERKPP	0.01	nM ⁻¹ .s ⁻¹	33, 35, 36 (SI.I) + [4,12- 13,16]
806	RP_ShP_G_GABP + ERKPP <-> RP_ShP_G_GABP_ERKPP	c606r		0.1	s ⁻¹	33, 35, 36 (SI.I) + [4,12- 13,16]
807	RP_ShP_G_GABP_ERKPP -> RP_ShP_G + GABPP + ERKPP	c607	c607*RP_ShP_G_GABP_ERKPP	1	s ⁻¹	33, 35, 36 (SI.I) + [4,12- 13,16]

808	RP_G_GABP + ERKPP <-> RP_G_GABP_ERKPP	c608f	c608f*RP_G_GABP*ERKPP - c608r*RP_G_GABP_ERKPP	0.01	nM ⁻¹ .s ⁻¹	33, 35, 36 (SI.I) + [4,12-13,16]
809	RP_G_GABP + ERKPP <-> RP_G_GABP_ERKPP	c608r		0.1	s ⁻¹	33, 35, 36 (SI.I) + [4,12-13,16]
810	RP_G_GABP_ERKPP -> RP_G + GABPP + ERKPP	c609	c609*RP_G_GABP_ERKPP	1	s ⁻¹	33, 35, 36 (SI.I) + [4,12-13,16]
811	ERBP_ShP_G_GABP + ERKPP <-> ERBP_ShP_G_GABP_ERKPP	c610f	c610f*ERBP_ShP_G_GABP*ERKPP - c610r*ERBP_ShP_G_GABP_ERKPP	0.01	nM ⁻¹ .s ⁻¹	33, 35, 36 (SI.I) + [4,12-13,16]
812	ERBP_ShP_G_GABP + ERKPP <-> ERBP_ShP_G_GABP_ERKPP	c610r		0.1	s ⁻¹	33, 35, 36 (SI.I) + [4,12-13,16]
813	ERBP_ShP_G_GABP_ERKPP -> ERBP_ShP_G + GABPP + ERKPP	c611	c611*ERBP_ShP_G_GABP_ERKPP	1	s ⁻¹	33, 35, 36 (SI.I) + [4,12-13,16]
814	ERBP_G_GABP + ERKPP <-> ERBP_G_GABP_ERKPP	c612f	c612f*ERBP_G_GABP*ERKPP - c612r*ERBP_G_GABP_ERKPP	0.01	nM ⁻¹ .s ⁻¹	33, 35, 36 (SI.I) + [4,12-13,16]
815	ERBP_G_GABP + ERKPP <-> ERBP_G_GABP_ERKPP	c612r		0.1	s ⁻¹	33, 35, 36 (SI.I) + [4,12-13,16]
816	ERBP_G_GABP_ERKPP -> ERBP_G + GABPP + ERKPP	c613	c613*ERBP_G_GABP_ERKPP	1	s ⁻¹	33, 35, 36 (SI.I) + [4,12-13,16]
817	ERB3P_G_GABP + ERKPP <-> ERB3P_G_GABP_ERKPP	c614f	c614f*ERB3P_G_GABP*ERKPP - c614r*ERB3P_G_GABP_ERKPP	0.01	nM ⁻¹ .s ⁻¹	33, 35, 36 (SI.I) + [4,12-13,16]
818	ERB3P_G_GABP + ERKPP <-> ERB3P_G_GABP_ERKPP	c614r		0.1	s ⁻¹	33, 35, 36 (SI.I) + [4,12-13,16]
819	ERB3P_G_GABP_ERKPP -> ERB3P_G + GABPP + ERKPP	c615	c615*ERB3P_G_GABP_ERKPP	1	s ⁻¹	33, 35, 36 (SI.I) + [4,12-13,16]
820	ERB3P_ShP_G_GABP + ERKPP <-> ERB3P_ShP_G_GABP_ERKPP	c616f	c616f*ERB3P_ShP_G_GABP*ERKPP - c616r*ERB3P_ShP_G_GABP_ERKPP	0.01	nM ⁻¹ .s ⁻¹	33, 35, 36 (SI.I) + [4,12-13,16]
821	ERB3P_ShP_G_GABP + ERKPP <-> ERB3P_ShP_G_GABP_ERKPP	c616r		0.1	s ⁻¹	33, 35, 36 (SI.I) + [4,12-13,16]
822	ERB3P_ShP_G_GABP_ERKPP -> ERB3P_ShP_G + GABPP + ERKPP	c617	c617*ERB3P_ShP_G_GABP_ERKPP	1	s ⁻¹	33, 35, 36 (SI.I) + [4,12-13,16]
823	GABP + ERKPP <-> GABP_ERKPP	c618f	c618f*GABP*ERKPP - c618r*GABP_ERKPP	0.01	nM ⁻¹ .s ⁻¹	33, 35, 36 (SI.I) + [4,12-13]
824	GABP + ERKPP <-> GABP_ERKPP	c618r		0.1	s ⁻¹	33, 35, 36 (SI.I) + [4,12-13]
825	GABPP + PhoA <-> GABPP_PhоА	c619f	c619f*GABPP*PhoA - c619r*GABPP_PhоА	0.01	nM ⁻¹ .s ⁻¹	33, 35, 36 (SI.I) + [4,12-13]
826	GABPP + PhoA <-> GABPP_PhоА	c619r		0.1	s ⁻¹	33, 35, 36 (SI.I) + [4,12-13]
827	GABPP_PhоА -> GABP + PhoA	c620	c620*GABPP_PhоА	1	s ⁻¹	33, 35, 36 (SI.I) + [4,12-13]

828	GABP_ERKPP -> GABPP + ERKPP	c621	c621*GABP_ERKPP	1	s ⁻¹	33, 35, 36 (SI.I) + [4,12-13]
829	ARF + MDM2 <-> [ARF_MDM2]	c622f	c622f*ARF*MDM2 - c622r*[ARF_MDM2)	0.01	nM ⁻¹ .s ⁻¹	40, 41 (SI.I) + [12-13]
830	ARF + MDM2 <-> [ARF_MDM2)	c622r		0.001	s ⁻¹	40, 41 (SI.I) + [12-13]
831	CYCLIND1 + CDK4 <-> CYCLIND1_CDK4	c623f	c623f*CYCLIND1*CDK4 - c623r*CYCLIND1_CDK4	0.01	nM ⁻¹ .s ⁻¹	92 (SI.I) + [12-13]
832	CYCLIND1 + CDK4 <-> CYCLIND1_CDK4	c623r		0.1	s ⁻¹	92 (SI.I) + [12-13]
833	CYCLINE + CDK2 <-> CYCLINE_CDK2	c624f	c624f*CYCLINE*CDK2 - c624r*CYCLINE_CDK2	0.01	nM ⁻¹ .s ⁻¹	92 (SI.I) + [12-13]
834	CYCLINE + CDK2 <-> CYCLINE_CDK2	c624r		0.1	s ⁻¹	92 (SI.I) + [12-13]
835	E2F + DP1 <-> E2F_DP1	c625f	c625f*E2F*DP1 - c625r*E2F_DP1	0.01	nM ⁻¹ .s ⁻¹	93, 94 (SI.I) + [12-13]
836	E2F + DP1 <-> E2F_DP1	c625r		0.1	s ⁻¹	93, 94 (SI.I) + [12-13]
837	E2F_DP1 + RB <-> E2F_DP1_RB	c626f	c626f*E2F_DP1*RB - c626r*E2F_DP1_RB	0.01	nM ⁻¹ .s ⁻¹	93, 94 (SI.I) + [12-13]
838	E2F_DP1 + RB <-> E2F_DP1_RB	c626r		0.1	s ⁻¹	93, 94 (SI.I) + [12-13]
839	CYCLIND1_CDK4 + RB <-> CYCLIND1_CDK4_RB	c627f	c627f*CYCLIND1_CDK4*RB - c627r*CYCLIND1_CDK4_RB	0.01	nM ⁻¹ .s ⁻¹	92 (SI.I) + [12-13]
840	CYCLIND1_CDK4 + RB <-> CYCLIND1_CDK4_RB	c627r		0.1	s ⁻¹	92 (SI.I) + [12-13]
841	CYCLIND1_CDK4_RB -> CYCLIND1_CDK4 + RBP	c628	c628*CYCLIND1_CDK4_RB	1	s ⁻¹	92 (SI.I) + [12-13]
842	CYCLINE_CDK2 + RBP <-> CYCLINE_CDK2_RBP	c629f	c629f*CYCLINE_CDK2*RBP - c629r*CYCLINE_CDK2_RBP	0.01	nM ⁻¹ .s ⁻¹	92 (SI.I) + [12-13]
843	CYCLINE_CDK2 + RBP <-> CYCLINE_CDK2_RBP	c629r		0.1	s ⁻¹	92 (SI.I) + [12-13]
844	CYCLINE_CDK2_RBP -> CYCLINE_CDK2 + RBPP	c630	c630*CYCLINE_CDK2_RBP	1	s ⁻¹	92 (SI.I) + [12-13]
845	RBPP + Pho14 <-> RBPP_Ph014	c631f	c631f*RBPP*Pho14 - c631r*RBPP_Ph014	0.01	nM ⁻¹ .s ⁻¹	92 (SI.I) + [12-13]
846	RBPP + Pho14 <-> RBPP_Ph014	c631r		0.1	s ⁻¹	92 (SI.I) + [12-13]
847	RBPP_Ph014 -> RBP + Pho14	c632	c632*RBPP_Ph014	1	s ⁻¹	92 (SI.I) + [12-13]
848	RBP + Pho14 <-> RBP_Ph014	c633f	c633f*RBP*Pho14 - c633r*RBP_Ph014	0.01	nM ⁻¹ .s ⁻¹	92 (SI.I) + [12-13]
849	RBP + Pho14 <-> RBP_Ph014	c633r		0.1	s ⁻¹	92 (SI.I) + [12-13]
850	RBP_Ph014 -> RB + Pho14	c634	c634*RBP_Ph014	1	s ⁻¹	92 (SI.I) + [12-13]
851	E2F_DP1_RB + TFBSV <-> E2F_DP1_RB_TFBSV	c635f	c635f*E2F_DP1_RB*TFBSV - c635r*E2F_DP1_RB_TFBSV	0.01	nM ⁻¹ .s ⁻¹	92, 93 (SI.I) + [12-13]
852	E2F_DP1_RB + TFBSV <-> E2F_DP1_RB_TFBSV	c635r		0.1	s ⁻¹	92, 93 (SI.I) + [12-13]

853	E2F_DP1 + TFBSV <-> E2F_DP1_TFBSV	c636f	c636f*E2F_DP1*TFBSV - c636r*E2F_DP1_TFBSV	0.01	nM ⁻¹ .s ⁻¹	92, 93 (SI.I) + [12-13]
854	E2F_DP1 + TFBSV <-> E2F_DP1_TFBSV	c636r		0.1	s ⁻¹	92, 93 (SI.I) + [12-13]
855	CYCLIND1_CDK4 + P16 <-> CYCLIND1_CDK4_P16	c637f	c637f*CYCLIND1_CDK4*P16 - c637r*CYCLIND1_CDK4_P16	0.01	nM ⁻¹ .s ⁻¹	92, 93 (SI.I) + [12-13]
856	CYCLIND1_CDK4 + P16 <-> CYCLIND1_CDK4_P16	c637r		0.1	s ⁻¹	92, 93 (SI.I) + [12-13]
857	CDC25C + ERKPP <-> CDC25C_ERKPP	c642f	c642f*CDC25C*ERKPP - c642r*CDC25C_ERKPP	0.01	nM ⁻¹ .s ⁻¹	26, 27 (SI.I) + [12-13]
858	CDC25C + ERKPP <-> CDC25C_ERKPP	c642r		0.01	s ⁻¹	26, 27 (SI.I) + [12-13]
859	CDC25C_ERKPP -> CDC25CP + ERKPP	c643	c643*CDC25C_ERKPP	10	s ⁻¹	26, 27 (SI.I) + [12-13]
860	CDC25CP + Pho16 <-> CDC25CP_Ph016	c644f	c644f*CDC25CP*Pho16 - c644r*CDC25CP_Ph016	0.01	nM ⁻¹ .s ⁻¹	26, 27 (SI.I) + [12-13]
861	CDC25CP + Pho16 <-> CDC25CP_Ph016	c644r		10	s ⁻¹	26, 27 (SI.I) + [12-13]
862	CDC25CP_Ph016 -> CDC25C + Pho16	c645	c645*CDC25CP_Ph016	0.1	s ⁻¹	26, 27 (SI.I) + [12-13]
863	Pb_MYC -> MYC_mRNA	c646	c646*MYC_mRNA_Gen	0.00005	s ⁻¹	[21]
864	MYC_mRNA -> null	c647	c647*MYC_mRNA	0.00027	s ⁻¹	95 (SI.I) + [22]
865	PKP_PIP2 + PI3K_inhibitor <-> PKP_PIP2_PI3K_inhibitor	c648f	c648f*PKP_PIP2*PI3K_inhibitor - c648r*PKP_PIP2_PI3K_inhibitor	0.01	nM ⁻¹ .s ⁻¹	[23]
866	PKP_PIP2 + PI3K_inhibitor <-> PKP_PIP2_PI3K_inhibitor	c648r		1.5	s ⁻¹	[23]
867	Pb_CCND1 -> CCND1_mRNA	c649	c649*CCND1_mRNA_Gen	0.00005	s ⁻¹	[21]
868	CCND1_mRNA -> null	c650	c650*(ERKPPcont / ERKPP) * CCND1_mRNA	0.0000057	s ⁻¹	96 (SI.I) + [22]
869	GSKP + AZAKEN <-> GSKP_AZAKEN	c651f	c651f*GSKP*AZAKEN - c651r*GSKP_AZAKEN	0.01	nM ⁻¹ .s ⁻¹	[23]
870	GSKP + AZAKEN <-> GSKP_AZAKEN	c651r		0.18	s ⁻¹	[23]

Supplementary Table 2.2 - Species Initial Concentration

Supplementary Table 2.2 reports the total concentration of 81 basic species (the total concentration of each species involved in biochemical reactions, adding up all the modified forms and complexes in which a given basic species is involved).

We considered growth factors (EGF, TGF β , WNT) non-consumable. We considered the GDP and GTP species to be in large excess (non-consumable).

	Molecular species as written in the rates equations (simplified notation)	Concentrations (nM)	Molecular species as written in MIM's cartouches	Extrapolations from Annotation List References (ST 1.1) + Notes / Ref. listed below
1	R	100	EGFR (ErbB family)	[1-10]
2	EGF	0.1		[7]
3	PLCy	105		[1-10]
4	Grb	85	Grb2	[1-10]
5	SOS	10		[1-10]
6	Shc	100		[1-10]
7	Ras	85		[1-10]
8	GDP	500		[1-10]
9	GTP	10000		[1-10]
10	Raf	50	BRAF	[1-10]
11	Pase1 (BRAF phosphatase)	50	Pase1	[1-10]
12	MEK	200		[1-10]
13	Pase2 (MEK phosphatase)	50	Pase7	[1-10]
14	ERK	200		[1-10]
15	Pase3 (ERK phosphatase)	100	MKP3	[1-10]
16	GAP	12		[1-10]
17	Pase5 (SOS phosphatase)	50		[1-10]
18	GAB	50		[1-10]
19	PTEN	50		[1-10]
20	PhoA (GAB1 phosphatase)	100	Pase3	[1-10]
21	AKT	100		[1-10]

22	PDK1	100		[1-10]
23	TAKT (AKT phosphatase)	50	PHLPP	[1-10]
24	GSK	50	GSK3β	[1-10]
25	PhoB (PI3K phosphatase)	50	PI3K inactivator	[1-10]
26	PhoC (GSK3β)	20	Pase4	[1-10]
27	PI3K	200		[1-10]
28	APC	100		[22,29]
29	PhoE (AXN, APC, BetaCatenin, LRP5/6 phosphatase)	10	Pase6	49, 54, 55 (<i>SI.I</i>) + [29]
30	PTP (BetaCateninY654)	100	PTP1B	[1-10]
31	ERB	1	ErbB2 (ErbB family)	[1-10]
32	PTP1E (Shc phosphatase)	50		[1-10]
33	PaseX (PLCy phosphatase)	50	Pase2	[1-10]
34	ERB3	1	ErbB3 (ErbB family)	[1-10]
35	Cadh	50	E-Cadherin	[1-10]
36	TGF	0.01	TGFβ	[30]
37	PP1C	10		77 – 81 (<i>SI.I</i>) + [29]
38	SMADII	25		77 – 81 (<i>SI.I</i>) + [29]
39	TBRI	100	TGFβ receptor I	77 – 81 (<i>SI.I</i>) + [29]
40	TBRII	100	TGFβ receptor II	77 – 81 (<i>SI.I</i>) + [29]
41	SMADIII	5		77 – 81 (<i>SI.I</i>) + [29]
42	TAK	25	TAK1	82 – 84 (<i>SI.I</i>) + [29]
43	NLK	50		82 – 84 (<i>SI.I</i>) + [29]
44	TCFLEF	15	TCF7L2	[22,29]

45	Pase8 (TCF7L2 phosphatase)	10		[29]
46	Pase9 (TAK phosphatase)	10		82 – 84 (<i>SI.I</i>) + [29]
47	Pase10 (NLK phosphatase)	10		82 – 84 (<i>SI.I</i>) + [29]
48	SMAD4	25		77 – 81 (<i>SI.I</i>) + [29]
49	PP1A (SMADII, SMADIII phosphatase)	10	PPM1A	77 – 81 (<i>SI.I</i>) + [29]
50	TFBS	0.00166	TFBS _{TCF7L2} (DNA BINDING SITE)	[29,31]
51	AP1	10		16, 17 (<i>SI.I</i>) + [29]
52	Pase12 (AP1 phosphatase)	20		[29]
53	TFBSII	0.00083	TFBS _{AP1} (DNA BINDING SITE)	[29,31]
54	WNT	0.01		[29,32]
55	FRZ	100		70 – 75 (<i>SI.I</i>) + [29]
56	LRP6	100		70 – 75 (<i>SI.I</i>) + [29]
57	DVL	100		70 – 75 (<i>SI.I</i>) + [22,29]
58	AXN	0.02	Axin	70 – 75 (<i>SI.I</i>) + [22,29]
59	BetaCatenin_generator	0.01		[29]
60	PIP2_Gen	0.01		[29]
61	PKC	50		28 – 29 (<i>SI.I</i>) + [29]
62	TAB	25	TAB2	82 – 84 (<i>SI.I</i>) + [29]
63	GROUCHO	25		[29]
64	TFBSI	0.00083	TFBS _{SMAD} (DNA BINDING SITE)	[29,31]
65	MDM2	10		[29]
66	TP53gen	0.1		[29]
67	Pho13 (MDM2 phosphatase)	50	Pase13	92 -94 (<i>SI.I</i>) + [29]

68	TFBSIV	0.00083	TFBS _{TP53} (DNA BINDING SITE)	[29,31]
69	ARF	10		92 (<i>SI.I</i>) + [29]
70	CYCLIND1	10		92 (<i>SI.I</i>) + [29]
71	CDK4	10		92 (<i>SI.I</i>) + [29]
72	CYCLINE	10		92 (<i>SI.I</i>) + [29]
73	CDK2	10		92 (<i>SI.I</i>) + [29]
74	RB	10		92 -94 (<i>SI.I</i>) + [29]
75	E2F	10		92 -94 (<i>SI.I</i>) + [29]
76	DP1	10		92 -94 (<i>SI.I</i>) + [29]
77	Pho14 (RB phosphatase)	10	Pase14	[29]
78	TFBSV	0.00083	TFBS _{E2F-DP1} (DNA BINDING SITE)	[29,31]
79	P16	10		92 -94 (<i>SI.I</i>) + [29]
80	Pho16 (CDC25C phosphatase)	5	Pase11	[29]
81	CDC25C (ErbB family phosphatase)	50		[29]

Supplementary references and notes to Table 2.1 – Reaction List and to Supplementary Table 2.2 - Species Initial Concentration:

1. Castagnino N, Tortolina L, Balbi A, Pesenti R, Montagna R, Ballestrero A, Soncini D, Moran E, Nencioni A and Parodi S. Dynamic simulations of pathways downstream of ERBB-family, including mutations and treatments: concordance with experimental results. Curr Cancer Drug Targets. 2010; 10(7):737-757.
2. Kholodenko BN, Demin OV, Moehren G and Hoek JB. Quantification of short term signaling by the epidermal growth factor receptor. The Journal of biological chemistry. 1999; 274(42):30169-30181.
3. Blinov ML, Faeder JR, Goldstein B and Hlavacek WS. A network model of early events in epidermal growth factor receptor signaling that accounts for combinatorial complexity. Bio Systems. 2006; 83(2-3):136-151.

4. Birtwistle MR, Hatakeyama M, Yumoto N, Ogunnaike BA, Hoek JB and Kholodenko BN. Ligand-dependent responses of the ErbB signaling network: experimental and modeling analyses. *Molecular systems biology*. 2007; 3:144.
5. Wolf J, Dronov S, Tobin F and Goryanin I. The impact of the regulatory design on the response of epidermal growth factor receptor-mediated signal transduction towards oncogenic mutations. *FEBS J*. 2007; 274(21):5505-5517.
6. Chen WW, Schoeberl B, Jasper PJ, Niepel M, Nielsen UB, Lauffenburger DA and Sorger PK. Input-output behavior of ErbB signaling pathways as revealed by a mass action model trained against dynamic data. *Molecular systems biology*. 2009; 5:239.
7. Borisov N, Aksamitiene E, Kiyatkin A, Legewie S, Berkhout J, Maiwald T, Kaimachnikov NP, Timmer J, Hoek JB and Kholodenko BN. Systems-level interactions between insulin-EGF networks amplify mitogenic signaling. *Molecular systems biology*. 2009; 5:256.
8. Schoeberl B, Eichler-Jonsson C, Gilles ED and Muller G. Computational modeling of the dynamics of the MAP kinase cascade activated by surface and internalized EGF receptors. *Nature biotechnology*. 2002; 20(4):370-375.
9. Kiyatkin A, Aksamitiene E, Markevich NI, Borisov NM, Hoek JB and Kholodenko BN. Scaffolding protein Grb2-associated binder 1 sustains epidermal growth factor-induced mitogenic and survival signaling by multiple positive feedback loops. *The Journal of biological chemistry*. 2006; 281(29):19925-19938.
10. Kholodenko BN, Hoek JB and Westerhoff HV. Why cytoplasmic signalling proteins should be recruited to cell membranes. *Trends in cell biology*. 2000; 10(5):173-178.
11. Stites EC, Trampont PC, Ma Z and Ravichandran KS. Network analysis of oncogenic Ras activation in cancer. *Science*. 2007; 318(5849):463-467.
12. The references associated with the Annotation List give information about all the interactions described in our MIM. If a good quality experimental paper says, for instance, that protein subspecies A (after a given posttranslational modification) interacts well with the molecule B, we can assume that we will have a 95% of [A:B].
13. There will be a free 5% of the less abundant partner. This could be a general default assumption, based on semi-quantitative information. The diffusion limit is $7 \times 10^9 \cdot M^{-1} \cdot s^{-1}$. However, considering the very crowded cellular environment, the very large size of many multi-protein complexes, the fact that only a

- fraction of protein–protein encounters will be productive, the contribution of the association rate to the equilibrium dissociation constant was fixed at $107 \cdot M^{-1} \cdot s^{-1}$, except for older values obtained by previous papers.
- 14. Similarly, a reasonable first order default dissociation rate constant could be in the order of $10^{-2} \cdot 10^{-3} \cdot s^{-1}$. This ranges will insure a good affinity between the two interacting species. We have utilized the semi-quantitative information implicitly present in the papers quoted in the References accompanying the Annotation List according to the above considerations, to fill up gaps concerning rates and concentrations.
 - 15. Numerical values have been interpolated by taking into account the constraints imposed by: a) existing values; b) molecular anatomy of the network; and c) indirect evidences at the molecular, cellular and clinical level, that we tried to satisfy. In general, the network system imposed relatively narrow ranges (3-5 times intervals) of the interpolated values. .
 - 16. Leahy DJ. A molecular view of anti-ErbB monoclonal antibody therapy. *Cancer cell*. 2008; 13(4):291-293.
 - 17. Verveer PJ, Wouters FS, Reynolds AR and Bastiaens PI. Quantitative imaging of lateral ErbB1 receptor signal propagation in the plasma membrane. *Science*. 2000; 290(5496):1567-1570.
 - 18. The protein-protein interaction reactions of the receptors family ErbB was described in a simplified way, attributing the same rates to all the members of the family.
 - 19. Zi Z and Klipp E. Constraint-based modeling and kinetic analysis of the Smad dependent TGF-beta signaling pathway. *PloS one*. 2007; 2(9):e936.
 - 20. Clarke DC, Betterton MD and Liu X. Systems theory of Smad signalling. *Systems biology*. 2006; 153(6):412-424.
 - 21. Vilar JM, Jansen R and Sander C. Signal processing in the TGF-beta superfamily ligand-receptor network. *PLoS computational biology*. 2006; 2(1):e3.
 - 22. Lee E, Salic A, Kruger R, Heinrich R and Kirschner MW. The roles of APC and Axin derived from experimental and theoretical analysis of the Wnt pathway. *PLoS biology*. 2003; 1(1):E10.
 - 23. see in the main text “Derivation of a Transcription Rate Function for MYC and CCND1” and S4.
 - 24. β -catenin, PIP2 and TP53 were endowed with a slow production and degradation rate. In this way, the model would tend to a steady state rather than to a continuous accumulation or complete destruction of the two molecules. .

25. β -catenin protein will be rapidly degraded, and therefore set on a lower concentration level, in the presence of an intact destruction complex (Axin:APC:GSK3 β). The model simulates a very slow degradation of a mutated β -catenin in HCT116 cells, or an APC inactivation in HT29 cells, and therefore a very slow β -catenin degradation also in these cells. .
26. PIP3, IP3, DAG were endowed with a slow degradation rate. In this way, the model would tend to a steady state rather than to a continuous accumulation of these molecules.
27. mRNA of MYC and CCND1 were endowed with a slow production and degradation rate. In this way, the model would tend to a steady state rather than to a continuous accumulation or complete destruction of the two messengers. See main text “Derivation of a Transcription Rate Function for MYC and CCND1” and S4 for the transcription rates of MYC (MYC_mRNA_Gen) and CCND1 (CCND1_mRNA_Gen) .
28. Inhibitors were implemented as follows: according to the information given by the company selling the inhibitor (see S3.1: Details about cell cultures and reagents) and according to the concentration of inhibitor used, we calculated different inhibition levels for each inhibitor.
29. Numerical values have been interpolated by taking into account the constraints imposed by: a) existing values; b) molecular anatomy of the network.
30. Wakefield LM, Smith DM, Masui T, Harris CC and Sporn MB. Distribution and modulation of the cellular receptor for transforming growth factor-beta. The Journal of cell biology. 1987; 105(2):965-975.
31. We assume that activators and repressor complexes can bind DNA in different sites. In the case of concentration value of TFBS, we considered two binding site: one binding site for TCF4 and one binding site for SMAD4. .
32. Carlson ME, Conboy MJ, Hsu M, Barchas L, Jeong J, Agrawal A, Mikels AJ, Agrawal S, Schaffer DV and Conboy IM. Relative roles of TGF-beta1 and Wnt in the systemic regulation and aging of satellite cell responses. Aging cell. 2009; 8(6):676-689.

Supplementary Material 3.1 - Cell cultures and reagents

Cells were cultured in DMEM (Gibco), supplemented with 10% heat-inactivated fetal bovine serum (FBS) (Hyclone), 2mM L-glutamine (Gibco) and 1% Penicillin-Streptomycin solution (Gibco). No EGF was added to our medium. Considering that we gave 10% serum, the corresponding simulations were performed at 1/10 the physiologic EGF concentration, therefore at 0.01 nM. The following inhibitors were used: MEK inhibitor CI-1040 (also known as PD184352) (Sigma-Aldrich) (kindly provided by Dr. Alex von Kriegsheim), PI3K inhibitor PI-103 (Sigma-Aldrich/Tocris) (kindly provided by Dr. Natalia Volinsky), AKT inhibitor Perifosine (Selleck), GSK3 β inhibitor 1-Azakenpaullone (Sigma-Aldrich), and Tankyrase inhibitor XAV939 (Sigma-Aldrich). Perifosine was dissolved in ethanol (Et-OH), while all others inhibitors were dissolved in DMSO. At the level of final dilution we had [(1 ul Et-OH + 3ul DMSO)/(1 ml culture medium)]. We used CI-1040 at a final concentration of 2 μ M (IC50 \approx 300nM. Inhibition of the target in our simulations: around 80% for both cell lines). We used PI-103 at 500nM (IC50 \approx 150nM. Inhibition of the specific target in our simulations: around 85% for both cell lines). We used Perifosine at 20 and 40 μ M (IC50 \approx 4.8 μ M, inhibition of the specific target in our simulations \approx 50% (20 μ M) or \approx 70% (40 μ M) for both cell lines. We used Azakenpaullone at 1 μ M (IC50 \approx 18nM, inhibition of the specific target in our simulations \approx 98% for HT29). We used XAV939 at 1 μ M (IC50 7.5nM, inhibition of the specific target in our simulations \approx 99% for both cell lines). These inhibition levels are derived from the IC50s given in the product data-sheets and our subsequent computations performed using our reaction list (Supplementary Table 2.1).

Supplementary material 3.2 - Western Blots: Methods and raw results

Preliminary experiments: We performed preliminary experiments to determine the optimal time to assay the proteins after addition of inhibitors, and to examine the effect of complete media change either on the day before addition of inhibitors or at the same time as inhibitors were added (data not shown).

We performed preliminary experiments to determine the optimal time to assay the proteins after addition of inhibitors (5', 10', 20', 30', 40' and 60' min), and to examine the effect of complete media change either on the day before addition of inhibitors or at the same time as inhibitors were added (data not shown). From these experiments we selected 30 min as a representative time to measure changes for protein and phospho-protein levels. A quasi plateau effect had been reached in the time interval 10' - 60' min. The timing of complete fresh media change did not alter the trend of experimental results, as long as controls were treated in the same manner. We also considered the practically negligible role of the vehicles used for

our inhibitors [(EtOH 1ul + DMSO 3 ul)/(1 ml culture medium)] (data not shown). After these preliminary experiments, all the combinations of different inhibitors were examined at 30' min incubation, after a change with complete fresh medium.

We seeded cells in 6 wells plates, to obtain an 80-90% confluence at the time of pharmacological treatment. After incubation with inhibitors, the cells were washed twice with cold PBS and lysed with lysis buffer (25mM Tris-phosphate (pH 7.8), 2mM DTT, 2mM EDTA, 2mM EGTA 10% glycerol, 1% Triton X-100) in the presence of two phosphatase inhibitors (50 mM NaF, 5 mM Na₃VO₄) and a protease inhibitor cocktail (Sigma-Aldrich). We sonicated all lysates for 10 seconds at power 2 with a MISONIX XL-2000 series sonicator. Thirty micrograms of whole lysate were resolved, for all samples, using an 8% acrylamide gel electrophoresis under reducing conditions. We transferred it to a PVDF membrane. The resulting membranes were blocked with 5% BSA (Sigma-Aldrich) diluted in a TBS solution with 0.1% Tween 20 (TBST), for 1 hour. Membranes were then incubated with primary antibodies: [HER2/ErbB2 (29D8) (#2165)]; [EGF receptor (D38B1) (#4267)]; [α/β -Tubulin (#2148)]; [β -Actin (#4970)]; [PTEN (#9552)]; [AKT (pan) (#4691)]; [phospho-AKT (Ser473) (#4060)]; [p44/42 MAPK (Erk1/2) (#9102)]; [phospho-44/42 MAPK (Erk1/2) (Thr202/Tyr204) (#9101)]. We used dilutions and protocols suggested by the supplier (Cell Signaling Technology). For the evaluation of phospho/dephospho ratios of AKT and ERK1/2, first we performed the detection using antibodies for phosphorylated states and, after stripping, the membranes were re-probed using the anti-total proteins antibodies. The stripping procedure adopted is according to Yee-Guide Yeung and E. Richard Stanley [1], based on the use of Guanidine hydrochloride. The stripped membranes were saturated with a solution of TBST- MILK 5%. We performed the detection using a secondary horseradish peroxidase-linked goat anti-rabbit antibody (Santa-Cruz) at a dilution of 1:5000 and an ECL chemi-luminescence system (Thermo Scientific). After Western blotting, we estimated the intensity of the bands obtained by a ChemidocXSR station using the software QuantityOne (Bio-Rad).

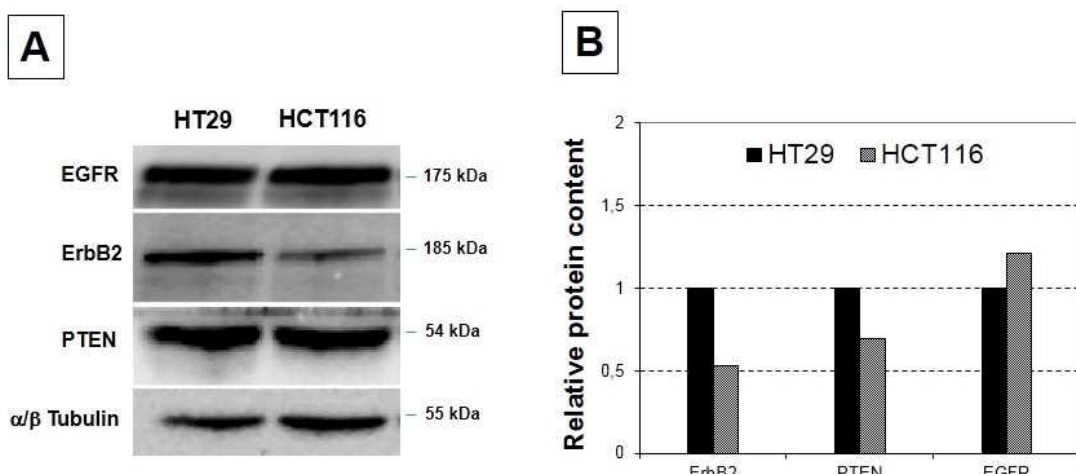
We used the reads from total protein amount of the same stripped membrane to standardize all the values obtained for the phosphorylated state. To obtain a comprehensive assessment of the phosphorylated versus non phosphorylated ratio change, for each experimental condition, the data were further expressed as values related to the "not treated" condition of the same membrane, were the ratio were arbitrary fixed to be equal to 1. For both cell lines the treatments were replicated by three independent experiments and the statistical analysis of the data were approached by GraphPad Prism 5.

PTEN, ErbB2, EGFR expression analysis in HCT116 and HT29 cancer lines

HCT116 and HT29 mutations / alterations present in our MIM are according to Cancer Cell Line Encyclopedia [2, 3].

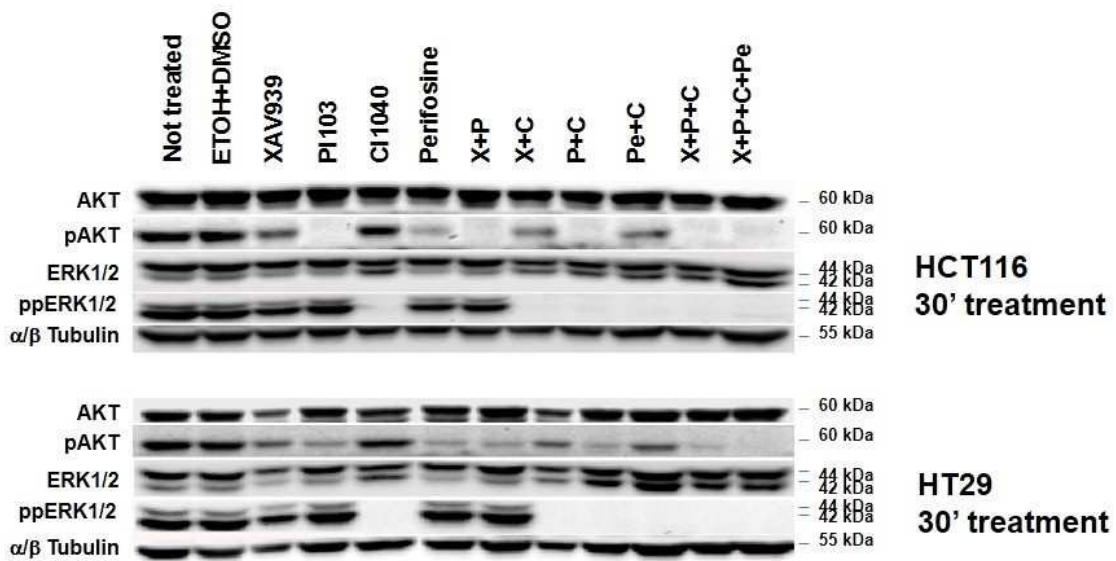
To determine the concentrations to be used in the modeling of our MIM, for the cell lines used for our experimental verifications, we performed a semi-quantitative determination by western blot analysis, for protein PTEN, ErbB2 and EGFR. Two total cell lysates were used for each cell line, corresponding to untreated samples, obtained from independent experiments. We transferred and evaluated all samples on the same PVDF membrane and we normalized the results using the anti-tubulin antibody.

HCT116 had not completely lost PTEN, despite the homozygous mutation in the 3'-UTR of its messenger, but showed only a reduction of expression of about 35%, compared to the HT29 cancer line. Concerning the expression of EGF's receptors, HT29 showed a double amount of ErbB2 compared to HCT116, while had a reduction of expression of about 20% with regard to the presence of EGFR.



Supplementary Figure 3.2.1: PTEN, ErbB2, EGFR expression analysis. Panel A: evaluation of the relative content of ErbB2, PTEN, and EGFR, in HT29 and HCT116 cell lines. We used tubulin to normalize the values. Here we show a representative panel for the semi-quantitative comparison.

Panel B: The histogram shows the relative protein content for ErbB2, PTEN and EGFR in HT29 and HCT116 cells respectively, obtained by averaging the values from two independent experiments. To better compare the relative protein content in the two cell lines, for each protein the values obtained in the HT29 cell line, were made = 1.

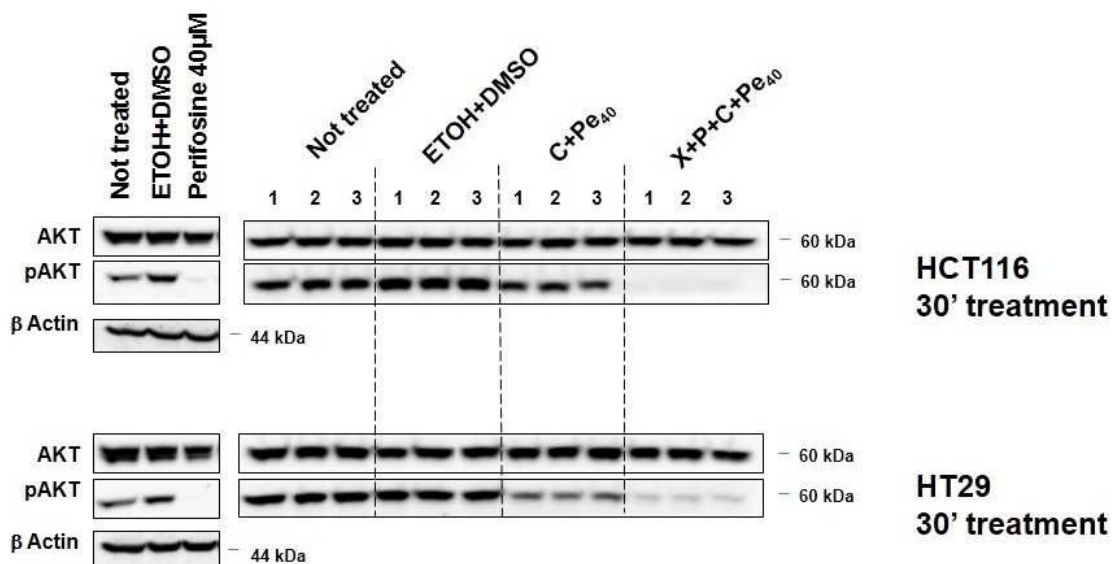


Supplementary Figure 3.2.2: pAKT/AKT and ppERK1/2/ERK ratio analyses in HT26 and HCT116 cell lines.
Representative panel of a semi-quantitative analysis for pAKT/AKT and ppERK1/2/ERK ratio change during a pharmacological treatment of 30 minutes in HCT116 and HT29 cell lines, respectively.

We resolved 30 ug of total lysate for each experimental condition by 8% acrylamide gel electrophoresis under reducing conditions. The values referred to phosphorylated proteins (pAKT and ppERK1/2) were normalized using the real total amount of the same protein present on the PVDF membrane, detected after stripping and re-probing (AKT and ERK1/2).

We introduced a further loading control using an α/β Tubulin antibody.

Inhibitors' abbreviations: XAV939 (X), PI-103 (P), CI-1040 (C), Perifosine (Pe).



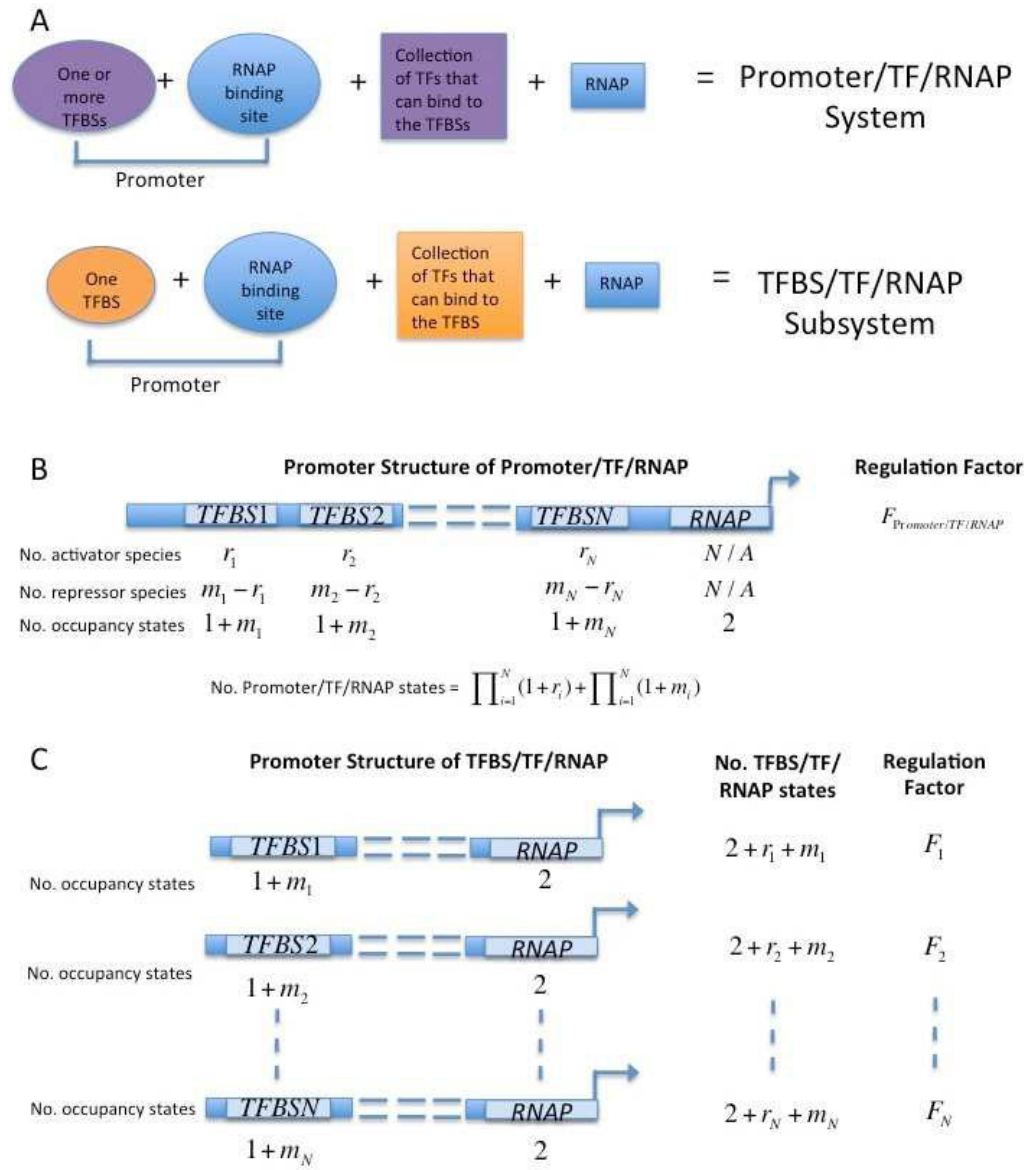
Supplementary Figure 3.2.3: pAKT/AKT ratio analysis in HT26 and HCT116 cell lines, using Perifosine 40uM.

Representative panels of a semi-quantitative analyses for pAKT/AKT ratio change during pharmacological treatments of 30 minutes in HCT116 and HT29 cell lines by using Perifosine 40uM alone (panels on the left) or in combination with others inhibitors (panels on the right). The panels on the left show only one representative experiment of a total of three evaluated in the main text for the treatments with Perifosine 40uM alone, while the panels on the right show all the biological triplicate experiments on the same membrane of the treatments with inhibitors' combinations. We resolved 30 ug of total lysate for each experimental condition by 8% acrylamide gel electrophoresis under reducing conditions. The values referred to phosphorylated protein pAKT was normalized using the real total amount of the same protein present on the PVDF membrane. We introduced a further loading control using an β -Actin antibody. Inhibitors' abbreviations: XAV939 (X), PI-103 (P), CI-1040 (C), Perifosine (Pe40).

References to Supplementary Material 3.2 - Western Blots

1. Yeung YG and Stanley ER. A solution for stripping antibodies from polyvinylidene fluoride immunoblots for multiple reprobing. Analytical biochemistry. 2009; 389(1):89-91.
2. The Cancer Cell Line Encyclopedia.
3. Barretina J, Caponigro G, Stransky N, Venkatesan K, Margolin AA, Kim S, Wilson CJ, Lehar J, Kryukov GV, Sonkin D, Reddy A, Liu M, Murray L, Berger MF, Monahan JE, Morais P, et al. The Cancer Cell Line Encyclopedia enables predictive modelling of anticancer drug sensitivity. Nature. 2012; 483(7391):603-607.

Supplementary Figure 4.1 - Illustration of the transcription factors and transcription factor binding sites considered in the *Promoter/TF/RNAP* and *TFBS/TF/RNAP* systems



Supplementary Figure 4.1. Illustration of the transcription factors and transcription factor binding sites considered in the *Promoter/TF/RNAP* and *TFBS/TF/RNAP* systems. A. *Promoter/TF/RNAP* and *TFBS/TF/RNAP* are collections of promoter binding sites (ovals) and the proteins that bind to them (rectangles). Binding sites and their binding proteins can be associated with RNAP (blue) or TFs (purple or

orange). $Promoter/TF/RNAP$ consists of one or more TFBSs, an RNAP binding site, all TFs that can bind to the TFBSs and RNAP. $TFBS/TF/RNAP$ consists of one TFBS, an RNAP binding site and all TFs that can bind to the TFBS. **B.** $Promoter/TF/RNAP$ is illustrated for a promoter with N TFBSs. The n^{th} TFBS can be unoccupied or occupied by any one of the m_n TFs assumed to bind to that site, for $n = 1, \dots, N$. Activators constitute r_n of the m_n TFs. The regulation factor of the gene represented by $Promoter/TF/RNAP$ is denoted by $F_{Promoter/TF/RNAP}$. The number of terms constituting $F_{Promoter/TF/RNAP}$ equals the number of possible occupancy states of $Promoter/TF/RNAP$.

Supplementary Material 4.2 - Literature background describing the involvement of key transcription factors and transcription factor binding sites in regulation of MYC and CCND1 transcription

The first step in building the thermo-statistical model involves identifying key transcription factor binding sites (TFBSs) responsible for MYC and CCND1 activation and repression, as well as the main TFs that bind to them. We have considered only some of the most important and best studied TFs (see reviews on MYC transcription [1, 2] and CCND1 transcription [3, 4]).

We start with TCF7L2, also known as TCF4, which is the most prominently expressed member of the TCF family of TFs in the intestinal epithelium, and a crucial transcriptional regulator in intestinal cells in particular [1, 5, 6]. TCF7L2 binding sites (termed $TFBS_{TCF7L2}$ in our model) have been found in both the MYC and CCND1 promoters, and have been shown to bind a number of complexes responsible for activation or repression of transcription. A complex of TCF7L2 and β -catenin can activate transcription of either gene through binding to $TFBS_{TCF7L2}$ [7-10]. Phosphorylation of β -catenin at Y654 in the cytoplasm results in its release from cadherins (especially type E) and facilitates its migration to the nucleus, with a consequent increase in TCF-mediated transcriptional activity [8, 11]. TCF7L2 binding sites can also bind the transcription activator complex TCF7L2-SMAD4, or, in contrast, mediate repression of transcription by binding a complex of TCF7L2 and GROUCHO [12-14].

SMAD4 can alternatively heterodimerise with TGF- β receptor regulated SMADs (SMAD2 or SMAD3), whose affinity for nuclear factors increases upon their phosphorylation (15, 16). These SMAD complexes can then bind to a SMAD binding site ($TFBS_{SMAD}$) on MYC, repressing its transcription [15-17]. A similar inhibitory role of the TGF- β pathway on CCND1 transcription has been described [18, 19]. SMAD4 (most likely complexed with phosphorylated SMAD2 or SMAD3) binds to the promoter region of CCND1 upon TGF- β treatment, repressing transcription [20].

AP1 (activating protein-1) is the collective term applied to dimeric transcription factors with subunits consisting of Jun, Fos or ATF (activating transcription factor) [21]. AP1, depending on its composition, has

been shown to activate or repress CCND1, and its activity can be modulated by phosphorylation [3, 22]. In the model, we assume a net-positive effect of AP1 on CCND1 transcription [23-25], where CCND1 has a consensus AP1 ($TFBS_{AP1}$) site in its promoter [3, 25]. A canonical AP1 responsive element has also been identified in the MYC promoter [26] and MYC transcription is known to be activated by the MAPK pathway, which mediates AP1 phosphorylation [27].

The tumor suppressor protein TP53 binds to the MYC promoter on a $TFBS_{TP53}$ site and represses MYC transcription through a mechanism that involves histone deacetylation [28]. TP53 also represses CCND1 transcription indirectly, by down regulating the transcriptional co-activator Bcl-3 [4, 29]. Additionally, the CCND1 promoter contains a functional (ChIP confirmed) human NF- κ B binding site at -39bp, which binds TP53 [4].

MYC and CCND1 are target genes of E2F, a family of proteins that require a dimerization partner (DP) protein in order to bind DNA [30, 31]. RB protein transrepresses E2F target genes through binding to E2F-DP complexes on the gene promoter at a $TFBS_{E2F-DP1}$ site [17, 30]. Multi-phosphorylation of RB results in dissociation of RB from E2F-DP1 and subsequent activation of the E2F-DP1 complex, allowing for activation of transcription [17, 30, 31].

For convenience, we introduce shorthand designations for the TF activator and repressor complexes that bind to the promoter regions of MYC and CCND1 in our model. We assume that activators β -Catenin-TCF7L2 (x_1), p β -Catenin(Y654)-TCF7L2 (x_1p), SMAD4-TCF7L2 (x_2) and repressor GROUCHO-TCF7L2 (y_1) compete for binding to the same site, $TFBS_{TCF7L2}$. Likewise, pSMAD2-SMAD4 (y_2) and pSMAD3-SMAD4 (y_3) repressor complexes compete for $TFBS_{SMAD4}$. AP1 (x_3) and pAP1 (x_3p) bind mutually exclusively to $TFBS_{AP1}$. Finally, we assume that TP53 (y_4) binds to $TFBS_{TP53}$, and that E2F-DP1 (x_4) competes with its repressor counterpart E2F-DP1-RB (y_5) for $TFBS_{E2F-DP1}$.

Supplementary Material 4.3 - Derivation of the transcription rate function for MYC and CCND1

Regulation of transcription is typically multi-factorial, involving a series of transcriptional activators, repressors and co-factors that control the recruitment of the transcriptional machinery and RNA Polymerase (RNAP) to the transcription start site [32, 33]. With reference to eukaryotic / mammalian cells mRNAs, we have in mind RNAP II. Several useful tools have been employed to investigate the relationship between active TF concentrations and the mRNA levels of genes under their control. One approach is that of a statistical thermodynamic framework [34-36], which we have applied to relate MYC and CCND1 transcription rates to the concentrations of their upstream transcriptional activator and repressor complexes.

The first step in building the thermo-statistical model was to identify key transcription factor binding sites (TFBSs) responsible for activation or repression of MYC and CCND1 transcription, as well as the main TFs that bind to them (see Fig. 2 and Supplementary Material 4.2 for details). As these genes have similar key transcriptional regulators, for the purposes of the model we assume that they have equivalent promoter regions and the same transcription rates. The entire system consisting of all five TFBSs, all TFs considered in the MIM and RNAP (RNA-Polymerase), is denoted as a *Promoter/TF/RNAP* system, whereas the designation *TFBS/TF/RNAP* refers to a subsystem of *Promoter/TF/RNAP* where only one TFBS, the corresponding TFs and RNAP are included (Supplementary Fig. 4.1). For instance, TFBS_{TCF7L2} together with the competing activator complexes β-Catenin- TCF7L2, pβ-CateninY654-TCF7L2, SMAD4-TCF7L2 and repressor complex GROUCHO-TCF7L2, and the RNAP binding site is denoted as *TFBS_{TCF7L2}/TF/RNAP*.

Transcription occurs when RNAP binds to the promoter, and the transcription rate is assumed to be proportional to the probability that RNAP is bound [34, 37]. Promoter-TF interactions change the probability of RNAP binding to the promoter and, therefore, the transcription rate. There are many possible states in which the individual *TFBS/TF/RNAP* subsystems and the entire *Promoter/TF/RNAP* system can reside. These states tell us, which (if any) TFs are bound to TFBSs, and whether RNAP is bound. Two rules impact on the number of possible states of *TFBS/TF/RNAP* (or *Promoter/TF/RNAP*). First, we assume that RNAP and a repressor TF cannot be simultaneously bound to the promoter region, and secondly, we assume that

two or more TFs competing for a TFBS cannot be simultaneously bound to it. According to Boltzmann statistics, each state can be assigned a statistical weight, and the probability of occurrence of each state is proportional to its statistical weight. The proportionality constant is the sum of statistical weights over all potential states. Expressions for the statistical weights for different *TFBS/TF/RNAP* states are given elsewhere (Supplementary Material 4.5, Supplementary Tables 4.7- 4.12), while here we describe the probability of RNAP being bound to or unbound from the promoter, $P(\text{RNAP}_{\text{bound}})$, in terms of these weights. The probability $P(\text{RNAP}_{\text{bound}})$ is proportional to the sum of the statistical weights for all DNA states where RNAP is bound, denoted as $S(\text{RNAP}_{\text{bound}})$. Similarly, the probability of RNAP not being bound to the DNA is proportional to the sum of the statistical weights of all states where RNAP is not bound to the DNA, denoted as $S(\text{RNAP}_{\text{unbound}})$.

We describe these relationships mathematically as,

$$P(\text{RNAP}_{\text{bound}}) = \frac{S(\text{RNAP}_{\text{bound}})}{Z}, \quad P(\text{RNAP}_{\text{unbound}}) = \frac{S(\text{RNAP}_{\text{unbound}})}{Z} \quad (1)$$

where the proportionality coefficient Z is the partition function equal to the sum of $S(\text{RNAP}_{\text{bound}})$ and $S(\text{RNAP}_{\text{unbound}})$.

Consequently,

$$P(\text{RNAP}_{\text{bound}}) = \frac{S(\text{RNAP}_{\text{bound}})}{S(\text{RNAP}_{\text{bound}}) + S(\text{RNAP}_{\text{unbound}})} \quad (2)$$

To simplify the algebraic expressions, it is convenient to introduce the regulation factor of a gene, F_{reg} , which is directly expressed in terms of $P(\text{RNAP}_{\text{bound}})$, as follows [35, 36]. We take the sum of the statistical weights of all DNA states where RNAP is bound to the promoter and divide it by the sum of the statistical weights where RNAP is not bound, and normalize it by the weight of the reference state of RNAP binding (in the absence of all TFs). This weight is expressed as $\frac{[\text{RNAP}]}{K_{\text{RNAP}}}$, where $[\text{RNAP}]$ denotes the cellular concentration of RNAP and K_{RNAP} is the equilibrium dissociation constant of the RNAP-DNA complex [38].

For a consideration about possible values in mammalian cells (in the absence of all TFs) of the ratio $\frac{[\text{RNAP}]}{K_{\text{RNAP}}}$, look at Supplementary Material 4.6.

F_{reg} is defined as,

$$F_{reg} = \left(\frac{[RNAP]}{K_{RNAP}} \right)^{-1} \frac{S(RNAP_{bound})}{S(RNAP_{unbound})} = \left(\frac{[RNAP]}{K_{RNAP}} \right)^{-1} \frac{P(RNAP_{bound})}{P(RNAP_{unbound})} = \\ = \left(\frac{[RNAP]}{K_{RNAP}} \right)^{-1} \frac{P(RNAP_{bound})}{1 - P(RNAP_{bound})} \quad (3)$$

From Eqn. 3, it follows that the probability of RNAP to be bound to the promoter can be expressed in terms of the regulation factor, as follows,

$$P(RNAP_{bound}) = \frac{1}{1 + \left(\frac{[RNAP]}{K_{RNAP}} F_{reg} \right)^{-1}} \quad (4)$$

We now need to decompose the probability $P(RNAP_{bound})$ into the relative contributions of each TFBS in recruiting RNAP (or inhibiting the recruitment of RNAP) to its binding site, assuming independence of TFBSs. Importantly, the regulation factor of a gene with multiple independent TFBSs is expressed as the product of the regulation factors for each *TFBS/TF/RNAP* subsystem (see a mathematical derivation in Supplementary Material 4.4). Therefore, the regulation factor for our genes of interest is given by,

$$F_{Promoter/TF/RNAP} = F_{TCF7L2} * F_{SMAD4} * F_{AP1} * F_{TP53} * F_{E2F-DP1} \quad (5)$$

where $F_{Promoter/TF/RNAP}$ is the regulation factor of the entire *Promoter/TF/RNAP* system and F_{TCF7L2} , F_{SMAD} , F_{AP1} , F_{TP53} and $F_{E2F-DP1}$ are the regulation factors of the *TFBS/TF/RNAP* subsystems, corresponding to the independent single sites, $TFBS_{TCF7L2}$, $TFBS_{SMAD4}$, $TFBS_{AP1}$, $TFBS_{TP53}$ and $TFBS_{E2F-DP1}$, respectively. The transcription rates of MYC and CCND1 are obtained from Eqn. 5, as described in Supplementary Material 4.6.

Supplementary Material 4.4 - Derivation of the regulation factor $F_{Promoter/TF/RNAP}$ in terms of the regulation factors of independent $TFBS/TF/RNAP$ subsystems

Consider a gene promoter with N distinct TFBSSs, where at each site there are a number of different types of activator and repressor TF complexes competing for binding to the DNA. To find an expression for the probability that RNAP is bound to the promoter we need to consider all possible promoter-binding patterns that can occur, exhaustively allocating statistical weights to all combinatorial possibilities. We assume that all TFBSSs are non-overlapping and each promoter-bound activator TF can interact with RNAP, decreasing the free energy of RNAP binding to the promoter. Rather than listing all possible states of the promoter, we show here that we can simplify derivation of the regulation factor of the full promoter, $F_{Promoter/TF/RNAP}$, by writing it as a product of the regulation factors of the individual TFBSSs on the promoter as follows (Eqn. 5 of Supplementary Document 4.3):

$$F_{Promoter/TF/RNAP} = F_{TCF7L2} * F_{SMAD} * F_{AP1} * F_{TP53} * F_{E2F-DP1} \quad (1)$$

In the general case, where there are N independent TFBSSs, and F_n is the regulation factor for the $TFBS/TF/RNAP$ subsystem number n , we claim that the regulation factor of the full system can be expressed as the product of all F_n :

$$F_{Promoter/TF/RNAP} = \prod_{n=1}^N F_n \quad (2)$$

The remainder of this section is dedicated to providing a proof for Eqn. 2, a convenient shortcut for computing the regulation factor of a gene with many TFBSSs, as previously proposed in the literature without a formal proof (1). We first rewrite Eqn. 2 in terms of probabilities of RNAP binding to the N-site promoter (also known as the *Promoter/TF/RNAP* system), as follows:

$$\begin{aligned}
& \left(\frac{[RNAP]}{K_{RNAP}} \right)^{-1} \frac{P(RNAP_{bound})}{P(RNAP_{unbound})} \\
&= \prod_{n=1}^N \left(\frac{[RNAP]}{K_{RNAP}} \right)^{-1} \frac{P(RNAP_{bound} | \text{only TFBS } n \text{ occupied})}{P(RNAP_{unbound} | \text{only TFBS } n \text{ occupied})}
\end{aligned} \tag{3}$$

We aim now to prove that Eqn. 3 (which is equivalent to Eqn. 2) holds for an N-site promoter by splitting the probabilities into their statistical weight components (see Supplementary Document 4.5 for an example of how to calculate statistical weights). Suppose that at each site $n = 1, \dots, N$ there are m_n types of TF complexes (of which r_n are activators, $0 \leq r_n \leq m_n$) competing for binding to the DNA. For each site n we order the numbering of the m_n TF species at each site such that the activators have the lower valued subscripts and define the functions, h_n and g_n , as follows

$$h_n = \sum_{i=1}^{m_n} \frac{[TF_{n,i}]}{K_{TF_{n,i}}}, \quad g_n = \sum_{i=1}^{r_n} \frac{[TF_{n,i}]}{K_{TF_{n,i}}} e^{-\Delta\varepsilon_{RNAP-TF_{n,i}}}, \tag{4}$$

where $TF_{n,i}$ is the i^{th} TF species competing for TFBS n , $K_{TF_{n,i}}$ is the equilibrium dissociation constant of $TF_{n,i}$ and TFBS n , and $\Delta\varepsilon_{RNAP-TF_{n,i}}$ (in units of RT) is the negative-valued change in the free energy of RNAP binding to the promoter induced by $TF_{n,i}$ bound to TFBS n . The function h_n equals the total statistical weight of occupancy of TFBS n by activator or repressor TFs (within the *Promoter/TF/RNAP* system) when all other TFBSs are unoccupied and RNAP is not bound to the promoter h_n . The function g_n equals the total statistical weight of occupancy of TFBS n , when all other TFBSs are free but RNAP is bound to the DNA.

For independent TFBSs, the statistical weights representing the occupancy of multiple sites with RNAP being bound or not bound to the promoter can be written in terms of sums and products of the elementary h_n and g_n terms, as presented below [36]. The statistical weight of all possible cases of occupancy of one or more than one TFBS when RNAP is not bound is given by the sums and products of the corresponding h_n terms, leading directly to the following expression for the probability $P(RNAP_{unbound})$ of RNAP being not bound to the promoter,

$$\begin{aligned}
& P(RNAP_{unbound}) \\
&= (1 + \Sigma_{i=1}^N h_i + \Sigma_{i=1}^N h_i \Sigma_{j=i+1}^N h_j + \Sigma_{i=1}^N h_i \Sigma_{j=i+1}^N h_j \Sigma_{k=j+1}^N h_k + \dots + \Sigma_{i_1=1}^N h_{i_1} \Sigma_{i_2=i_1+1}^N h_{i_2} * \dots \\
&\quad * \Sigma_{i_{n-1}=N-1}^N h_{i_{n-1}} + \Sigma_{i_1=1}^N h_{i_1} \Sigma_{i_2=i_1+1}^N h_{i_2} * \dots * \Sigma_{i_{n-1}=N-1}^N h_{i_{n-1}} * \Sigma_{i_n=N}^N h_{i_n}) / Z
\end{aligned} \tag{5}$$

where the successive terms correspond to the promoter states when RNAP is unbound and no TF is bound to DNA, only one TFB is occupied, two TFBs are occupied, ..., and all N TFBs are occupied. Z is the standard partition function that is the sum of statistical weights of all possible promoter-binding scenarios. The probability $P(RNAP_{unbound})$ is a polynomial expression of N arguments h_1, h_2, \dots, h_N and can be factorized by extracting h_1 from the expression Eqn. 5 as follows:

$$\begin{aligned}
& P(RNAP_{unbound}) \\
&= (1 + (h_1 + \Sigma_{i=2}^N h_i) + (h_1 \Sigma_{j=2}^N h_j + \Sigma_{i=2}^N h_i \Sigma_{j=i+1}^N h_j) \\
&\quad + (h_1 \Sigma_{j=2}^N h_j \Sigma_{k=j+1}^N h_k + \Sigma_{i=2}^N h_i \Sigma_{j=i+1}^N h_j \Sigma_{k=j+1}^N h_k) + \dots + (h_1 \Sigma_{i_2=2}^N h_{i_2} * \dots * \Sigma_{i_{n-1}=N-1}^N h_{i_{n-1}} \\
&\quad + \Sigma_{i_1=2}^N h_{i_1} \Sigma_{i_2=i_1+1}^N h_{i_2} * \dots * \Sigma_{i_{n-1}=N-1}^N h_{i_{n-1}}) + (h_1 \Sigma_{i_2=2}^N h_{i_2} * \dots * \Sigma_{i_{n-1}=N-1}^N h_{i_{n-1}} * \Sigma_{i_n=N}^N h_{i_n}) / Z \\
&= ((1 + h_1) + (1 + h_1) \Sigma_{i=2}^N h_i + (1 + h_1) \Sigma_{i=2}^N h_i \Sigma_{j=i+1}^N h_j + \dots \\
&\quad + (1 + h_1) \Sigma_{i_1=2}^N h_{i_1} \Sigma_{i_2=i_1+1}^N h_{i_2} * \dots * \Sigma_{i_{n-1}=N-1}^N h_{i_{n-1}} + (1 + h_1) \Sigma_{i_1=2}^N h_{i_1} \Sigma_{i_2=i_1+1}^N h_{i_2} * \dots \\
&\quad * \Sigma_{i_{n-1}=N-1}^N h_{i_{n-1}} * \Sigma_{i_n=N}^N h_{i_n}) / Z \\
&= (1 + h_1)(1 + \Sigma_{i=2}^N h_i + \Sigma_{i=2}^N h_i \Sigma_{j=i+1}^N h_j + \Sigma_{i_1=2}^N h_{i_1} \Sigma_{i_2=i_1+1}^N h_{i_2} * \dots * \Sigma_{i_{n-1}=N-1}^N h_{i_{n-1}} \\
&\quad + \Sigma_{i_1=2}^N h_{i_1} \Sigma_{i_2=i_1+1}^N h_{i_2} * \dots * \Sigma_{i_{n-1}=N-1}^N h_{i_{n-1}} * \Sigma_{i_n=N}^N h_{i_n}) / Z
\end{aligned} \tag{6}$$

We can now extract the h_2 terms in the same way:

$$\begin{aligned}
P(RNAP_{unbound}) &= (1 + h_1)(1 + (h_2 + \sum_{i=3}^N h_i)) + (h_2 \sum_{j=3}^N h_j + \sum_{i=3}^N h_i \sum_{j=i+1}^N h_j) \\
&\quad + (h_2 \sum_{i_2=3}^N h_{i_2} * \dots * \sum_{i_{n-1}=N-1}^N h_{i_{n-1}} + \sum_{i_1=3}^N h_{i_1} \sum_{i_2=i_1+1}^N h_{i_2} * \dots * \sum_{i_{n-1}=N-1}^N h_{i_{n-1}}) \\
&\quad + (h_2 \sum_{i_2=3}^N h_{i_2} * \dots * \sum_{i_{n-1}=N-1}^N h_{i_{n-1}} * \sum_{i_n=N}^N h_{i_n} + \sum_{i_1=3}^N h_{i_1} \sum_{i_2=i_1+1}^N h_{i_2} * \dots * \sum_{i_{n-1}=N-1}^N h_{i_{n-1}} \\
&\quad * \sum_{i_n=N}^N h_{i_n})/Z \\
&= (1 + h_1)(1 + h_2)(1 + \sum_{i=3}^N h_i + \sum_{i=3}^N h_i \sum_{j=i+1}^N h_j + \sum_{i_1=3}^N h_{i_1} \sum_{i_2=i_1+1}^N h_{i_2} * \dots \\
&\quad * \sum_{i_{n-1}=N-1}^N h_{i_{n-1}} + \sum_{i_1=3}^N h_{i_1} \sum_{i_2=i_1+1}^N h_{i_2} * \dots * \sum_{i_{n-1}=N-1}^N h_{i_{n-1}} * \sum_{i_n=N}^N h_{i_n})/Z
\end{aligned} \tag{7}$$

Continuing in this manner for h_3, h_4, \dots, h_N leads to the simplified expression

$$P(RNAP_{unbound}) = \prod_{i=1}^N (1 + h_i)/Z \tag{8}$$

In order to derive the probability $P(RNAP_{bound})$ of RNAP being bound to the promoter, we reuse the assumption that each TFBS acts independently facilitating or repressing RNAP binding. This means that TFs bound to different TFBSs do not directly interact with each other and independently contribute or repress the RNAP binding to the promoter. These assumptions allow us to generate a simplified expression for $P(RNAP_{bound})$ in terms of g_1, g_2, \dots, g_N similar to that derived for $P(RNAP_{unbound})$ as follows:

$$\begin{aligned}
P(RNAP_{bound}) &= \frac{[RNAP]}{K_{RNAP}} (1 + \sum_{i=1}^N g_i + \sum_{i=1}^N g_i \sum_{j=i+1}^N g_j + \sum_{i=1}^N g_i \sum_{j=i+1}^N g_j \sum_{k=j+1}^N g_k + \dots \\
&\quad + \sum_{i_1=1}^N g_{i_1} \sum_{i_2=i_1+1}^N g_{i_2} * \dots * \sum_{i_{n-1}=N-1}^N g_{i_{n-1}} + \sum_{i_1=1}^N g_{i_1} \sum_{i_2=i_1+1}^N g_{i_2} * \dots * \sum_{i_{n-1}=N-1}^N g_{i_{n-1}} \\
&\quad * \sum_{i_n=N}^N g_{i_n})/Z \\
&= \frac{[RNAP]}{K_{RNAP}} \prod_{i=1}^N (1 + g_i)/Z = \left(\frac{[RNAP]}{K_{RNAP}} \right)^{-N+1} \prod_{i=1}^N \frac{[RNAP]}{K_{RNAP}} \frac{(1 + g_i)}{Z}
\end{aligned} \tag{9}$$

The second equality follows by analogy with the expression for $P(RNAP_{unbound})$.

Thus, by Eqns. (3 (Supplementary Material 4.3), 8 and 9) we can write the following:

$$F_{Promoter/TF/RNAP} = \left(\frac{[RNAP]}{K_{RNAP}} \right)^{-1} \frac{P(RNAP_{bound})}{P(RNAP_{unbound})} = \left(\frac{[RNAP]}{K_{RNAP}} \right)^{-N} \frac{\prod_{i=1}^N \frac{[RNAP]}{K_{RNAP}}^{(1+g_i)/Z}}{\prod_{i=1}^N (1+h_i)/Z} \quad (10)$$

The usefulness of Eqn. 10 is shown in the following expression, where Z_1, Z_2, \dots, Z_N are the partition functions for the *TFBS/TF/RNAP* subsystems where only TFBS1, TFBS2, ..., or TFBSN can be occupied by TFs, respectively:

$$\begin{aligned} & \left(\frac{[RNAP]}{K_{RNAP}} \right)^{-1} \frac{P(RNAP_{bound})}{P(RNAP_{unbound})} = \left(\frac{[RNAP]}{K_{RNAP}} \right)^{-N} \frac{\prod_{i=1}^N \frac{[RNAP]}{K_{RNAP}}^{(1+g_i)/Z_i}}{\prod_{i=1}^N \frac{1+h_i}{Z_i}} \\ & = \left(\frac{[RNAP]}{K_{RNAP}} \right)^{-N} \prod_{i=1}^N \frac{P(RNAP_{bound} | \text{only TFBS } n \text{ occupied})}{P(RNAP_{unbound} | \text{only TFBS } n \text{ occupied})} \end{aligned} \quad (11)$$

Thus, we have proved that Eqn. 2 holds. Therefore, we can compute the regulation factor for a complex *Promoter/TF/RNAP* system by calculating the individual regulation factors for each *TFBS/TF/RNAP* subsystem and using the above equation.

It follows that for MYC and CCND1 transcription Eqn. 1 holds (which is Eqn. 5 of Supplementary Material 4.3).

Supplementary Material 4.5 - Example: Detailed derivation of the regulation factor $F_{E2F-DP1}$ for the *TFBS/TF/RNAP* subsystem associated with the E2F-DP1 transcription factor binding site

As an illustrative example, we present here a derivation of the regulation factor $F_{E2F-DP1}$ for the E2F-DP1 binding-site (*TFBS_{E2F-DP1}*) in terms of the activator (E2F-DP1, x_4) and repressor (E2F-DP1-RB, y_5) concentrations. The shorthand notation for the activators and repressors is as defined in Supplementary

Material 4.2 and Supplementary Fig. 4.1. The regulation factors F_{TFBS} for the remaining TFBSSs are expressed in Supplementary Tables 4.7 - 4.12. There are five possible states of the $TFBS_{E2F-DP1}/TF/RNAP$ subsystem (Table 4.7): state 1 is the unbound promoter reference state, state 2 where only $RNAP$ is bound, states 3 and 4 where the activator x_4 is bound in the absence or presence of $RNAP$, respectively, and state 5 where only the repressor y_5 is bound to the promoter (y_5 and $RNAP$ cannot bind to the DNA simultaneously, as we assume that transcription cannot occur in the presence of the repressor). The statistical weight of each of these states is determined by the product of a cellular concentration term and a Boltzmann factor. The concentration determines the number of ways this state (i) can occur, and the Boltzmann factor $\exp(-\varepsilon_i/RT)$ of state i is the exponential of minus the free energy change of the state relative to the reference state, where free energy changes arise from association and dissociation of complexes of TFs, RNAP and DNA. The free energy change ε_i is measured in units of RT (R is the gas constant, T is absolute temperature). Since we deal with free energy changes rather than absolute values we assume zero free energy of the reference state of the unbound promoter, and consequently a statistical weight equal to 1. Two of the five possible states of $TFBS_{E2F-DP1}/TF/RNAP$ subsystem have RNAP bound to the promoter (states 2 and 4, Supplementary Table 4.7), where the activator x_4 is either unbound or promoter-bound. Their statistical weights (w_2 and w_4 , respectively) are expressed as,

$$w_2 = \frac{[RNAP]}{K_{RNAP}}, \quad w_4 = \frac{[x_4][RNAP]}{K_{x_4} K_{RNAP}} e^{-\varepsilon_{x_4 R} / RT} \quad (1)$$

where K_{x_4} is the dissociation constant of the activator x_4 and $TFBS_{E2F-DP1}$, $\varepsilon_{x_4 R}$ is the free energy change of RNAP binding induced by the interaction of E2F-DP1 and the transcriptional machinery, and concentrations are denoted by square brackets. For the three remaining states (1, 3 and 5), RNAP is unbound, and their statistical weights are given by,

$$w_1 = 1, \quad w_3 = [x_4]/K_{x_4}, \quad w_5 = [y_5]/K_{y_5} \quad (2)$$

Using Eqn. 3 (Supplementary Material 4.3), we obtain the regulation factor $F_{E2F-DP1}$ as the ratio of probabilities of *RNAP* being bound or not bound to the gene promoter as follows:

$$F_{E2F-DP1} = \left(\frac{[RNAP]}{K_{RNAP}} \right)^{-1} \frac{w_2 + w_4}{w_1 + w_3 + w_5} = \frac{1 + \frac{[x_4]}{K_{x_4}} e^{-\frac{\varepsilon_{x_4} R}{RT}}}{1 + \frac{[x_4]}{K_{x_4}} + \frac{[y_5]}{K_{y_5}}} = \frac{1 + A_6 \frac{[x_4]}{K_{x_4}}}{1 + \frac{[x_4]}{K_{x_4}} + \frac{[y_5]}{K_{y_5}}} \quad (3)$$

The Boltzmann factor $A_6 = e^{-\varepsilon_{x_4} R / RT}$ is larger than 1, since the free energy change $\varepsilon_{x_4} R$ is negative, because the activator complex E2F-DP1 lowers the energy of RNAP binding to DNA.

The regulation factors for the other *TFBS/TF/RNAP* subsystems in the model are derived in the same manner as presented here. The regulation factors and statistical weights of associated promoter states are shown in Supplementary Tables 4.7 – 4.11, and summarized in Supplementary Table 4.12.

Supplementary Material 4.6 - Final expression for the transcription rate of MYC and CCND1.

Introductory note: Regulation of RNA Polymerase II (RNAP for short) transcription is a very complex event in mammals (and eukaryotes) [39]. RNAP itself is made of 12 subunits in humans. Sequence-specific DNA binding factors establish a bridge / communication with general/basal factors through an assortment of co-regulators (mediator complex). Recognition sites for sequence-specific factors tend to be arranged in clusters. In addition, there is associated involvement of chromatin-remodeling factors which catalyze covalent modifications of histones and other proteins. Complexity is further increased by cis-acting at long distance sequences (> 1kbp), either upstream or downstream of RNA transcription start, controlled by specific enhancer/regulator proteins. Post-translational modifications can modulate the DNA affinity of sequence-specific factors. Specific phosphorylations can for instance increase this affinity [39].

A chain of events starting with the cooperative presence of sequence specific factors co-opts mediator-complex-proteins and finally the core-transcription-complex containing RNAP [40]. In the absence of this chain of events, RNA polymerase II is generally thought to recognize, at low affinity, DNA non-specifically, with a weak intrinsic preference for Inr (initiator) consensus sequences (Py-Py-A-N-T/A-Py-Py in mammals) [40].

In calculation of the transcription rate in the thermostatistical model, the number of RNAP molecules in the nucleus of mammalian cells must be considered. Hieda *et al.* [41], in Table 1 of their work, report the number of the different forms of the largest (catalytic) subunit of RNA polymerase II, for HeLa cells. They report the total number of RNAPII nuclear molecules to be approximately 320,000. Maul and Deaven [42], in Table 1 of their work, give an estimation of the nuclear volume of different cell types. For HeLa cells, the nuclear volume was found to be approximately $374 \mu\text{m}^3$ ($3.74 \cdot 10^{-13}$ liters). Dividing the number of nuclear molecules by the ratio of Avogadro's number to nuclear volume, RNAPII nuclear molarity can be estimated to be around $1 \cdot 10^{-4}$ M.

K_{RNAP} is the equilibrium dissociation constant for a non-specific binding of RNAP II to chromatin-DNA, in the absence of all TFs. Because of a non-specific type of binding, K_{RNAP} will tend to be high (rapid

dissociation of RNAP from chromatin-DNA). For this base-line non-specific chromatin-DNA binding, we estimated the K_{RNAP} equilibrium dissociation constant to be roughly around $10^{-2} - 10^{-3}$ M. Accordingly, we have tested the predictions of our simulations arranging the value of $[RNAP]/K_{RNAP}$ between .01 and .1. Concordance with experimental results remained quite good, substantially invariant for the two values.

Computation of transcription rates: By the results of Supplementary Material 4.4 and the expressions of the regulation factors for the other TFBSS (Supplementary Tables 4.7 - 4.11), we obtain the regulation factor for the *Promoter/TF/RNAP* system of our genes of interest, as follows,

$$\begin{aligned}
 F_{Promoter/TF/RNAP} &= \frac{1 + A_1 \frac{[x_1]}{K_{x_1}} + A_2 \frac{[x_1 p]}{K_{x_1 p}} + A_3 \frac{[x_2]}{K_{x_2}}}{1 + \frac{[x_1]}{K_{x_1}} + \frac{[x_1 p]}{K_{x_1 p}} + \frac{[x_2]}{K_{x_2}} + \frac{[y_1]}{K_{y_1}}} * \frac{1 + A_4 \frac{[x_3]}{K_{x_3}} + A_5 \frac{[x_3 p]}{K_{x_3 p}}}{1 + \frac{[x_3]}{K_{x_3}} + \frac{[x_3 p]}{K_{x_3 p}}} * \frac{1 + A_6 \frac{[x_4]}{K_{x_4}}}{1 + \frac{[x_4]}{K_{x_4}} + \frac{[y_5]}{K_{y_5}}} \\
 &\quad * \frac{1}{1 + \frac{[y_2]}{K_{y_2}} + \frac{[y_3]}{K_{y_3}}} * \frac{1}{1 + \frac{[y_4]}{K_{y_4}}}
 \end{aligned} \tag{1}$$

Here the K values denote the equilibrium dissociation constants of the TF-TFBS complexes, and the A_i terms are dimensionless multipliers (the Boltzmann factors, whose expressions are given in Supplementary Tables 4.7 - 4.11). The multipliers A_i are larger than 1, because RNAP binding to DNA is energetically favorable, and therefore has a negative free energy.

Finally, the probability that RNAP is bound to the promoter is obtained from Eqns. 1 and 4 of Supplementary Material 4.4) .

$$\begin{aligned}
& P(RNAP_{bound}) \\
&= \frac{[RNAP]}{K_{RNAP}} \left(\left(1 + A_1 \frac{[x_1]}{K_{x_1}} + A_2 \frac{[x_1 p]}{K_{x_1 p}} + A_3 \frac{[x_2]}{K_{x_2}} \right) * \left(1 + A_4 \frac{[x_3]}{K_{x_3}} + A_5 \frac{[x_3 p]}{K_{x_3 p}} \right) * \left(1 + A_6 \frac{[x_4]}{K_{x_4}} \right) \right) \\
&\quad / \left(\frac{[RNAP]}{K_{RNAP}} \left(\left(1 + A_1 \frac{[x_1]}{K_{x_1}} + A_2 \frac{[x_1 p]}{K_{x_1 p}} + A_3 \frac{[x_2]}{K_{x_2}} \right) * \left(1 + A_4 \frac{[x_3]}{K_{x_3}} + A_5 \frac{[x_3 p]}{K_{x_3 p}} \right) * \left(1 + A_6 \frac{[x_4]}{K_{x_4}} \right) \right) \right. \\
&\quad + \left(1 + \frac{[x_1]}{K_{x_1}} + \frac{[x_1 p]}{K_{x_1 p}} + \frac{[x_2]}{K_{x_2}} + \frac{[y_1]}{K_{y_1}} \right) * \left(1 + \frac{[y_2]}{K_{y_2}} + \frac{[y_3]}{K_{y_3}} \right) * \left(1 + \frac{[x_3]}{K_{x_3}} + \frac{[x_3 p]}{K_{x_3 p}} \right) * \left(1 + \frac{[y_4]}{K_{y_4}} \right) \\
&\quad \left. * \left(1 + \frac{[x_4]}{K_{x_4}} + \frac{[y_5]}{K_{y_5}} \right) \right) \quad (2)
\end{aligned}$$

The K and A terms are dissociation constants and exponential functions of free energy changes, respectively, as previously described.

We assume in our model that no one TFBS or TF dominates the control of the promoter over the transcription rate, but that phosphorylated TFs have a greater affinity for the transcriptional machinery than their unphosphorylated counterparts [43, 44]. Therefore, we choose $A_1, A_3, A_4 = 2$ and $A_2, A_5 = 10$. Similar values with similar ratios also provided a satisfactory fit between the qPCR data and the output of the simulated MIM.

The transcription rate is proportional to the probability $P(RNAP_{bound})$ of RNAP being bound to the gene of interest [38], and taking into account the mRNA decay rate k_{deg} , we finally obtain the equation for the time evolution of mRNA concentrations, which we use in our model,

$$\frac{d}{dt} mRNA = k * P(RNAP_{bound}) - k_{deg} mRNA \quad (3)$$

Supplementary Table 4.7 - Computation of regulation factor $F_{E2F-DP1}$

Promoter-Bound (0 or 1)			Statistical Weight of the Promoter State
x_4	y_5	$RNAP$	
0	0	0	$w_1 = 1$
0	0	1	$w_2 = \frac{[RNAP]}{K_{RNAP}}$
1	0	0	$w_3 = \frac{[x_4]}{K_{x_4}}$
1	0	1	$w_4 = A_6 \frac{[x_4][RNAP]}{K_{x_4} K_{RNAP}}, A_6 = e^{\frac{-\varepsilon_{x_4 R}}{RT}}$
0	1	0	$w_5 = \frac{[y_5]}{K_{y_5}}$
$F_{E2F-DP1} = \left(\frac{[RNAP]}{K_{RNAP}} \right)^{-1} \frac{w_2 + w_4}{w_1 + w_3 + w_5} = \frac{1 + A_6 \frac{[x_4]}{K_{x_4}}}{1 + \frac{[x_4]}{K_{x_4}} + \frac{[y_5]}{K_{y_5}}}$			

Supplementary Table 4.7 - Computation of regulation factor $F_{E2F-DP1}$. Enumeration and statistical weight evaluation of each possible state for a promoter subsystem ($TFBS_{E2F-DP1}/TF/RNAP$) with an $RNAP$ site and a single $TFBS_{E2F-DP1}$ that binds either activator complex E2F-DP1 (x_4) or transcriptional repressor complex E2F-DP1-RB (y_5). The parameter $\varepsilon_{x_4 R}$ is the free energy change of RNAP binding, induced by the interaction of x_4 and the transcriptional machinery. This free energy change is negative for an activator, thus the Boltzmann factor A_6 is positive. The function $F_{E2F-DP1}$ is the regulation factor associated with $TFBS_{E2F-DP1}/TF/RNAP$.

Supplementary Table 4.8 - Computation of regulation factor F_{TCF7L2}

Promoter-Bound(0 or 1)					Statistical Weight of the Promoter State
x_1	x_1p	x_2	y_1	$RNAp$	
0	0	0	0	0	$w_1 = 1$
0	0	0	0	1	$w_2 = \frac{[RNAp]}{K_{RNAp}}$
1	0	0	0	0	$w_3 = \frac{[x_1]}{K_{x_1}}$
1	0	0	0	1	$w_4 = A_1 \frac{[x_1][RNAp]}{K_{x_1} K_{RNAp}}, A_1 = e^{-\frac{\varepsilon_{x_1} R}{RT}}$
0	1	0	0	0	$w_5 = \frac{[x_1p]}{K_{x_1p}}$
0	1	0	0	1	$w_6 = A_2 \frac{[x_1p][RNAp]}{K_{x_1p} K_{RNAp}}, A_2 = e^{-\frac{\varepsilon_{x_1p} R}{RT}}$
0	0	1	0	0	$w_7 = \frac{[x_2]}{K_{x_2}}$
0	0	1	0	1	$w_8 = A_3 \frac{[x_2][RNAp]}{K_{x_2} K_{RNAp}}, A_3 = e^{-\frac{\varepsilon_{x_2} R}{RT}}$
0	0	0	1	0	$w_9 = \frac{[y_1]}{K_{y_1}}$
$F_{TCF7L2} = \left(\frac{[RNAp]}{K_{RNAp}} \right)^{-1} \left(\frac{w_2 + w_4 + w_6 + w_8}{w_1 + w_3 + w_5 + w_7 + w_9} \right)$					
$= \frac{1 + A_1 \frac{[x_1]}{K_{x_1}} + A_2 \frac{[x_1p]}{K_{x_1p}} + A_3 \frac{[x_2]}{K_{x_2}}}{1 + \frac{[x_1]}{K_{x_1}} + \frac{[x_1p]}{K_{x_1p}} + \frac{[x_2]}{K_{x_2}} + \frac{[y_1]}{K_{y_1}}}$					

Supplementary Table 4.8 - Computation of regulation factor F_{TCF7L2} . The F_{TCF7L2} regulation factor for the $TFBS_{TCF7L2}/TF/RNAp$ subsystem is computed via enumeration and statistical weight evaluation of each possible state of the system. This site has three activator TF complexes and one repressor TF complex

competing for binding to it: β -Catenin-TCF7L2 (x_1), p β -Catenin(Y654)-TCF7L2 (x_1p), SMAD4-TCF7L2 (x_2) and repressor GROUCHO-TCF7L2 (y_1). There are nine possible states of $TFBS_{TCF7L2}/TF/RNAP$: each of the activator complexes singly binding to the DNA where the $RNAP$ is bound or not bound to its site, the unbound (reference) state, the inhibitor y_1 -bound state and the state where $RNAP$ is bound without the presence of an activator. Note that where we consider a transcriptional repressor we assume that $RNAP$ cannot bind to the promoter to activate transcription. The parameters ε_{x_1R} , ε_{x_1pR} and ε_{x_2R} (measured in units of RT) are the free energy changes of $RNAP$ binding induced by the interaction of bound x_1 , x_1p or x_2 with the transcriptional machinery. These free energy changes are negative for activators, thus the multipliers A_1 , A_2 and A_3 are positive.

Supplementary Table 4.9 - Computation of regulation factor F_{SMAD4}

Promoter-Bound (0 or 1)			Statistical Weight of the Promoter State
y_2	y_3	$RNAP$	
0	0	0	$w_1 = 1$
0	0	1	$w_2 = \frac{[RNAP]}{K_{RNAP}}$
1	0	0	$w_3 = \frac{[y_2]}{K_{y_2}}$
0	1	0	$w_4 = \frac{[y_3]}{K_{y_3}}$
$F_{SMAD4} = \left(\frac{[RNAP]}{K_{RNAP}}\right)^{-1} \frac{w_2}{w_1 + w_3 + w_4} = \frac{1}{1 + \frac{[y_2]}{K_{y_2}} + \frac{[y_3]}{K_{y_3}}}$			

Supplementary Table 4.9 - Computation of regulation factor F_{SMAD4} . The F_{SMAD4} regulation factor for the $TFBS_{SMAD4}/TF/RNAP$ subsystem is computed via enumeration and statistical weight evaluation of each possible state of the system. There are four states of this promoter: each of the repressor complexes, pSMAD2(S467)-SMAD4 (y_2) and pSMAD3(S425)-SMAD4 (y_3), singly binding to the DNA, the unbound (reference) state and the state where only $RNAP$ is bound. Note that where we consider a transcriptional repressor we assume that $RNAP$ cannot bind to the promoter to activate transcription.

Supplementary Table 4.10 - Computation of regulation factor F_{AP1}

Promoter-Bound (0 or 1)			Statistical Weight of the Promoter State
x_3	x_3p	$RNAP$	
0	0	0	$w_1 = 1$
0	0	1	$w_2 = \frac{[RNAP]}{K_{RNAP}}$
1	0	0	$w_3 = \frac{[x_3]}{K_{x_3}}$
1	0	1	$w_4 = A_4 \frac{[RNAP][x_3]}{K_{RNAP} K_{x_3}}, A_4 = e^{-\frac{\varepsilon_{x_3} R}{RT}}$
0	1	0	$w_5 = \frac{[x_3p]}{K_{x_3p}}$
0	1	1	$w_6 = A_5 \frac{[RNAP][x_3p]}{K_{RNAP} K_{x_3p}}, A_5 = e^{-\frac{\varepsilon_{x_3p} R}{RT}}$
$F_{AP1} = \left(\frac{[RNAP]}{K_{RNAP}} \right)^{-1} \left(\frac{w_2 + w_4 + w_6}{w_1 + w_3 + w_5} \right) = \frac{1 + A_4 \frac{[x_3]}{K_{x_3}} + A_5 \frac{[x_3p]}{K_{x_3p}}}{1 + \frac{[x_3]}{K_{x_3}} + \frac{[x_3p]}{K_{x_3p}}}$			

Supplementary Table 4.10 - Computation of regulation factor F_{AP1} . The F_{AP1} regulation factor for the $TFBS_{AP1}/TF/RNAP$ subsystem is computed via enumeration and statistical weight evaluation of each possible state of the system. There are six possible states of this promoter: each of the activator complexes, AP1 (x_3) and pAP1 (x_3p) singly binding to the DNA with or without the presence of $RNAP$, the unbound (reference) state and the state where only $RNAP$ is bound. The parameters ε_{x_3R} and ε_{x_3pR} (measured in units of RT) are the free energy changes of RNAP binding induced by the binding of x_3 or x_3p to the transcriptional machinery. These free energy changes are negative for activators, thus the multipliers A_4 and A_5 are positive.

Supplementary Table 4.11 - Computation of regulation factor F_{TP53}

Promoter-Bound (0 or 1)		Statistical Weight of the Promoter State
y_4	$RNAP$	
0	0	$w_1 = 1$
0	1	$w_2 = \frac{[RNAP]}{K_{RNAP}}$
1	0	$w_3 = \frac{[y_4]}{K_{y_4}}$
$F_{TP53} = \left(\frac{[RNAP]}{K_{RNAP}} \right)^{-1} \frac{w_2}{w_1 + w_3} = \frac{1}{1 + \frac{[y_4]}{K_{y_4}}}$		

Supplementary Table 4.11 - Computation of regulation factor F_{TP53} . The F_{TP53} regulation factor for the $TFBS_{TP53}/TF/RNAP$ subsystem is computed via enumeration and statistical weight evaluation of each possible state of the system. There are three states of this promoter: the repressor TP53 (y_4) bound to the promoter, the unbound (reference) state and the state where only $RNAP$ is bound. Note that where we consider a transcriptional repressor we assume that $RNAP$ cannot bind to the promoter to activate transcription.

Supplementary Table 4.12 - Summary of regulation factor expressions

TF Binding Site	Regulation Factor Name	Regulation Factor Expression
$TFBS_{TCF7L2}$	F_{TCF7L2}	$\frac{1+A_1\frac{[x_1]}{K_{x_1}}+A_2\frac{[x_1p]}{K_{x_1}p}+A_3\frac{[x_2]}{K_{x_2}}}{1+\frac{[x_1]}{K_{x_1}}+\frac{[x_1p]}{K_{x_1}p}+\frac{[x_2]}{K_{x_2}}+\frac{[y_1]}{K_{y_1}}}$
$TFBS_{SMAD4}$	F_{SMAD4}	$\frac{1}{1+\frac{[y_2]}{K_{y_2}}+\frac{[y_3]}{K_{y_3}}}$
$TFBS_{AP1}$	F_{AP1}	$\frac{1+A_4\frac{[x_3]}{K_{x_3}}+A_5\frac{[x_3p]}{K_{x_3}p}}{1+\frac{[x_3]}{K_{x_3}}+\frac{[x_3p]}{K_{x_3}p}}$
$TFBS_{TP53}$	F_{TP53}	$\frac{1}{1+\frac{[y_4]}{K_{y_4}}}$
$TFBS_{E2F-DP1}$	$F_{E2F-DP1}$	$\frac{1+A_6\frac{[x_4]}{K_{x_4}}}{1+\frac{[x_4]}{K_{x_4}}+\frac{[y_5]}{K_{y_5}}}$

Supplementary Table 4.12 - Summary of regulation factor expressions. The regulation factor expressions for each of the TCF7L2, SMAD4, AP1, TP53 and E2F-DP1 binding sites, which bind TF complexes of TCF7L2, SMAD4, AP1, TP53 and E2F-DP1, respectively.

References

1. Wierstra I and Alves J. The c-myc promoter: still MysterY and challenge. *Adv Cancer Res.* 2008; 99:113-333.
2. Levens D. How the c-myc promoter works and why it sometimes does not. *J Natl Cancer Inst Monogr.* 2008; (39):41-43.
3. Klein EA and Assoian RK. Transcriptional regulation of the cyclin D1 gene at a glance. *J Cell Sci.* 2008; 121(Pt 23):3853-3857.
4. Guo ZY, Hao XH, Tan FF, Pei X, Shang LM, Jiang XL and Yang F. The elements of human cyclin D1 promoter and regulation involved. *Clin Epigenetics.* 2011; 2(2):63-76.
5. Korinek V, Barker N, Morin PJ, vanWichen D, deWeger R, Kinzler KW, Vogelstein B and Clevers H. Constitutive transcriptional activation by a beta-catenin-Tcf complex in APC(-/-) colon carcinoma. *Science.* 1997; 275(5307):1784-1787.
6. van de Wetering M, Sancho E, Verweij C, de Lau W, Oving I, Hurlstone A, van der Horn K, Batlle E, Coudreuse D, Haramis AP, Tion-Pon-Fong M, Moerer P, van den Born M, Soete G, Pals S, Eilers M, et al. The beta-catenin/TCF-4 complex imposes a crypt progenitor phenotype on colorectal cancer cells. *Cell.* 2002; 111(2):241-250.
7. He TC, Sparks AB, Rago C, Hermeking H, Zawel L, da Costa LT, Morin PJ, Vogelstein B and Kinzler KW. Identification of c-MYC as a target of the APC pathway. *Science.* 1998; 281(5382):1509-1512.
8. Piedra J, Martinez D, Castano J, Miravet S, Dunach M and de Herreros AG. Regulation of beta-catenin structure and activity by tyrosine phosphorylation. *Journal of Biological Chemistry.* 2001; 276(23):20436-20443.
9. Shtutman M, Zhurinsky J, Simcha I, Albanese C, D'Amico M, Pestell R and Ben-Ze'ev A. The cyclin D1 gene is a target of the beta-catenin/LEF-1 pathway. *Proceedings of the National Academy of Sciences of the United States of America.* 1999; 96(10):5522-5527.
10. Tetsu O and McCormick F. beta-catenin regulates expression of cyclin D1 in colon carcinoma cells. *Nature.* 1999; 398(6726):422-426.

11. van Veelen W, Le NH, Helvensteijn W, Blonden L, Theeuwes M, Bakker ERM, Franken PF, van Gurp L, Meijlink F, van der Valk MA, Kuipers EJ, Fodde R and Smits R. beta-catenin tyrosine 654 phosphorylation increases Wnt signalling and intestinal tumorigenesis. *Gut*. 2011; 60(9):1204-1212.
12. Arce L, Pate KT and Waterman ML. Groucho binds two conserved regions of LEF-1 for HDAC-dependent repression. *Bmc Cancer*. 2009; 9.
13. Daniels DL and Weis WI. beta-catenin directly displaces Groucho/TLE repressors from Tcf/Lef in Wnt-mediated transcription activation. *Nature Structural & Molecular Biology*. 2005; 12(4):364-371.
14. Lim SK and Hoffmann FM. Smad4 cooperates with lymphoid enhancer-binding factor 1/T cell-specific factor to increase c-myc expression in the absence of TGF-beta signaling. *Proceedings of the National Academy of Sciences of the United States of America*. 2006; 103(49):18580-18585.
15. Chen CR, Kang YB, Siegel PM and Massague J. E2F4/5 and p107 as Smad cofactors linking the TGF beta receptor to c-myc repression. *Cell*. 2002; 110(1):19-32.
16. Massague J, Seoane J and Wotton D. Smad transcription factors. *Genes & Development*. 2005; 19(23):2783-2810.
17. Yagi K, Furuhashi M, Aoki H, Goto D, Kuwano H, Sugamura K, Miyazono K and Kato M. c-myc is a downstream target of the Smad pathway. *Journal of Biological Chemistry*. 2002; 277(1):854-861.
18. Ko TC, Sheng HM, Reisman D, Thompson EA and Beauchamp RD. Transforming Growth-Factor-Beta-1 Inhibits Cyclin D1 Expression in Intestinal Epithelial-Cells. *Oncogene*. 1995; 10(1):177-184.
19. Mithani SK, Balch GC, Shiou SR, Whitehead RH, Datta PK and Beauchamp RD. Smad3 has a critical role in TGF-beta-mediated growth inhibition and apoptosis in colonic epithelial cells. *Journal of Surgical Research*. 2004; 117(2):296-305.
20. Ding ZH, Wu CJ, Chu GC, Xiao YH, Ho D, Zhang JF, Perry SR, Labrot ES, Wu XQ, Lis R, Hoshida Y, Hiller D, Hu BL, Jiang S, Zheng HW, Stegh AH, et al. SMAD4-dependent barrier constrains prostate cancer growth and metastatic progression. *Nature*. 2011; 470(7333):269-+.

21. Karin M, Liu Z and Zandi E. AP-1 function and regulation. *Curr Opin Cell Biol.* 1997; 9(2):240-246.
22. Shaulian E and Karin M. AP-1 in cell proliferation and survival. *Oncogene.* 2001; 20(19):2390-2400.
23. Albanese C, Johnson J, Watanabe G, Eklund N, Vu D, Arnold A and Pestell RG. Transforming p21ras mutants and c-Ets-2 activate the cyclin D1 promoter through distinguishable regions. *The Journal of biological chemistry.* 1995; 270(40):23589-23597.
24. Bakiri L, Lallemand D, Bossy-Wetzel E and Yaniv M. Cell cycle-dependent variations in c-Jun and JunB phosphorylation: a role in the control of cyclin D1 expression. *EMBO J.* 2000; 19(9):2056-2068.
25. Zhang HS, Yan B, Li XB, Fan L, Zhang YF, Wu GH, Li M and Fang J. PAX2 protein induces expression of cyclin D1 through activating AP-1 protein and promotes proliferation of colon cancer cells. *The Journal of biological chemistry.* 2012; 287(53):44164-44172.
26. Iavarone C, Catania A, Marinissen MJ, Visconti R, Acunzo M, Tarantino C, Carlomagno MS, Bruni CB, Gutkind JS and Chiariello M. The platelet-derived growth factor controls c-myc expression through a JNK- and AP-1-dependent signaling pathway. *The Journal of biological chemistry.* 2003; 278(50):50024-50030.
27. Kerkhoff E, Houben R, Loffler S, Troppmair J, Lee JE and Rapp UR. Regulation of c-myc expression by Ras/Raf signalling. *Oncogene.* 1998; 16(2):211-216.
28. Ho JSL, Ma WL, Mao DYL and Benchimol S. p53-dependent transcriptional repression of c-myc is required for G(1) cell cycle arrest. *Molecular and Cellular Biology.* 2005; 25(17):7423-7431.
29. Rocha S, Martin AM, Meek DW and Perkins ND. p53 Represses cyclin D1 transcription through down regulation of Bcl-3 and inducing increased association of the p52 NF-kappa B subunit with histone deacetylase 1. *Molecular and Cellular Biology.* 2003; 23(13):4713-4727.
30. Bracken AP, Ciro M, Cocito A and Helin K. E2F target genes: unraveling the biology. *Trends in Biochemical Sciences.* 2004; 29(8):409-417.
31. Chen HZ, Tsai SY and Leone G. Emerging roles of E2Fs in cancer: an exit from cell cycle control. *Nature Reviews Cancer.* 2009; 9(11):785-797.

32. Carey MF. Transcriptional activation. A holistic view of the complex. *Current biology : CB*. 1995; 5(9):1003-1005.
33. Posern G and Treisman R. Actin' together: serum response factor, its cofactors and the link to signal transduction. *Trends Cell Biol*. 2006; 16(11):588-596.
34. Frank TD, Carmody AM and Kholodenko BN. Versatility of cooperative transcriptional activation: a thermodynamical modeling analysis for greater-than-additive and less-than-additive effects. *PloS one*. 2012; 7(4):e34439.
35. Garcia HG, Sanchez A, Kuhlman T, Kondev J and Phillips R. Transcription by the numbers redux: experiments and calculations that surprise. *Trends Cell Biol*. 2010; 20(12):723-733.
36. Bintu L, Buchler NE, Garcia HG, Gerland U, Hwa T, Kondev J and Phillips R. Transcriptional regulation by the numbers: models. *Current opinion in genetics & development*. 2005; 15(2):116-124.
37. Brewster RC, Jones DL and Phillips R. Tuning promoter strength through RNA polymerase binding site design in *Escherichia coli*. *PLoS computational biology*. 2012; 8(12):e1002811.
38. Frank TD, Cheong A, Okada-Hatakeyama M and Kholodenko BN. Catching transcriptional regulation by thermostatistical modeling. *Physical biology*. 2012; 9(4):045007.
39. Kadonaga JT. Regulation of RNA polymerase II transcription by sequence-specific DNA binding factors. *Cell*. 2004; 116(2):247-257.
40. Smale ST and Kadonaga JT. The RNA polymerase II core promoter. *Annual review of biochemistry*. 2003; 72:449-479.
41. Hieda M, Winstanley H, Maini P, Iborra FJ and Cook PR. Different populations of RNA polymerase II in living mammalian cells. *Chromosome research : an international journal on the molecular, supramolecular and evolutionary aspects of chromosome biology*. 2005; 13(2):135-144.
42. Maul GG and Deaven L. Quantitative determination of nuclear pore complexes in cycling cells with differing DNA content. *J Cell Biol*. 1977; 73(3):748-760.
43. Carey M. The enhanceosome and transcriptional synergy. *Cell*. 1998; 92(1):5-8.

44. Pyrzynska B, Mosieniak G and Kaminska B. Changes of the trans-activating potential of AP-1 transcription factor during cyclosporin A-induced apoptosis of glioma cells are mediated by phosphorylation and alterations of AP-1 composition. *Journal of neurochemistry*. 2000; 74(1):42-51.

Supplementary Material 5.1 Examples of behaviors of the model

Our rational modeling approach makes it possible to calculate the effect of all altered proteins (present in the MIM) or a given compound (at any dose) from the point of inhibition down to transcriptional effects. As an example to provide insight into the workings of the MIM we will describe the effect of the MEK inhibitor CI-1040 in HCT116 cells. Considering the "physiological model" (no mutations/alterations) and a concentration of EGF = 0.01 nM (expected in the presence of 10% calf serum), the physiologic concentration of MEKKPP is 2.18 nM, however given the KRAS mutation present in HCT116 cells, this goes up to 80.79 nM (all MEKPP complexes included). Due to the elevated active MEK, activated ERKPP also goes up from .046 nM, in the physiologic model, to 127.51 nM, in the HCT116 model.

In the presence of the MEK inhibitor, CI-1040 (2 μ M), a new complex was formed [MEKPP:CI-1040]. The residual MEKPP complexes have now a concentration of 24.15 nM, while the concentrations of ERKPP complexes is now down to 17.51 nM. As a result, the downstream components of the pathway are also suppressed reducing the transcription of CCND1 and MYC. The original HCT116 transcription level of c-MYC is = 0.0396 nM. Adding the MEK inhibitor, the c-MYC transcription level goes down to 0.0188 nM. The parallel values for CCND1 are the following: original HCT116 transcription level of CCND1 = 1.874 nM. In the presence of MEK inhibitor we go down to 0.516 nM.

Our model makes it easier to examine both positive and negative feedbacks in the signaling networks and how these are affected by mutations (sometimes competing mutations) or inhibitor treatments.

An example of how the model can be used to elucidate and quantify complicated competing mutational effects is AKT phosphorylation. A KRAS mutation introduced in the physiologic model produces a negative feedback to AKT-P, while an additional PI3K mutation increases AKT-P. Again starting from a physiologic model with EGF = 0.01 nM, a mutated KRAS increases ERKPP (from 0.046 nM to 134.17 nM). This in turn increases phosphorylation of CDC25C (from 12.95 nM to 49.73 nM) which reduces phosphorylated ErbB family proteins (from 6.95 nM to 1.61 nM), through CDC25C phosphatase activity. Reduced ErbBs decrease AKT-P (from 13.52 to 4.93 nM). Conversely, due to the PI3K mutation, activated PI3K increases (from 6.38 nM to 199.6 nM); this in turn increases activated AKT-P (from 13.52 nM to 63.8 nM). Taken together the effects of these two competing (with respect to AKT-P) mutations result in AKT-P becoming 62.02 nM, compared to 13.52 nM in the physiologic model. Considering the effects of the additional four mutations (TGF β R-II, E-Cadherin, PTEN, β -catenin) also present in HCT116 cells, AKT-P becomes 67.01 nM.

This is just one example, but our model can be used to quickly examine the combined effect of any number of mutations and inhibitors, on the level of any of the proteins present in the MIM, accounting not only for linear relationships but also the numerous intricate feedbacks which occur in this signaling network.

Supplementary Material 5.2 Starting from physiologic model: no mutations, KRAS mutation. Inhibitors: no inhibitors, panErb inhibitor, MEK inhibitor, both inhibitors

	EGFRP Family	ERKPP	AKTP	c-MYC	CCND1
Physiologic	1 (5.89)	1 (0.046)	1 (13.52)	1 (0.0039)	1 (0.1853)
Physiologic + PanErb Inhibitor	.18 (1.06)	0.037 (0.0018)	0.18 (2.49)	.37 (0.0014)	.014 (0.0026)
Physiologic + CI-1040	1.03 (6.07)	0.98 (0.045)	1.02 (13.79)	1.01 (0.0039)	0.99 (0.1828)
Physiologic + PanErb Inhibitor + CI-1040	0.18 (1.06)	0.037 (0.017)	0.18 (2.49)	.37 (0.0014)	.014 (0.0025)
KRAS mutated	0.129 (0.76)	2919 (134.17)	0.36 (4.93)	2.75 (0.0108)	2.75 (0.51)
KRAS mutated + PanErb Inhib.	0.055 (0.324)	2893 (133.10)	0.17 (2.30)	1.66 (0.00647)	1.64 (0.304)
KRAS mutated + CI-1040	0.130 (0.76)	450 (20.71)	0.37 (4.96)	1.26 (0.00491)	0.16 (0.030)
KRAS mutated + PanErb Inhib. + CI-1040	0.055 (0.324)	430 (19.80)	0.17 (2.30)	0.74 (0.00298)	0.09 (0.0904)

Comment: EGFR-P, ERKPP and AKT-P (all P-complexes were added together in the computation, for each signaling-protein), modeling at 30 min – 1 h, show a reasonable relative trend, see also Fig. 2 and 4 of (56, reference in main text). C-MYC and CCND1 mRNAs, at 4 – 8 h, show a more integrated behavior, closer to cell growth inhibition in the paper of Misale et al. (56, reference in main text). Consider the last four lines of Table *Supplementary Material 5.2* above, versus Fig. 5 of (56, reference in main text).

We give relative values normalized to 1 for the physiologic condition, and nM values in parenthesis.

Supplementary Material 6 - Simulated and Experimental Data

In Tables Supplementary Material 6.1 (HCT116) and Supplementary Material 6.2 (HT29) we report simulated and experimental values for ERKPP and AKTP proteins (controls normalized to 1) in the presence of different inhibitors, both alone and in association, in HCT116 and HT29 CRC lines, respectively. Experiments performed at 30 min.

In Tables Supplementary Material 6.3 and 6.4 we report simulated and experimental values for MYC and CCND1 mRNA levels (controls normalized to 1) in the presence of different inhibitors, in HCT116 and HT29 CRC lines, respectively. In HCT116 CRC line associations of inhibitors were also explored. Experiments performed both at 4h and 8h are reported and utilized for statistical analyses.

P-PROTEINS EXPERIMENTS PERFORMED WITH HCT116 CANCER LINE

Table Supplementary Material 6.1		ERKPP and AKTP levels in HCT116 cell line		
ERKPP				
	Experimental Data		Simulated Data	
Controls	1.000	1.000	1.000	1.000
XAV939 (X)	0.747	1.861	0.568	1.000
PI103 (P)	0.956	1.806	0.494	1.015
CI1040 (C)	0.065	0.339	0.101	0.113
Perifosine 20 (Pe ₂₀)	0.676	1.228	0.759	1.016
Perifosine 40 (Pe ₄₀)	0.958	1.107	0.838	1.021
X + P	0.618	0.998	1.224	1.015
X + C	0.046	0.185	0.175	0.113
P + C	0.039	0.248	0.137	0.120
C + Pe ₂₀	0.031	0.102	0.103	0.120
C + Pe ₄₀	0.045	0.026	0.022	0.122
X + P + C	0.042	0.108	0.097	0.120
Pe20 + X + P + C	0.026	0.077	0.073	0.126
Pe40 + X + P + C	0.022	0.019	0.013	0.127
AKTP				
	Experimental Data		Simulated Data	
Controls	1.000	1.000	1.000	1.000
XAV939 (X)	0.728	0.634	0.993	1.000
PI103 (P)	0.259	0.396	0.566	0.800
CI1040 (C)	0.935	1.137	1.328	1.000
Perifosine 20 (Pe ₂₀)	0.494	0.703	0.950	0.571
Perifosine 40 (Pe ₄₀)	0.171	0.243	0.132	0.395
X + P	0.312	0.343	0.480	0.800
X + C	0.771	0.649	1.349	1.000
P + C	0.418	0.456	0.461	0.801
C + Pe ₂₀	0.731	0.446	0.649	0.572
C + Pe ₄₀	0.908	0.844	0.812	0.395
X + P + C	0.439	0.370	0.382	0.801
Pe20 + X + P + C	0.417	0.282	0.456	0.319
Pe40 + X + P + C	0.135	0.135	0.138	0.198

P-PROTEINS EXPERIMENTS PERFORMED WITH HT29 CANCER LINE

Table Supplementary Material 6.2 ERKPP and AKTP levels in HT29 cell line				
ERKPP				
	Experimental Data			Simulated Data
Controls	1.000	1.000	1.000	1.000
XAV939 (X)	1.002	0.951	0.787	1.000
PI103 (P)	1.207	0.517	0.688	1.021
CI1040 (C)	0.094	0.357	0.041	0.157
Perifosine 20 (Pe ₂₀)	1.212	0.461	0.630	1.033
Perifosine 40 (Pe ₄₀)	1.959	1.892	1.282	1.043
X + P	0.942	0.353	0.796	1.021
X + C	0.110	0.146	0.057	0.157
P + C	0.081	0.144	0.037	0.176
C + Pe ₂₀	0.066	0.145	0.033	0.187
C + Pe ₄₀	0.423	0.108	0.063	0.197
X + P + C	0.063	0.136	0.026	0.176
Pe20 + X + P + C	0.056	0.155	0.025	0.203
Pe40 + X + P + C	0.058	0.030	0.017	0.208
AKTP				
	Experimental Data			Simulated Data
Controls	1.000	1.000	1.000	1.000
XAV939 (X)	0.567	0.641	0.485	1.000
PI103 (P)	0.298	0.246	0.353	0.672
CI1040 (C)	0.943	0.321	0.468	1.000
Perifosine 20 (Pe ₂₀)	0.285	0.215	0.220	0.498
Perifosine 40 (Pe ₄₀)	0.080	0.239	0.153	0.328
X + P	0.235	0.225	0.276	0.672
X + C	0.637	0.762	0.577	1.000
P + C	0.253	0.231	0.211	0.673
C + Pe ₂₀	0.336	0.385	0.236	0.498
C + Pe ₄₀	0.471	0.401	0.384	0.328
X + P + C	0.142	0.148	0.214	0.673
Pe20 + X + P + C	0.120	0.116	0.090	0.215
Pe40 + X + P + C	0.180	0.163	0.181	0.127

Tables Supplementary Material 6.1 and 6.2: Protein levels indicated as ratio ppERK/ERK and pAKT/AKT, 30 min

treatments. Tables Supplementary Material 6.1 referred to HCT116 cells, Table Supplementary Material 6.2 referred to HT29

cells. Not treated samples normalized to 1. For combination treatments inhibitor names were abbreviated as follows; XAV939 (X), PI-103 (P), CI-1040 (C), Perifosine (Pe)

mRNA EXPERIMENTAL RESULTS PERFORMED WITH HCT116 CANCER LINE

Table Supplementary Material 6.3		<u>MYC mRNA levels HCT116 cell line</u>			
		Experimental Data			Simulated Data
4h Control	1.000	1.000	1.000	1.000	1.000
8h Control	1.000	1.000	1.000	1.000	1.000
4h CI1040 (C)	0.366	0.352	0.264	0.310	0.484
8h CI1040 (C)	0.465	0.415	0.593	0.406	0.473
4h PI103 (P)	1.399	1.274	1.144	1.154	0.972
8h PI103 (P)	1.291	1.392	1.798	1.555	0.969
4h XAV939 (X)	0.978	0.918	0.803	0.793	1.000
4h P + C	0.391	0.449	0.420	0.382	0.477
4h X + C	0.262	0.231	0.198	0.202	0.484
4h X + P	0.987	0.815	0.856	0.781	0.972
4h X + P + C	0.269	0.279	0.279	0.241	0.477
<u>CCND1 mRNA levels HCT116 cell line</u>					
		Experimental Data			Simulated Data
4h Control	1.000	1.000	1.000	1.000	1.000
8h Control	1.000	1.000	1.000	1.000	1.000
4h CI1040 (C)	0.571	0.548	0.349	0.530	0.512
8h CI1040 (C)	0.250	0.225	0.294	0.218	0.275
4h PI103 (P)	0.885	0.882	0.736	0.776	0.999
8h PI103 (P)	1.064	0.961	1.248	1.088	0.998
4h XAV939 (X)	0.990	0.947	0.866	0.853	1.000
4h P + C	0.345	0.418	0.370	0.412	0.533
4h X + C	0.636	0.589	0.496	0.521	0.512
4h X + P	0.706	0.711	0.677	0.727	0.999
4h X + P + C	0.448	0.446	0.439	0.435	0.533

Tables Supplementary Material 6.3: MYC and CCND1 mRNA levels referred to HCT116 cells

Not treated samples normalized to 1. For combination treatments inhibitor names were abbreviated as follows; XAV939 (X), PI-103 (P), CI-1040 (C).

mRNA EXPERIMENTAL RESULTS PERFORMED WITH HT29 CANCER LINE

Table Supplementary Material 6.4 MYC mRNA levels HT29 cell line					
	Experimental Data				Simulated Data
4h Control	1.000	1.000	1.000	1.000	1.000
8h Control	0.780	0.999	0.820	1.041	1.000
4h CI1040 (C)	0.102	0.115	0.106	0.109	0.556
8h CI1040 (C)	0.067	0.052	0.060	0.055	0.547
4h PI103 (P)	0.942	1.105	0.956	1.257	1.049
8h PI103 (P)	1.047	1.019	0.909	0.956	1.050
4h Azakenpaullone	1.164	1.229	1.016	1.277	1.000
8h Azakenpaullone	1.409	1.334	1.168	1.316	1.000
CCND1 mRNA levels HT29 cell line					
	Experimental Data				Simulated Data
4h Control	1.000	1.000	1.000	1.000	1.000
8h Control	0.936	0.811	0.960	0.916	1.000
4h CI1040 (C)	0.522	0.398	0.487	0.467	0.655
8h CI1040 (C)	0.162	0.103	0.130	0.133	0.440
4h PI103 (P)	0.929	0.948	0.773	1.118	1.005
8h PI103 (P)	0.952	0.909	0.753	0.987	1.010
4h Azakenpaullone	1.212	0.985	1.012	1.089	1.000
8h Azakenpaullone	1.350	1.190	0.995	1.383	1.000

Tables Supplementary Material 6.4: CCND1 mRNA and MYC levels referred to HT29 cells.

Not treated samples normalized to 1. For combination treatments inhibitor names were abbreviated as follows; XAV939 (X), PI-103 (P), CI-1040 (C).